

Looking below the surface:

Intraoperative assessment of resection margins in oral cancer surgery

Yassine Aaboubout

Colofon

Looking Below the Surface: Intraoperative Assessment of Resection Margins in Oral Cancer Surgery.

Author: Yassine Aaboubout ISBN: 978-94-6510-931-2

Cover design by Grisha Karakozov

Layout and printing by Optima Grafische Communicatie, Rotterdam, the Netherlands (www.ogc.nl)

Copyright © 2025 Y. Aaboubout, Rotterdam, The Netherlands.

All rights reserved. Save expectations stated by law, no part of this thesis may be reproduced, stored in a retrieval system of any nature, or transmitted, in whole or in part, in any form or by any means, electronic, mechanical, photocopying, recording or otherwise, included in a complete or partial transcription, without the written permission of the author, or - when appropriate - of the publishers of the presented publications.

Looking Below the Surface: Intraoperative Assessment of Resection Margins in Oral Cancer Surgery.

Een blik onder het oppervlak: intra-operatieve beoordeling van resectiemarges in mondholte kanker chirurgie.

Thesis

to obtain the degree of Doctor from the
Erasmus University Rotterdam
by command of the
rector magnificus

Prof. dr. ir. A.J. Schuit

and in accordance with the decision of the Doctorate Board.

The public defence shall be held on Thursday, 23 October 2025 at 15:30 hrs

by

Yassine Aaboubout born in The Hague, The Netherlands

Erasmus University Rotterdam

(zafung

DOCTORAL COMMITTEE

Promotors: Prof. dr. S. Koljenović

Prof. dr. R.J. Baatenburg de Jong

Other members: Prof. dr. B. Kremer

Prof. dr. I.W. Schie Prof. dr. B. Weynand

Co-promotors: Dr. ir. G.J. Puppels

Paranymphs: Dr. M.R. Nunes Soares

Dr. R.W.H Smits



TABLE OF CONTENTS

Chapter 1	General introduction	9
Chapter 2	Performance of intraoperative assessment of resection margins in oral cancer surgery: A review of literature	29
Chapter 3	Intraoperative assessment of resection margins in oral cavity cancer: This is the way	53
Chapter 4	Intraoperative assessment of resection margins by Raman spectroscopy to guide oral cancer surgery	75
Chapter 5	Experimental study on needle insertion force to minimize tissue deformation in tongue tissue	111
Chapter 6	Is the depth of invasion a marker for elective neck dissection in early oral squamous cell carcinoma?	129
Chapter 7	Specimen-driven intraoperative assessment of resection margins should be standard of care for oral cancer patients	147
Chapter 8	General discussion and outlook	161
Chapter 9	Summary	175
Chapter 10	Samenvatting	181
Chapter 11	Appendix List of abbrevations Affiliations of contributing authors	187 189 191
	List of publications PhD portfolio	193 195
	Dankwoord	195
	About the author	200



GENERAL INTRODUCTION



EPIDEMIOLOGY

In 2020, more than 19 million new cases of cancer were diagnosed worldwide. In the same year, nearly 10 million patients died of cancer. Almost 900.000 of these newly diagnosed cancers, originated from the head and neck region. The head and neck region consists of the oral cavity, nasopharynx, oropharynx, hypopharynx, and larynx. Oral cavity cancer contributed to more than 1/3 of the cases (377.000) with an annual mortality of more than 177.000. This ranks oral cavity cancer among the 17 most prevalent cancers worldwide¹. The majority (> 90%) of oral cavity cancers is squamous cell carcinoma that originates from the squamous epithelium lining of the mucosa.

Many risk factors contribute to the development of oral cavity cancer including tobacco, alcohol, diet, viruses (for example, EBV, HHV8, and CMV), and radiation². Tobacco consumption (smoking or chewing) remains the most important risk factor next to alcohol consumption. The chewing of tobacco has become more prevalent worldwide³.

Another important risk factor is betel quid chewing. Being the fourth most used addictive substance worldwide and the most prevalent among the population from Southeast Asia³⁻⁵. Betel quid chewing increases the risk of developing oral/oropharyngeal cancer 2.5-fold, and in combination with tobacco 7.7-fold⁶.

For oral cavity squamous cell carcinoma (OCSCC), the average 5-year survival is 50%, with little to no improvement in the last decades. The survival depends heavily on the tumor stage, age, ethnicity, comorbidity, and the exact location of the tumor in the oral cavity⁷. Another significant factor with an adverse effect on survival is the presence of lymph node metastasis⁸. One positive lymph node reduces the 5-year overall survival by 23%, whereas 10 or more positive lymph nodes reduce the 5-year overall survival by 85%.

The standard treatment modalities for OCSCC are surgery, radiotherapy, or a combination of these modalities. However, surgery is the mainstay of OCSCC treatment¹⁰.

SURGICAL ONCOLOGY

History

Since ancient times, solid tumors were often surgically removed. For example, in 440 BCE, Atossa the queen of Persia noticed a bleeding lump on her breast which was

excised by one of her slaves¹¹. Moving forward, Galen (CE 129-199), the Greek scholar and the most prominent and acknowledged physician and surgeon in the history of medicine (**Figure 1.1**), introduced the term "oncos" (ancient Greek for tumor). He used the Hippocratic term "karkinos" (carcinoma) only for malignant tumors. He states in his thesis the *Opera Omnia*: "Cancer is curable at an early stage, the excision of the tumor must include healthy tissue around the growth and the surgeon must be sure to remove the roots of the disease, otherwise, a cure cannot be attained"^{12,13}.

During the Islamic Golden Age, the Persian scholar Ibn-e Sina (980-1037), Avicenna (his Latinized name), was known as a physician, mathematician, encyclopedist, philosopher, astronomer, and politician (Figure 1.1). However, he was best known for his many contributions to the medical field, in particular surgery. He devoted several chapters to surgery in his medical encyclopedia Al-Qanun fi al-Tibb (The Canon of Medicine). Reports showed that Avicenna was specialized in head and neck surgery¹⁴. His interest in the head and neck region made him develop new surgical tools and techniques, including the tonsillectomy and the cutting of the lingual frenulum in patients with ankyloglossia. It was also reported that the use of a tracheotomy in suffocating patients originated from him14. Moreover, Avicenna introduced the tracheotomy cannula, a tube made of either silver or gold to be placed after the tracheotomy to assist breathing¹⁵. Avicenna had different approaches for benign and malignant tumors, one-step ligation or excision versus surgical removal (in steps). He tried to focus on the preoperative differentiation of these tumors. For malignant tumors, Avicenna recommended as early and as wide as possible resection. He also stated "If you treat a recent onset cancerous lesion, it may be possible to prevent its growth and establishment. ... If cancer is treated at an early stage, it is sometimes possible to cure the patient; however, if the tumor is established, a cure becomes impossible. ... One should completely remove the cancerous lesion, its surrounding involved tissues and vessels ..."14,16.

Going forward to the Victorian era, most surgeons until the early decades of the nineteenth century did not attend an university. Some surgeons were even unable to read or write. The surgeon was often the first doctor to be approached by the poor.

The art of surgery comes from a long tradition of being trained through apprenticeships. The value of these apprenticeships depended and still depends heavily on the master's capability.

A systematic form of education came into view around 1815 in London, which was driven by a demand for uniformity in the medical world. At this time, those that



Figure 1.1. Left - Galen of Pergamum (Claudius Galenus, or in French, Claude Galien), undated lithograph by Pierre-Roch Vigneron (1789-1872). Right - Ibn-e Sina (Avicenna) With the Courtesy of the National Library of Medicine (Image ID: B029612)

wanted to become a surgeon had to attend lectures and clinics for at least 6 months, to obtain a license from the Royal College of Surgeons. However, if one wanted to become a member of the Royal College of Surgeons, one had to spend at least 6 years attending lectures and clinics. During this period surgeons evolved from ill-trained technicians to modern surgical specialists¹⁷.

An important problem during surgery was the patient's pain management, which was solved by the introduction of ether. In 1842, the American surgeon, Crawford Williamson Long from Georgia became the first to operate with the administration of ether. It is worthwhile to mention that during this operation Long removed a tumor from the neck. To confirm the effects of ether, Long performed 7 more operations with the administration of ether and published his findings in 1848. At the same time, the American dentist William Thomas Green Morton from Boston became famous for the use of ether for pain-free tooth extraction. Morton published his findings in 1846^{17,18}.

Thus, with the introduction of ether, the era of pain-free surgery had commenced. Before the introduction of ether, the surgeon had to operate as fast as possible, with all its consequences, such as incomplete tumor resection. Now, the surgeon could permit longer procedures which enabled more extensive and precise resections.

Moreover, this encouraged the surgeons to operate more frequently. However, this "improved" practice had a drawback, because multiple patients were treated with the same unwashed instruments. This resulted in a flare-up of postoperative infections, which led to death in the majority of patients.

During the same period, the French chemist and biologist Louis Pasteur wanted to investigate the cause of spoiled vats of wine. He discovered that this was caused by living agents (bacteria) or as he called it "the world of the infinitely small". Based on the publications of Pasteur, (*Recherches sur le putrefaction, 1863*), the British surgeon, Joseph Jackson Lister, professor at the University of Glasgow, hypothesized that these same bacteria could cause postoperative infections¹⁹.

Lister was a microscope enthusiast from a very young age, as his college supervisor would say: "He had a better microscope than any man in college". At this time, the use of the microscope for scientific purposes was yet to be established and many believed at the beginning of the nineteenth century that the microscope was a threat to the medical establishment. Nevertheless, Lister, with the help of his microscope and the publications of Pasteur, succeeded in his mission to abolish postoperative infections by using carbolic acid to wash open injuries or the wound bed after surgery. The number of postoperative infections decreased significantly by the use of carbolic acid and Lister published his findings in the Lancet in 1867^{17,19,20}. Until then, carbolic acid was known for preserving food, as a parasiticide, and in some cases as a deodorant. The surgical procedures became even more sanitary after the introduction of rubber gloves by the American surgeon William Stewart Halsted, professor at Johns Hopkins Hospital²¹.

In 1890, Halsted performed the first radical mastectomy in the US. Halsted was extremely aggressive in his surgical approach, not only did he remove the breast, but also the musculus pectoralis major, lymph nodes near the collar bone, and lymph nodes in the armpit. Some colleagues in Europe eventually even removed ribs. The aim was to achieve more local control and save more lives. If the surgical approach was not aggressive enough, this was classified as "mistaken kindness to the patient" and/or "surgeons with weak knives take lives" 11,22.

Despite all the improvements in surgery, the complete resection of a tumor remained a problem.

Present

In today's medicine, the goal of oncological surgery remains: the complete removal of the tumor but sparing healthy tissue as much as possible.

In the case of tumors in the oral cavity, the surgeon will aim for an adequate margin (i.e., the shortest distance between the tumor border and resection surface is > 5 mm of healthy tissue surrounding the tumor). In the complex region of the head and neck, the surgeon is often caught between a rock and a hard place. Removing too much healthy tissue can lead to disfigurement and will impair functions such as mastication and swallowing. Insufficient tissue removal leading to an inadequate resection is detrimental to the prognosis of the patient.

The Royal College of Pathologists defines margins as clear (> 5 mm), close (1-5 mm), and positive (< 1 mm). Clear margins are regarded as adequate, whereas close and positive margins are regarded as inadequate²³. Patients with an adequate resection have higher survival and a reduction in local recurrence. However, adequate resections are seldom achieved (15%-26%)²⁴⁻²⁶. This is due to the complex anatomy and the fact that the surgeon can intraoperatively only rely on preoperative imaging, visual inspection, and palpation. To improve the number of adequate resections the surgeon needs intraoperative guidance.

INTRAOPERATIVE ASSESSMENT OF RESECTION MARGINS (IOARM)

There are many oncological prognostic factors (i.e., patient and tumor characteristics). However, the resection margin is the only prognostic factor the physician can influence. An adequate resection improves the prognosis (higher survival and a reduction in local recurrence)²⁴⁻²⁶. To improve the number of adequate resections, the resection margins need to be assessed intraoperatively.

Current practices

There are two schools of thought for intraoperative assessment, namely defect-driven IOARM and specimen-driven IOARM.

The defect-driven approach is the most commonly used method. A 2005 survey reported that this method is used by 76% of head and neck surgeons²⁷. In the defect-driven approach, the surgeon samples tissue from (suspicious) region(s) from the surgical wound bed. These tissue samples are analyzed by means of frozen section (i.e., tis-

sue is quickly frozen, cut by a microtome, and stained for immediate microscopic analysis). The main advantage of this method is that it can indicate the presence or absence of tumor. However, the pathologist cannot tell what the exact resection margin is. This will only be established by final histopathology (several days after the initial surgery). Besides, the frozen section procedure takes 20-30 minutes, this time can be doubled or even tripled (depending on the facilities of an institute) in case of multiple tissue samples.

The same 2005 survey showed that the specimen-driven IOARM method is only used by 14% of head and neck surgeons²⁷. However, the evidence is growing that the specimen-driven method is superior to the defect-driven method^{26,28-34}. This resulted in its recommendation by the American Joint Committee on Cancer (AJCC)³⁵. In the specimen-driven approach, the surgeon and pathologist sample tissue (grossing) from the freshly resected specimen. This method allows the pathologist to measure the exact resection margin in millimeters. Based on this measurement the pathologist can make a recommendation for an additional resection if needed (e.g., 3 mm margin was detected during IOARM and an additional resection of 2-3 mm is recommended).

In comparison to the defect-driven approach, the specimen-driven approach can be performed in different ways. The most used specimen-driven IOARM method is based on the grossing of suspicious regions. In this method, the surgeon and pathologist inspect and palpate the specimen to identify suspicious regions (i.e., inadequate margins). If a suspicious region is detected, the pathologist will make an incision at this location and will measure the resection margin macroscopically on the cross-section. Only if the tumor border cannot be macroscopically distinguished from surrounding tissue (e.g., fibrotic tissue, salivary gland tissue), a frozen section analysis is needed. This method is also described in detail in Chapter 3.

Some authors have tried to systematically sample a specimen. For example, Gokavarapu et al. have taken the approach of routinely performing frozen section analysis from five defined anatomical regions of the oral specimen³⁶. However, different reports show that this does not improve the accuracy and is not cost-effective, due to sampling bias³⁷⁻³⁹.

It is proven that specimen-driven IOARM improves the number of adequate resections and concomitantly improves patient outcome²⁶. It is important to stress that intraoperative assessment is only effective in combination with a precise relocation method. The crux of the matter is that the region with an inadequate margin that is detected during IOARM needs to be relocated in the wound bed for an additional resection.

Therefore, our institute developed a relocation method called "paired tagging", described in detail by van Lanschot et al. ⁴⁰ (**Figure 1.2**). This method consists of paired yellow numbered tags that are sutured on both sides of the intended resection line (superficial and deep). This way, one tag is on the specimen and one tag with the same number remains in the wound bed. This facilitates the surgeon to accurately relocate a region with an inadequate margin, based on the tags.

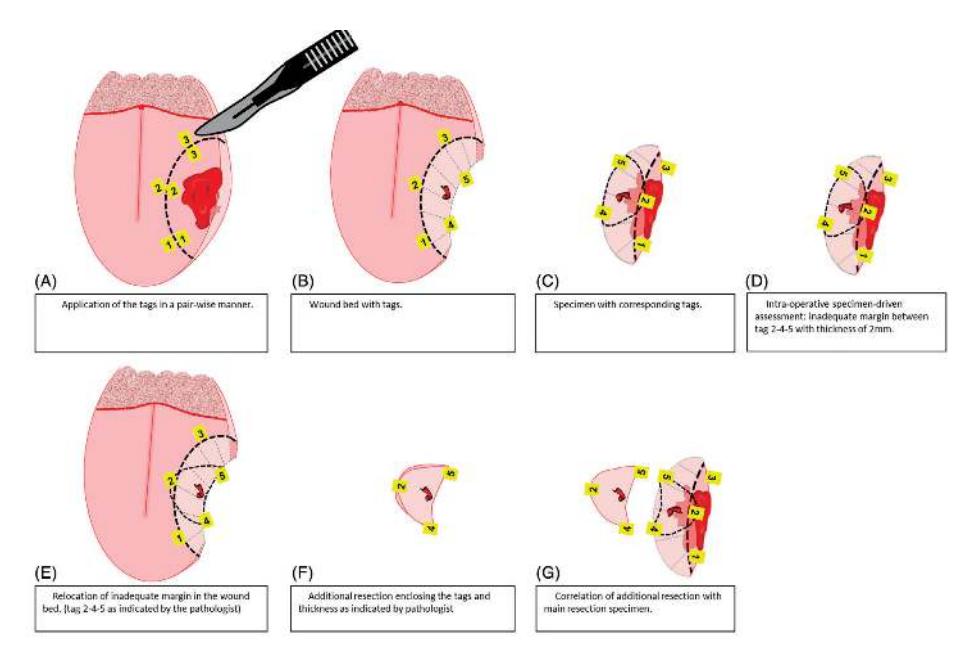


Figure 1.2. Paired tagging method, overview. A, Application of the tags in a pair-wise manner. B, Wound bed with tags. C, Specimen with corresponding tags. D, Intraoperative specimen-driven assessment: inadequate margins between tag 2-4-5 with thickness of 2 mm. E, Relocation of inadequate margins in the wound bed. (Tag 2-4-5 as indicated by the pathologist.) F, Additional resection enclosing the tags and thickness as indicated by pathologist. G, Correlation of additional resection with main resection specimen.

Reproduced with permission from MD, PhD, C.G.F. van Lanschot, Department of Otorhinolaryngology and Headand Neck Surgery, Erasmus MC, University Medical Center Rotterdam, Rotterdam, The Netherlands.

As previously described, many institutes use a method of IOARM. Every institute uses either the defect-driven or specimen-driven method. There is a lack of a unified protocol which makes the comparison of these methods difficult. However, these different methods do have one thing in common; a dedicated team of pathologists and surgeons, who are willing to improve patient care.

Nevertheless, the methods described above remain laborious and subjective which impairs their widespread implementation. The future of IOARM lies in objective techniques.

Recent developments in IOARM

Many different techniques can be used to develop a tool for IOARM, such as fluorescence, ultrasound, narrow-band imaging, confocal microscopy, high-resolution microendoscopy, optical coherence tomography, and Raman spectroscopy. A recent systematic review analyzed the different techniques for IOARM in OCSCC surgery⁴¹.

Fluorescence

Fluorescence-guided surgery is an optical imaging technique that relies on the interaction between tissue and light. A light source of a specific wavelength is used to excite fluorophores in the tissue resulting in light emission from the fluorophores. This emitted light can be detected by the eye or by a camera. Fluorophores can be endogenous (i.e., hemoglobin in autofluorescence imaging) or exogenous (i.e., fluorescein administered intravenously)³¹. Exogenous fluorophores need to bind to tumor-specific receptors, for example, the epidermal growth factor receptor (EGFR) which is present in > 90% of the head and neck squamous cell carcinomas. Antibodies like cetuximab or panitumumab can target EGFR and can be combined with a fluorescent dye (e.g., IR-Dye800CW). A recent report showed that panitumumab-IRDye800CW can be detected up to a depth of 6.3 mm in human tissue⁴¹.

However, there are disadvantages: systemic administration can cause adverse effects such as flushing, hypotension, tumor site irritation, and tachycardia, the administration must be performed several hours or 1 day before surgery, and the optimal dosage needs to be determined to achieve detectable binding to the tumor⁴³. To counter these disadvantages new research focuses on topical administration instead of intravenous administration. Studies have shown that for topical tracers (e.g., g-GLU-HMRG and 5-ALA-induced PPIX) an incubation of 10 minutes to 2.5 hours can be sufficient⁴⁴⁻⁴⁶. However, topical administration has been used off-label. Additionally, the maximum penetration depth is only limited to 1 mm⁴¹.

Ultrasound

Ultrasound (US) is a non-invasive, real-time technology, that is widely available. It is a well-known medical device that is used in many specialties. Recent reports show that US could be used as an IOARM tool in OCSCC. It started with a report that showed that the tumor thickness can be measured with US and therefore the tumor border can be detected by US^{47} . The use of US for IOARM has been reported, on the specimen and in the wound bed^{48,49}. Brouwer et al reported a mean (SD) difference of 1.1 (0.9) mm between the US and final histopathological margin and a Pearsons correlation coefficient of 0.79 (p < 0.01)⁴⁸. Helbig et al reported that the US measurement differed 0-4 mm from the final histopathology⁵⁰. Even though US is widely available it is still in its

infancy for the application for IOARM and has limited use for the wound bed. Songra et al analyzed the deep resection surface halfway through the resection, by placing a metal retractor into the surgical cut, to create an echogenic surface⁴⁹. This method is labor-intensive and could lead to false margins as tissue is compressed between the US probe and the metal retractor. Moreover, another limitation is that the accuracy depends on the experience and skill of the operator which makes it very subjective.

Raman spectroscopy

Raman spectroscopy is among the most auspicious technologies to be adopted for IOARM. It is a non-destructive optical technique that can provide real-time information about the molecular composition of tissue. Moreover, it requires no sample preparation and the ability to characterize tissues for diagnostic purposes has been extensively proven.

Raman effect

Light (photons) and matter can interact in four ways: absorption, reflection, transmission, and scattering. The scattering of light can either be elastic or inelastic. Most scattered light is unchanged in energy (elastic) and is called Rayleigh scattering (Figure 1.3A). Only a very small fraction, (i.e., 1 in a million to 1 in 100 million) of the photons has lost or gained energy through inelastic scattering by molecules. This last part is called Raman scattering (Figure 1.3 B/C).

In so-called Stokes-Raman scattering, an incoming photon transfers some of its energy to a molecule, thereby exciting a vibrational mode of the molecule. As a result, the scattered photon will have less energy than the incoming photon. Which is called the Raman shift. This Raman shift can be measured by means of a spectrometer. The Raman shift is expressed in wavenumbers (cm⁻¹).

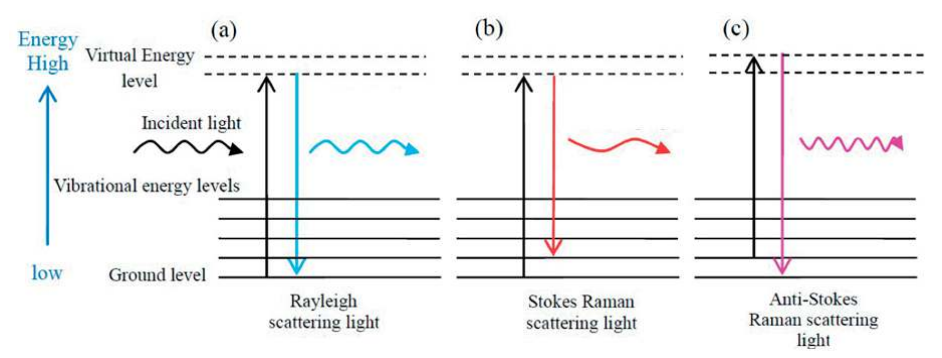


Figure 1.3. Schematic diagram of the energy transitions involved in Rayleigh scattering (a) and Raman scattering (b and c). Raman scattering occurs through the interaction of an incident photon with a molecular vibration mode, gaining (anti-Stokes scattering, blue-shifted) or losing (Stokes scattering, red-shifted) an amount of energy equal to that vibrational mode.

A molecule can have (many) different vibrational modes. The number of vibrational modes corresponds with the number of atoms in a molecule (3N-6 vibrational modes). The energy needed to excite these vibrations depends on the masses of the atoms and their chemical bonds. Also, secondary structure and interactions with other molecules can play a role. A typical Raman spectrum of a molecule consists of multiple narrow and sometimes broader bands of which the intensity is linearly dependent on the concentration of the molecules in a sample, see **Figure 1.4**.

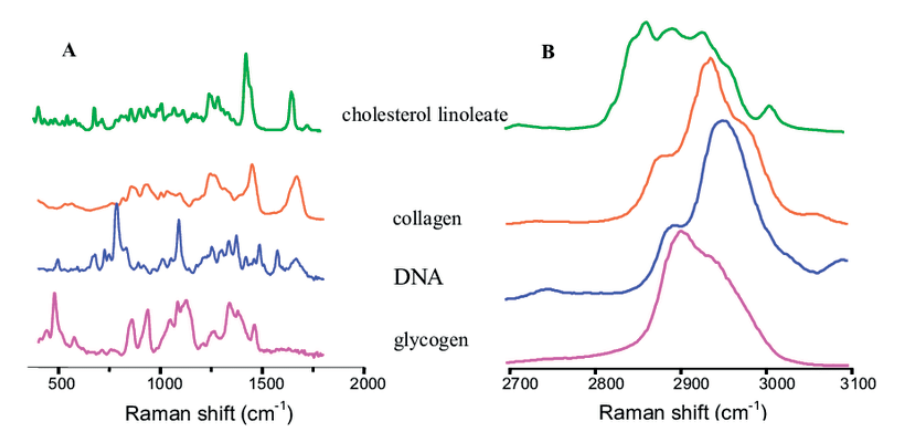


Figure 1.4. Raman spectra of commercially available pure chemical compounds, obtained in fingerprint region (A) and in high wavenumber region (B).

Two Raman spectral regions are most frequently used namely the fingerprint region (i.e., from 200 cm⁻¹ up to 2000 cm⁻¹) and the high wavenumber region (i.e., from 2400 cm⁻¹ up to 4000 cm⁻¹) (**Figure 1.4**). The fingerprint region consists of a very large number of possible vibrations and the high wavenumber region consists of information about the CH-, OH- and NH- stretching vibrations.

Recent developments in Raman spectroscopy in OCSCC surgery

Recent reports have shown that the water concentration measured with Raman spectroscopy on freshly resected tissue can be used to discriminate between healthy and tumor tissue with a sensitivity of 0.99 and a specificity of 0.92⁵¹.

The water concentration can be determined in the high wavenumber (HWVN) part of the Raman spectrum. It has been reported that for clinical applications the HWVN part of the Raman spectrum is as informative as the fingerprint region of the Raman spectrum⁵².

The use of the HWVN region has significant advantages.

- 1. The intensity of the acquired signal is much higher allowing for fast measurements.
- 2. Lower tissue autofluorescence background signal, which is known to interfere with the Raman signals.
- 3. It facilitates the use of fiber optics because no background signal is generated in the fiber material compared to the fingerprint region⁵³⁻⁵⁶. This makes it possible to use a single fiber to guide laser light to the tissue and collect Raman scattered light from the tissue. This allows measurements in depth below the tissue surface⁵⁷.

THIS THESIS

The goal of this thesis was two-fold: to improve/develop a subjective IOARM method and to develop an objective IOARM method. Here we describe a current standard of care at Erasmus MC, a subjective IOARM method performed by the pathologist and surgeon. Objective IOARM method based on Raman spectroscopy which was concomitantly developed is also described.

In chapter 2, a review of the performance of all types of IOARM that are currently employed in oral cancer surgery is presented. The IOARM performance consisted of the accuracy, sensitivity, and specificity in predicting margin status of the whole re-

section specimen, the reduction of inadequate resections and clinical relevance (i.e., overall survival, local recurrence, regional recurrence, local recurrence-free survival, disease-specific survival, adjuvant therapy). This chapter also emphasizes the need for a golden standard in intraoperative assessment. It shows that intraoperative assessment is more often the exception than the rule. Many of the included studies lack a detailed description of the IOARM method that was used.

Chapter 3 contains a detailed description of the subjective IOARM method that is currently the standard of care at Erasmus MC. This IOARM method can easily be implemented in any institute in oral cancer surgery and other surgical disciplines. Moreover, the measures prescribed in this protocol prevent any negative effects of the grossing of fresh tissue (i.e., deterioration of the anatomical orientation, shape, and size of the specimen). This protocol will stimulate and facilitate the wide adoption of specimen-driven IOARM.

In **chapter 4**, the development of a device for objective IOARM based on Raman spectroscopy is described. A device was created with a fiber-optic needle that is driven into the fresh resection specimen to determine the resection margins. First, the discriminating factors between tumor and surrounding healthy tissue were identified and used to determine the tumor border. Finally, these findings were validated and the first steps towards the implementation of the device were taken.

In **chapter 5**, the development phase of the needle of the device (described in chapter 4) is shown. The needle characteristics were optimized to minimize tissue displacement during the insertion. Moreover, the tissue displacement was further minimized by optimizing the insertion method itself.

In **chapter 6**, the depth of invasion, an important prognostic factor and a marker for elective neck dissection, was investigated. Currently, there is a need to pre- or intraoperatively measure the depth of invasion to enable as complete as possible planning of the operation. The incorporation of the measurement of the depth of invasion during the intraoperative assessment, with the Raman spectroscopy-based device, could be of added value.

In **chapter 7**, specimen-driven IOARM is recommended as a standard of care based on a broad review of the recent literature. This chapter describes the benefits and downfalls of the different methods of IOARM and the outlook.

Chapter 8, is a general discussion and an outlook on objective IOARM based on Raman spectroscopy in OCSCC.

Chapter 9 contains a summary of this thesis.

REFERENCES

- Globocan. Globocan 2020 [Internet]. Lyon (France): International Agency for Research on Cancer; 2020 [cited 2021 Apr 14]. Available from: https://gco.iarc.fr/today.
- Gupta K, Metgud R. Evidences suggesting involvement of viruses in oral squamous cell carcinoma. Patholog Res Int. 2013;2013:642496. doi:10.1155/2013/642496.
- 3. Kumar M, Nanavati R, Modi T, Dobariya C. Oral cancer: Etiology and risk factors: A review. J Cancer Res Ther. 2016;12(2):458-463. doi:10.4103/0973-1482.186696.
- Gupta PC, Warnakulasuriya S. Global epidemiology of areca nut usage. Addict Biol. 2002;7(1):77-83. doi:10.1080/13556210020091437.
- Lechner M, Breeze CE, Vaz F, Lund VJ, Kotecha B. Betel nut chewing in high-income countries—lack of awareness and regulation. Lancet Oncol. 2019;20(11):1512-1514. doi:10.1016/S1470-2045(18)30911-2.
- 6. Guha N, Warnakulasuriya S, Vlaanderen J, Straif K. Betel quid chewing and the risk of oral and oropharyngeal cancers: A meta-analysis with implications for cancer control. Int J Cancer. 2014;135(6):1433-1443. doi:10.1002/ijc.28643.
- 7. van der Ploeg T, Datema F, Baatenburg de Jong R, Steyerberg EW. Prediction of survival with alternative modeling techniques using pseudo values. PLoS One. 2014;9(6):e100234. doi:10.1371/journal.pone.0100234.
- 8. Hoesseini A, van Leeuwen N, Offerman MPJ, et al. Predicting survival in head and neck cancer: External validation and update of the prognostic model OncologIQ in 2189 patients. Head Neck. 2021;43(7):2072-2081. doi:10.1002/hed.26716.
- 9. Ho AS, Kim S, Tighiouart M, et al. Metastatic lymph node burden and survival in oral cavity cancer. J Clin Oncol. 2017;35(13):1445-1452. doi:10.1200/JCO.2016.71.1176.
- 10. Shah JP, Gil Z. Current concepts in management of oral cancer Surgery. Oral Oncol. 2009;45(4-5):301-308. doi:10.1016/j.oraloncology.2008.05.017.
- 11. Mukherjee S. The emperor of all maladies: A biography of cancer. 1st ed. New York: Scribner; 2010.
- 12. Stathopoulos P. Galen's contribution to head and neck surgery. J Oral Maxillofac Surg. 2017;75(6):1095-1096. doi:10.1016/j.joms.2017.01.036.
- 13. Toledo-Pereyra LH. Galen's contribution to surgery. J Hist Med Allied Sci. 1973;28(4):357-370. doi:10.1093/jhmas/XXVIII.4.357.
- 14. Dalfardi B, Mahmoudi Nezhad GS. Insights into Avicenna's contributions to the science of surgery. World J Surg. 2014;38(10):2540-2545. doi:10.1007/s00268-014-2477-3.
- 15. Shehata M. The ear, nose, and throat in Islamic medicine. J Int Soc Hist Islam Med. 2003;1(1):2-5.
- Eltorai I. Avicenna's view on cancer from his Canon. Am J Chin Med. 1979;7(2):103-111. doi:10.1142/S0192415X79000234.
- 17. Fitzharris L. The butchering art. 1st ed. New York: Scientific American/Farrar, Straus and Giroux: 2017.
- Hammonds WD, Steinhaus JE, Crawford W. Long: Pioneer physician in anesthesia. J Clin Anesth. 1993;5(4):306-311. doi:10.1016/0952-8180(93)90147-7.

- 19. Pitt D, Aubin JM. Joseph Lister: Father of modern surgery. Can J Surg. 2012;55(6):416-419. doi:10.1503/cjs.007112.
- 20. Lister BJ. The classic: On the antiseptic principle in the practice of surgery. 1867. Clin Orthop Relat Res. 2010;468(3):634-638. doi:10.1007/s11999-010-1320-x.
- 21. Kean S. The nurse who introduced gloves to the operating room. Distillations. Science History Institute. [cited 2021 Apr 14]. Available from: https://www.sciencehistory.org/distillations/the-nurse-who-introduced-gloves-to-the-operating-room.
- 22. Osborne MP. William Stewart Halsted: his life and contributions to surgery. Lancet Oncol. 2007;8(4):319-325. doi:10.1016/S1470-2045(07)70076-1.
- 23. Helliwell T, Woolgar J. Dataset for histopathology reporting of mucosal malignancies of the oral cavity. London, UK: Royal College of Pathologists; 2013.
- 24. Smits RWH, Koljenović S, Hardillo JA, et al. Resection margins in oral cancer surgery: Room for improvement. Head Neck. 2016;38(S1):E2197-E2203. doi:10.1002/hed.24075.
- 25. Varvares MA, Poti S, Kenyon B, et al. Surgical margins and primary site resection in achieving local control in oral cancer resections. Laryngoscope. 2015;125(10):2298-2307. doi:10.1002/lary.25397.
- 26. Smits RWH, van Lanschot CGF, Aaboubout Y, et al. Intraoperative assessment of the resection specimen facilitates achievement of adequate margins in oral carcinoma. Front Oncol. 2020;10:614593. doi:10.3389/fonc.2020.614593.
- 27. Meier JD, Oliver DA, Varvares MA. Surgical margin determination in head and neck oncology: Current clinical practice. The results of an International American Head and Neck Society member survey. Head Neck. 2005;27(7):573-581. doi:10.1002/hed.20269.
- 28. Amit M, Na'ara S, Leider-Trejo L, et al. Improving the rate of negative margins after surgery for oral cavity squamous cell carcinoma: A prospective randomized controlled study. Head Neck. 2016;38(S1):E1803-E1809. doi:10.1002/hed.24320.
- 29. Maxwell JH, Thompson LDR, Brandwein-Gensler MS, et al. Early oral tongue squamous cell carcinoma sampling of margins from tumor bed and worse local control. JAMA Otolaryngol Head Neck Surg. 2015;141(4):342-348. doi:10.1001/jamaoto.2015.1351.
- 30. Hinni ML, Zarka MA, Hoxworth JM. Margin mapping in transoral surgery for head and neck cancer. Laryngoscope. 2013;123(2):466-470. doi:10.1002/lary.23900.
- 31. Kain JJ, Birkeland AC, Udayakumar N, et al. Surgical margins in oral cavity squamous cell carcinoma: Current practices and future directions. Laryngoscope. 2020;130(1):128-138. doi:10.1002/lary.27943.
- 32. Kubik MW, Sridharan S, Varvares MA, et al. Intraoperative margin assessment in head and neck cancer: A case of misuse and abuse? Head Neck Pathol. 2020;14(4):998-1006. doi:10.1007/s12105-019-01121-2.
- 33. Barroso EM, Aaboubout Y, van der Sar LC, et al. Performance of intraoperative assessment of resection margins in oral cancer surgery: A review of literature. Front Oncol. 2021;11:628297. doi:10.3389/fonc.2021.628297.
- 34. Amin MB, Greene FL, Edge SB, et al. The eighth edition AJCC cancer staging manual: Continuing to build a bridge from a population-based to a more "personalized" approach to cancer staging. CA Cancer J Clin. 2017;67(2):93-99. doi:10.3322/caac.21388.

- 35. Lydiatt WM, Patel SG, O'Sullivan B, et al. Head and neck cancers—major changes in the American Joint Committee on Cancer eighth edition cancer staging manual. Cancer J Clin. 2018;68(1):55-63. doi:10.3322/caac.21389.
- 36. Gokavarapu S, Rao LMC, Mahajan M, Parvataneni N, Raju KVVN, Chander R. Revision of margins under frozen section in oral cancer: A retrospective study of involved margins in pT1 and pT2 oral cancers. Br J Oral Maxillofac Surg. 2015;53(8):686-692. doi:10.1016/j. bjoms.2015.04.018.
- Chaturvedi P, Datta S, Nair S, et al. Gross examination by the surgeon as an alternative to frozen section for assessment of adequacy of surgical margin in head and neck squamous cell carcinoma. Head Neck. Published online 2014. doi:10.1002/hed.23313
- 38. Mair M, Nair D, Nair S, et al. Intraoperative gross examination vs frozen section for achievement of adequate margin in oral cancer surgery. Oral Surg Oral Med Oral Pathol Oral Radiol. Published online 2017. doi:10.1016/j.oooo.2016.11.018
- 39. Datta S, Mishra A, Chaturvedi P, et al. Frozen section is not cost beneficial for the assessment of margins in oral cancer. Indian J Cancer. Published online 2019. doi:10.4103/ijc. IJC_41_18
- 40. Lanschot CGF, Mast H, Hardillo JA, et al. Relocation of inadequate resection margins in the wound bed during oral cavity oncological surgery: A feasibility study. Head Neck. 2019;41(7):2159-2166. doi:10.1002/hed.25690
- 41. Brouwer de Koning SG, Schaeffers AWMA, Schats W, van den Brekel MWM, Ruers TJM, Karakullukcu MB. Assessment of the deep resection margin during oral cancer surgery: A systematic review. Eur J Surg Oncol. Published online 2021. doi:10.1016/j.ejso.2021.04.016
- 42. van Keulen S, van den Berg NS, Nishio N, et al. Rapid, non-invasive fluorescence margin assessment: Optical specimen mapping in oral squamous cell carcinoma. Oral Oncol. Published online 2019. doi:10.1016/j.oraloncology.2018.11.012
- 43. Gao RW, Teraphongphom N, de Boer E, et al. Safety of panitumumab-IRDye800CW and cetuximab-IRDye800CW for fluorescence-guided surgical navigation in head and neck cancers. Theranostics. Published online 2018. doi:10.7150/thno.24487
- 44. Slooter MD, Handgraaf HJM, Boonstra MC, et al. Detecting tumour-positive resection margins after oral cancer surgery by spraying a fluorescent tracer activated by gamma-glutamyltranspeptidase. Oral Oncol. 2018;78:1-7. doi:10.1016/j.oraloncology.2017.12.006
- 45. Shimane T, Aizawa H, Koike T, Kamiya M, Urano Y, Kurita H. Oral cancer intraoperative detection by topically spraying a γ-glutamyl transpeptidase-activated fluorescent probe. Oral Oncol. Published online 2016. doi:10.1016/j.oraloncology.2015.12.003
- 46. Leunig A, Betz CS, Mehlmann M, et al. Detection of squamous cell carcinoma of the oral cavity by imaging 5-aminolevulinic acid-induced protoporphyrin IX fluorescence. Laryngoscope. Published online 2000. doi:10.1097/00005537-200001000-00015
- 47. Klein Nulent TJW, Noorlag R, Van Cann EM, et al. Intraoral ultrasonography to measure tumor thickness of oral cancer: A systematic review and meta-analysis. Oral Oncol. Published online 2018. doi:10.1016/j.oraloncology.2017.12.007
- 48. Brouwer de Koning SG, Karakullukcu MB, Lange CAH, Schreuder WH, Karssemakers LHE, Ruers TJM. Ultrasound aids in intraoperative assessment of deep resection margins of

- squamous cell carcinoma of the tongue. Br J Oral Maxillofac Surg. Published online 2020. doi:10.1016/j.bjoms.2019.11.013
- 49. Songra AK, Ng SY, Farthing P, Hutchison IL, Bradley PF. Observation of tumour thickness and resection margin at surgical excision of primary oral squamous cell carcinoma Assessment by ultrasound. Int J Oral Maxillofac Surg. Published online 2006. doi:10.1016/j.ijom.2005.07.019
- Helbig M, Flechtenmacher C, Hansmann J, Dietz A, Tasman AJ. Intraoperative B-mode endosonography of tongue carcinoma. Head Neck. Published online 2001. doi:10.1002/1097-0347(200103)23:3<233::AID-HED1024>3.0.CO;2-P
- 51. Barroso EM, Smits RWH, Schut TCB, et al. Discrimination between Oral Cancer and Healthy Tissue Based on Water Content Determined by Raman Spectroscopy. Anal Chem. Published online 2015. doi:10.1021/ac504362y
- 52. Koljenović S, Bakker Schut TC, Wolthuis R, et al. Tissue characterization using high wave number Raman spectroscopy. J Biomed Opt. 2005;10(3):031116. doi:10.1117/1.1922307
- 53. Santos LF, Wolthuis R, Koljenović S, Almeida RM, Puppels GJ. Fiber-Optic Probes for in Vivo Raman Spectroscopy in the High-Wavenumber Region. Anal Chem. 2005;77(20):6747-6752. doi:10.1021/ac0505730
- 54. Caspers PJ, Bruining HA, Puppels GJ, Lucassen GW, Carter EA. In Vivo Confocal Raman Microspectroscopy of the Skin: Noninvasive Determination of Molecular Concentration Profiles. J Invest Dermatol. 2001;116(3):434-442. doi:10.1046/j.1523-1747.2001.01258.x
- 55. Koljenović S, Bakker Schut TC, Wolthuis R, et al. Raman Spectroscopic Characterization of Porcine Brain Tissue Using a Single Fiber-Optic Probe. Anal Chem. 2007;79(2):557-564. doi:10.1021/ac0616512
- Nijssen A, Maquelin K, Santos LF, et al. Discriminating basal cell carcinoma from perilesional skin using high wave-number Raman spectroscopy. J Biomed Opt. Published online 2007. doi:10.1117/1.2750287
- 57. Caspers PJ, Lucassen GW, Bruining HA, Puppels GJ. Automated depth-scanning confocal Raman microspectrometer for rapid in vivo determination of water concentration profiles in human skin. J Raman Spectrosc. Published online 2000. doi:10.1002/1097-4555(200008/09)31:8/9<813::AID-JRS573>3.0.CO;2-7



PERFORMANCE OF INTRAOPERATIVE ASSESSMENT OF RESECTION MARGINS IN ORAL CANCER SURGERY: A REVIEW OF LITERATURE

Elisa M. Barroso, Yassine Aaboubout, Lisette C. van der Sar, Hetty Mast, Aniel Sewnaik, Jose A. Hardillo, Ivo ten Hove, Maria R. Nunes Soares, Lars Ottevanger, Tom C. Bakker Schut, Gerwin J. Puppels,† and Senada Koljenović1,†

Front Oncol. 2021 Mar 30;11:628297.



ABSTRACT

Introduction

Achieving adequate resection margins during oral cancer surgery is important to improve patient prognosis. Surgeons have the delicate task of achieving an adequate resection and safeguarding satisfactory remaining function and acceptable physical appearance, while relying on visual inspection, palpation, and preoperative imaging. Intraoperative assessment of resection margins (IOARM) is a multidisciplinary effort, which can guide towards adequate resections. Different forms of IOARM are currently used, but it is unknown how accurate these methods are in predicting margin status. Therefore, this review aims to investigate: 1) the IOARM methods currently used during oral cancer surgery, 2) their performance, and 3) their clinical relevance.

Methods

A literature search was performed in the following databases: Embase, Medline, Web of Science Core Collection, Cochrane Central Register of Controlled Trials, and Google Scholar (from inception to January 23, 2020). IOARM performance was assessed in terms of accuracy, sensitivity, and specificity in predicting margin status, and the reduction of inadequate margins. Clinical relevance (i.e., overall survival, local recurrence, regional recurrence, local recurrence-free survival, disease-specific survival, adjuvant therapy) was recorded if available.

Results

Eighteen studies were included in the review, of which 10 for soft tissue and 8 for bone. For soft tissue, defect-driven IOARM-studies showed the average accuracy, sensitivity, and specificity of 90.9%, 47.6%, and 84.4%, and specimen-driven IOARM-studies showed, 91.5%, 68.4%, and 96.7%, respectively. For bone, specimen-driven IOARM-studies performed better than defect-driven, with an average accuracy, sensitivity, and specificity of 96.6%, 81.8%, and 98%, respectively. For both, soft tissue and bone, IOARM positively impacts patient outcome.

Conclusion

IOARM improves margin-status, especially the specimen-driven IOARM has higher performance compared to defect-driven IOARM. However, this conclusion is limited by the low number of studies reporting performance results for defect-driven IOARM. The current methods suffer from inherent disadvantages, namely their subjective character and the fact that only a small part of the resection surface can be assessed in a short time span, causing sampling errors. Therefore, a solution should be sought in the field of objective techniques that can rapidly assess the whole resection surface.

INTRODUCTION

Every year, around 350,000 new patients are diagnosed worldwide with oral cavity cancer. Oral cavity squamous cell carcinoma (OCSCC) is the most prevalent oral cavity cancer type. The worldwide mortality rate is 175,000 per year and the 5-year overall survival is 64.8%^{1.4}.

Surgery is the primary treatment for OCSCC. The goal of surgery is the complete resection of the tumor with an adequate resection margin (i.e., the shortest distance between the tumor border and the resection surface is > 5 mm) while preserving as much healthy tissue as possible to minimize the loss of function (such as, mastication and swallowing) and facial disfigurement. The resection margin is an important predictor for patient outcome and is the only oncological prognostic factor that pathologists and surgeons can influence⁵⁻⁷.

For soft tissue, according to the Royal College of Pathologist (RCP), the resection margin is classified as clear when it is more than 5 mm, close when it is 1 to 5 mm, and positive when it is less than 1 mm⁸. Clear margins are regarded as adequate, whereas close and positive margins are regarded as inadequate. For bone, the RCP indicates that a resection is adequate when the bone resection surfaces are cancer-negative⁵.

It has been proven that inadequate resection margins in soft tissue result in a need for adjuvant therapy (re-excision or post-operative (chemo-) radiotherapy)⁸. Adjuvant therapy brings an additional burden for the patient and results in increased morbidity and reduced quality of life⁹. Furthermore, inadequate resection margins in soft tissue have a significantly negative effect (almost two fold reduction) on overall survival and disease-free survival^{5,7,10}. Patients with positive bone margins have a twofold reduction of disease-free and overall survival compared to patients with adequate bone margins¹¹⁻¹³.

However, achieving adequate resection margins in the oral cavity is often difficult due to its complex anatomy. During the operation the surgeon relies on pre-operative imaging, visual inspection and palpation.

Recent studies have shown that adequate margins are only achieved in a minority (15% - 26%) of the cases of soft tissue OCSCC^{5,7,10}. Segmental mandible resections have shown considerable improvement over the last years (0% - 14.6% positive bone margins). However, marginal mandible resections and partial maxillectomies still show a high rate of positive bone margins (16% - 35.7% and 44% - 60%, respectively)^{11,13-16}.

These results indicate that visual inspection, palpation, and preoperative imaging do not warrant adequate tumor resection. Besides, the final margin status is only known a few days (soft tissue) or weeks (bone) after surgery. If at that point an inadequate margin is encountered, a second surgery is not an option, nor effective, because an accurate relocation of the site of an inadequate margin is almost impossible in most cases⁶.

Furthermore, in the case of bone resections, an immediate bone reconstruction is performed (often with a free flap) to limit the loss of continuity and the adverse effects on function and aesthetics, making the second surgery undesirable.

Therefore, for optimal control of resection margins, the surgeon needs additional information during surgery. Intraoperative assessment of resection margins (IOARM) can provide this valuable information, enabling revision of margins (additional tissue resection) during the initial surgery to turn an inadequate resection into an adequate resection.

Two methods for soft tissue IOARM can be distinguished: the traditional defect-driven method and the specimen-driven method.

According to a 2005 survey, around 76% of the surgeons perform defect-driven IOARM, while only 14% perform specimen-driven IOARM during OCSCC surgery¹⁷. However, the evidence that specimen-driven IOARM is superior to defect-driven IOARM is growing^{5, 18-21}. Therefore, the American Joint Committee on Cancer (AJCC) has recommended specimen-driven IOARM as the standard of care since 2017²².

In the traditional defect-driven approach, the surgeon samples one or more suspicious pieces of tissue from the wound bed for analysis by frozen section (FS) (i.e., a tissue sample that has been quick-frozen, cut by a microtome, and stained immediately for rapid microscopic diagnosis). The major disadvantage of defect-driven IOARM is that it can only indicate the presence of a tumor-positive margin and it cannot provide the exact margin value in millimeters. In the recently recommended specimen-driven method, the margins are assessed on the specimen by visual inspection and palpation followed by perpendicular incisions with or without sampling of tissue for FS examination⁶. This approach provides immediate feedback on whether an additional resection is needed.

Here we review the performance of IOARM methods used during OCSCC surgery in predicting margin-status. The impact on patient outcome was assessed with respect

to overall survival, disease-specific survival, local recurrence and the need for adjuvant therapy.

MATERIALS AND METHODS

Search Strategy

A search was conducted in the following databases: Embase, Medline, Web of Science Core Collection, Cochrane Central Register of Controlled Trials, and Google Scholar. The following keywords and synonyms were used in the search filter: "oral cavity squamous cell carcinoma", "resection margin" and "intraoperative". Only studies written in English from inception of the database to the 23rd of January 2020 were considered.

The studies were first assessed for eligibility based on the title and abstract. The following inclusion criteria were used: 1) the majority (> 90%) of the patients were surgically treated for OCSCC and 2) the performance of an IOARM method was investigated. The following exclusion criteria used were: 1) the study did not follow the resection margin definition of the RCP, 2) the study comprised a non-human population, 3) the study is a review, a commentary or a letter to the editor. The full text of studies that met the previous criteria was screened to extract and analyze the data.

Data Analysis

Data Extraction

The included studies were divided based on the type of tissue assessed: soft tissue (group 1), and bone tissue (group 2).

The following patient and tumor characteristics were extracted independently by 3 researchers, when available: number of patients, male/female ratio (M/F), mean/median age (years), anatomical subsite, pathological TNM (pTNM) classification, and percentage of patients treated for primary disease. Type of IOARM was extracted from each of the included studies. The following IOARM performance variables were collected: true positives, true negatives, false positives, false negatives, accuracy (Acc.), sensitivity (Sens.), specificity (Spec.), positive predictive value (PPV) and negative predictive value (NPV). IOARM impact on patient outcome (e.g., overall survival (OS), disease-specific survival (DSS), local recurrence (LR) and the need for adjuvant therapy) was also collected.

Analysis of IOARM Performance and Impact on Patient Outcome.

Based on the extracted data, IOARM sampling and interpretation errors (a), and the reduction in inadequate resections (b) were calculated.

Sampling and Interpretation Errors

Two types of error can occur during IOARM: sampling error (SE) and interpretation error (IE).

SE is the proportion of inadequate resections that are not identified during IOARM. It occurs due to non-representative sampling of tissue resulting in underestimation of inadequate margins (e.g., tissue is sampled from two suspicious regions but final histopathology indicates that there is a close margin in a region not regarded as suspicious during IOARM).

Interpretation error refers to incorrect diagnosis of the sampled tissue, resulting in under or overestimation of inadequate margins during IOARM.

Reduction of Inadequate Resections

The reduction in the number of inadequate resections (IR) based on IOARM was calculated using

$$Reduction \, IR \, (\%) = \left(\frac{IR_i - IR_{Rev}}{IR_i}\right) \times 100$$

where:

 IR_i is the number of initially inadequate resections, without revision (additional resection);

 IR_{Rev} is the number of inadequate resections after revision.

RESULTS

A total of 1265 records were found in the different databases. After removing duplicates, 699 remained and were screened on title and abstract, see **Figure 2.1**. This resulted in exclusion of 626 records based on the criteria applied. Of the remaining 43 records, the full text was screened resulting in further exclusion of 25 records based on the criteria of this study, as mentioned above.

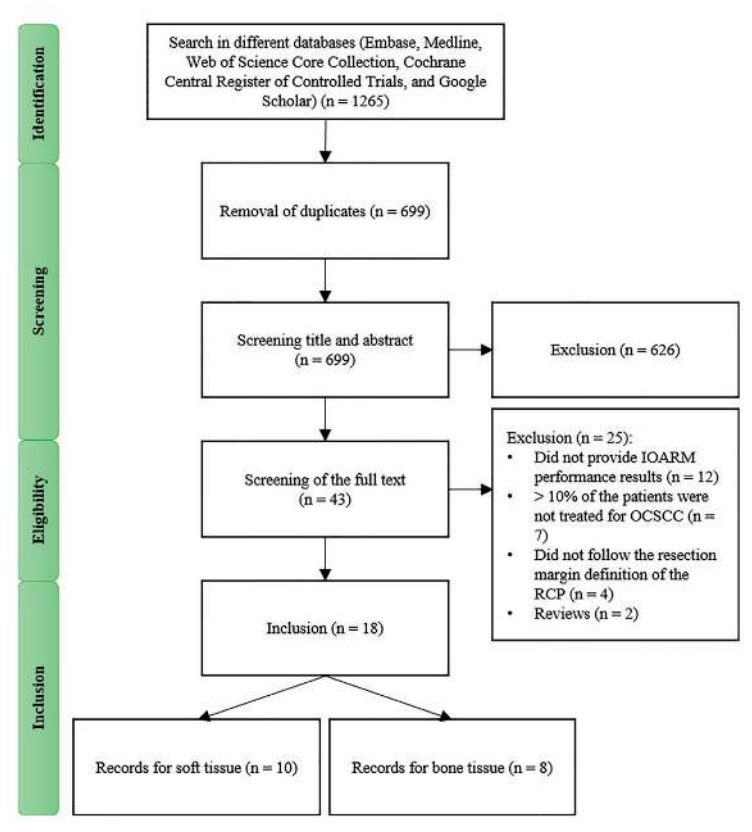


Figure 2.1. Flow diagram of the study selection process.

Group 1 - IOARM in Soft Tissue

Ten studies investigated the performance of IOARM methods in soft tissue^{19, 23-31}. The patients and tumor characteristics of the studies are shown in **Table 2.1**. The description of the IOARM methods and their performance in the studies included are shown in **Table 2.2**. The non-weighted average performance parameters for both methods were calculated over all studies that reported the necessary information (**Table 2.3**). For the specimen-driven method the reduction of inadequate resections after revision was 47.1%, based on the report of 5 studies^{23, 25, 26, 28, 30}. For the defect-driven method, one study has reported that the reduction in inadequate resections amounted 51.3%²⁷.

IOARM Impact on Patient Outcome

Overall Survival

One study reported that at 5 years follow-up there was no significant difference between defect-driven IOARM and no IOARM (p=0.836)²⁴. None of the other studies reported on OS.

Disease-Specific Survival

Pathak et al. showed that at 5 years follow-up there was no significant difference between defect-driven IOARM and no IOARM²⁴. None of the other studies reported on DSS.

Local Recurrence

Three studies reported results on LR^{24, 27, 28}. Two studies used defect-driven IOARM and one study used specimen-driven IOARM. For defect-driven LR of 14.4% (after 180 months of follow-up) and 23% (after 60 months of follow-up) were shown. For specimen-driven LR of 7.3% (after 14 months of follow-up) was shown^{24, 27, 28}. From the 3 articles reporting LR, only Pathak et al. compares the defect-driven IOARM group (supported by FS) with a control group without IOARM²². They showed that the IOARM group had 20.1% of primary failure rate (i.e., LR), while the control group had 25.2% of primary failure rate.

Adjuvant Therapy

Two studies have described the influence of IOARM on the need for adjuvant therapy^{19, 30}. Datta et al. showed that there was no significant reduction in the need for adjuvant therapy when comparing two groups of patients, patients treated with IOARM vs patients that did not receive IOARM³⁰. Amit et al. reported that from all patients that underwent defect-driven IOARM 35% required adjuvant therapy. In the specimen-driven IOARM group 8% required adjuvant therapy¹⁹.

Table 2.1. IOARM in soft tissue: patients and tumor characteristics.

	Primary disease(%)	ı	ı	100.0	85.8	100.0	100.0		
	Prior therapy(%)	0.0	0.0	0.0	3.5 ^{cT} 14.2 ⁵	0.0	ı	c	2
	Iumor characteristics pT1/pT2/pT3/pT4 (%) pN0/ pN1/pN2/pN3 (%)	30.6/16.3/14.4/38.7	30.8/40.1/10.3/18.8 73.3/15.9/9.9/0.5	18.0/45.0/18.0/19.0 65.7/19.8/14.0/0.5	14.7/26.6/9.1/49.7 -/-/-	35.3/32.0/5.8/26.9 57.0/14.1/28.9/0.0	45.0/21.0/4.0/30.0 71/10.0/19.0/<1.0	29.0/34.0/28.0/9.0	25.0/35.0/30.0/10.0 -/-/-
	Subsite(s) (%)	Oral cavity (100.0)	Floor of the mouth (42.8); Tongue (27.6); Gingiva/Alveolus (12.0); Buccal (8.2); Retromolar trigone (1.9); Hard palate (1.2)	Tongue (100.0)	Tongue (42.2); Buccal (42.2); Lower and upper alveolus (5.7); Hard palate (2.2); Floor of the mouth (0.7); Lip (0.7); Larynx (2.8); Hypopharynx (3.5)	Tongue (16.0); Floor of the mouth (45.0); Cheek (7.0); Maxilla and palate (8.0); Larynx/pharynx (8.0); Alveolus (14.0)	Tongue (45.0); Lower and upper alveolus (20.0); Floor of mouth (18.0); Other (17.0)	Tongue (49.0); Lip (16.0); Floor of the mouth (9.0); Hard palate (5.0); Buccal (9.0); Mandible (12.0)	Tongue (40.0); Lip (15.0); Floor of the mouth (10.0); Hard palate (5.0); Buccal (15.0); Mandible (15.0)
	Mean age (y)	1	64.0	48.0	1	59.0	61.0	59.0	70.0
-	M/F(%)	65.0/35.0	58.0/42.0	73.0/27.0	1	72.0/28.0	58.0/42.0	61.0/39.0	60.0/40.0
	Patients (N) (inclusion period)	49.0 (-)	416.0 (1973-2003)	877.0 (2007-2010)	141.0 (2011-2012)	156.0 (2004-2012)	406.0 (2005-2014)	51.0 (2011-2014)	20.0 (2011-2014)
	Author	Ord ²³	Pathak ²⁴	Chaturvedi ³¹	Chaturvedi ²⁵	Ettl ²⁸	Buchakjian ²⁷	A v v i t 19	

Table 2.1. IOARM in soft tissue: patients and tumor characteristics. (continued)

Patients (N)			Mean		Tumor characteristics		
(inclusion period) M/F(%)	W/F(%)		age (y)	Subsite(s) (%)	pT1/pT2/pT3/pT4 (%) pN0/ pN1/pN2/pN3 (%)	Prior therapy(%)	Primary disease(%)
435.0 (2014-2015) 65.0/35.0	65.0/35.	0	ı	Tongue (28.5); Floor of mouth (1.0); Buccal (48.5); Lower and upper alveolus (18.2); Retromolar trigone (2.1); Lower lip (1.4)	55.9′44.1" 42.5″/57.5‴	3.7 ^{CT} 3.2 ^{RT} 3.7 ^S	96.3
77.0 58.0/42.0 49.0 (2010-2014)	58.0/42.0		49.0	Tongue (38.0); Cheek (37.0); Palate (8.0); Other (17.0)	ı	0.0	ı
1237.0 (2012-2013)				Gingivobuccal complex (56.0); Tongue & floor of mouth (36.0); Lip (5.0); Hard palate & upper alveolus (3.0)			

*Percentage of pT1 and pT2.

**Percentage of pT3 and pT4.

"Percentage of pN+. "Percentage of pN-.

^{CT}Percentage of patients treated with neoadjuvant chemotherapy.

^{RT}Percentage of patients treated with radiation therapy prior to surgery.

^SPercentage of patients treated with secondary surgery.

Table 2.2. IOARM methods in soft tissue: description and performance.

		IOARM					IOARM PE	IOARM performance	e,			
Author	Method	Details of approach	Acc. (%)	Sens. (%)	Spec.(%) PPV(%)	PPV(%)	NPV(%)	IRi(%)	IR Rev.	ReductionIR(%)	SE(%)	IE(%)
Ord ²³	Specimen- driven	Gross examination and FS (taken from mucosal and deep margins)	83.7	30.0	97.0	75.0	84.4	22.4	18.4	17.8	20.0	1.0
Chaturvedi ³¹	Specimen- driven	Gross examination and FS (taken from mucosal and deep margins)	0.66	97.0	100.0	100.0	99.4	ı	12.2	ı	79.0	1
Chaturvedi ²⁵	Specimen- driven	Gross examination and FS (taken from mucosal and deep margins)	94.0	80.0	100.0	100.0	91.4	31.9	6.6	0.69	20.0	0.0
Ettl ²⁶	Specimen- driven	FS (taken from mucosal margins)	1	1	ı	1	1	51.3	32.0	37.6	1	1
	Coorimon	Gross examination alone	83.7	61.9	88.3	53.1	91.2				37.0	12.8
Mair ²⁸	driven	Gross examination and FS (taken from mucosal and deep margins)	92.9	45.5	98.8	83.3	93.5	15.6	7.4	52.6	48.0	7.7
Datta ³⁰	Specimen- driven	Gross examination and FS (taken from mucosal and deep margins)	95.4	73.1	100.0	0.99	94.8	18.8	7.8	58.5	4.3	0.0
Pathak ²⁴	Defect- driven	FS (taken from mucosal and deep margins)	1	1	70.4	1	1	ı		1	ı	1
Buchakjian ²⁷	Defect- driven	FS (taken from mucosal and deep margins)	1	48.0	72.0	57.0	65.0	37.0	18.0	51.3	64.9	10.1
Abbas ²⁹	Defect- driven	FS (taken from mucosal and deep margins)	6.06	72.7	95.3	9.99	93.9	ı		,	27.3	5.2
Amit ¹⁹	Specimen- driven	Gross examination and FS (taken	1	91.0	93.0	ı	1	ı	16.0	1	1	1
	Defect- driven	from mucosal and deep margins)		22.0	100.0			1	45.0			1

Table 2.3. The non-weighted average IOARM performance parameters for soft tissue: specimendriven vs defect-driven method.

Performance parameters (average)	Studies using specimen-driven method* (N)	Studies using defect-driven method (N)
Accuracy (%)	91.5 (6.0)	90.9 (1.0)
Sensitivity (%)	68.4 (7.0)	47.6 (3.0)
Specificity (%)	96.7 (7.0)	84.4 (3.0)
¹ PPV (%)	79.6 (6.0)	41.2 (2.0)
² NPV (%)	92.5 (6.0)	79.5 (2.0)
³ SE (%)	41.4 (6.0)	46.1 (2.0)
⁴IE (%)	4.3 (5.0)	7.7 (2.0)

*Four of 6 studies were from the same institute.

N represents the number of studies included in the calculation.

Group 2 - IOARM in Bone Tissue

Eight studies investigated the performance of IOARM on bone tissue^{11, 12, 32-37}. The patients and tumor characteristics are shown in **Table 2.4**. The description of the IOARM methods and their performance are shown in **Table 2.5**.

The non-weighted average performance parameters for both methods were calculated over all studies that reported the necessary information (**Table 2.6**). For the specimen-driven method the reduction of inadequate resections after revision was 78.4%, based on the report of 4 studies^{11, 32, 35, 36}. For the defect-driven method, one study has reported that the reduction in inadequate resections amounted 33%³⁷.

¹PPV - Positive predictive value.

²NPV - Negative predictive value.

³SE - Sampling error.

⁴IE - Interpretation error.

Table 2.4. IOARM in bone tissue: patients and tumor characteristics.

	Primary disease (%)	ı	ı	85.2	ı	0.06	89.2
	Prior therapy (%)	25.0 ^{RT}	0.0		ı	18.0 ^{кт} 4.0 ^{¢⊤}	
Tumor characteristics	pT1/pT2/pT3/pT4 (%) Prior pN0/pN1/pN2/pN3 (%) therapy (%)	ı	ı	-/-/-/100.0 37.0/19.0/44.0/-		ı	12.0/22.0/18.0/47.0 54.9/10.8/26.5/-
TuT.	Subsite(s) (%)	ı	Floor of mouth (30.0); Retromular (50.0); Buccal (15.0); Gingiva (5.0)	Floor of mouth (66.0); Lower and upper alveolus (19.0); Lip (4.0); Retromolar trigone (11.0)	•	Oral cavity (94.0); Oropharynx (6.0)	Floor of mouth (41.0); Mandible (33.0); Maxilla (14.0); Cheek (7.0); Tongue (2.0); Orb. (3.0)
	Type of surgery(%)	Mandible resection: segmental (55.0); marginal (45.0)	Segmental marginal mandibulectomy (100.0)	Segmental mandibulectomy (100.0)	Segmental/ marginal mandibulectomy (88.0); partial maxillectomy (12.0)	Mandible resection: segmental (80.0); marginal (20.0)	Segmental/ marginal/ lingual rim mandibulectomy (86.0), partial maxillectomy (13.0); other (1.0)
	Mean age (y)	57.0	67.0	59.0	56.0	ı	62.0
	M/F(%)	ı	65.0/35.0	63.0/37.0	68.0/32.0	ı	69.0/31.0
	Patients (N) (inclusion period)	16.0	20.0 (2006-2007)	27.0 (2005-2010)	45.0 (2010-2013)	51.0 (2003-2013)	102.0
	Author	Forrest ³²	Wysluch ³³	Bilodeau ³⁴	Nieberler ³⁵	Namin ³⁶	Nieberler ¹¹

Table 2.4. IOARM in bone tissue: patients and tumor characteristics. (continued)

	Primary disease (%)	82.9	100.0
	Prior therapy (%)		0.0
Tumor characteristics	pT1/pT2/pT3/pT4 (%) Prior Primary pN0/pN1/pN2/pN3 (%) therapy (%) disease (%)	5.7/25.7/20.0/42.9 51.4/11.4/28.6/-	-/-/-100.0 47.0/29.0/18.0/6.0
	Subsite(s) (%)	Floor of mouth (40.0); Mandible (28.6); Maxilla (5.7); Cheek (11.4); Tongue (5.7); Other (8.6)	Tongue (53.0); Floor of mouth (23.5); Retromolar trigone (23.5)
	Type of surgery(%)	Segmental/ partial/ lingual rim mandibulectomy (94.0); partial maxillectomy (3.0);	Segmental mandibulectomy (100.0)
Mean	age (y)	62.0	0.69
	M/F(%)	77.0/23.0	71.0/29.0 69.0
Dationte (N)	(inclusion period)	35.0 (2012-2014)	17.0 (2016-2018)
	Author	Nieberler ¹²	Cariati ³⁷

 $^{^{\}rm CT} \text{Percentage of patients treated with neoadjuvant chemotherapy.}$ $^{\rm RT} \text{Percentage of patients treated with radiation therapy prior to surgery.}$

Table 2.5. IOARM methods in bone tissue: description and performance.

	IOARM		IOARM				0	IOARM performance	erform	ance		
Author (year)	Method	Sampling tool	Tissue sample	Processing technique (%)	Acc. (%)	Sens. (%)	Spec. (%)	%)	NPV %	IRi (%)	Rev (%)	Reduction IR (%)
Forrest ³²	Specimen-driven	Currette	bone marrow	FS (100.0)	93.8	66.7	66.7 100.0 100.0 92.9 18.8	100.0	92.9	18.8	6.3	66.5
Wysluch ³³	Specimen-driven	Trephine drill technique	cortical bone	FS (100.0)	•	77.0	0.06		•		,	,
Nieberler ³⁵	Specimen-driven	Cytobrush	bone marrow	FS (100.0)	0.96	80.0	0.86	80.0		97.0 11.0 2.2.0	2.2.0	80.0
Namin ³⁶	Specimen-driven	Currette	bone marrow	FS (100.0)	100.0	100.0	100.0 100.0 100.0 100.0 100.0 19.0	100.0	100.0	19.0	0.0	100.0
Nieberler ¹¹	Specimen-driven	Cytobrush	bone marrow	FS (100.0)	99.0	88.9	99.0 88.9 100.0 100.0 98.9	100.0	98.9	8.8	2.9	67.1
Nieberler ¹²	Specimen-driven	Cytobrush	bone marrow	Fixation with cold methanol (59.0); Papanicolau staining (41.0)	94.0	78.0	78.0 100.0 100.0	100.0	92.9			
Bilodeau ³⁴	Defect-driven	Currette	bone marrow; Inf. alveolar nerve	FS (100.0)	89.0	50.0	89.0 50.0 100.0 100.0 87.5	100.0	87.5	•		
Cariati ³⁷	Defect-driven	Currette	bone marrow	FS (100.0)	76.5	33.3	85.7	33.3	85.7	17.6 11.8	1.8	33.0

IOARM Impact on Patient Outcome

Overall Survival

Nieberler et al. demonstrated that at 3 years follow-up OS was higher for patients treated with specimen-driven IOARM compared to the control group (OS: 70% vs 20%, respectively)¹¹. None of the other studies reported on OS.

Disease-Specific Survival

Nieberler et al. showed that at 3 years follow-up disease-free survival was higher for patients treated with specimen-driven IOARM compared to the control group (DSS: 80% vs 40%, respectively)¹¹. None of the other studies reported on DSS. Local Recurrence None of the studies demonstrated the impact of IOARM on LR.

Adjuvant Therapy

Nieberler et al. have also demonstrated that the group of patients treated with specimen-driven IOARM had a slightly lower rate of adjuvant therapy than the control group (52% RT vs 58% RT, respectively)¹¹. None of the other studies reported on the impact of IOARM on adjuvant therapy.

Table 2.6. The non-weighted average IOARM performance parameters for bone tissue: specimendriven vs defect-driven method.

Performance variables (average)	Studies using specimen-driven method (N)	Studies usingdefect-driven method (N)
Accuracy (%)	96.6 (5.0)	82.8 (2.0)
Sensitivity (%)	81.8 (6.0)	41.7 (2.0)
Specificity (%)	98 (6.0)	92.9 (2.0)
¹ PPV (%)	96 (5.0)	66.7 (2.0)
² NPV (%)	96.3 (5.0)	86.6 (2.0)
³ SE (%)	10.6 (5.0)	58.5 (2.0)
⁴ IE (%)	1.7 (5)	7.8 (2)

¹PPV - Positive predictive value.

N represents the number of studies included in the calculation.

DISCUSSION

Surgical treatment of OCSCC patients aims for complete tumor resection with adequate margins, which is the most important prognostic factor. This goal is seldom

²NPV - Negative predictive value.

³SE - Sampling error.

⁴IE - Interpretation error.

achieved, underlining that insufficient intraoperative information is available for optimal control of resection margins. IOARM can provide such information.

Here we review the literature reporting on IOARM in OCSCC surgery. The performance of different IOARM methods in predicting margin-status, and their impact on patient outcome were studied. Despite the pressing need for improving OCSCC surgery, only 18 studies were found that have reported on the performance of IOARM methods; 10 regarding soft tissue resection margins, and 8 regarding bone resection margins.

Of the 10 studies that investigated the performance of IOARM for soft tissue, 6 reported on the specimen-driven method, 3 on the defect-driven method and one on both. In the majority of the specimen-driven studies (4/6), the assessment was performed by gross examination of mucosal and deep margins, followed by FS analysis of locations judged suspicious for inadequate margins^{25, 28, 30, 31}. Mair et al. have assessed whether gross examination alone can be as accurate as gross examination combined with FS analysis and found no statistically significant difference in overall incidence of inadequate margins in both groups²⁸. In the 3 defect-driven IOARM-studies inspection of the wound bed by the surgeon followed by FS analysis of suspicious mucosal and deep margins was performed^{19, 27, 29}.

Patient outcome parameters are negatively affected by inadequate resections^{5, 7, 10}. The studies show that IOARM improves the rate of adequate operations and as a result leads to a decrease in adjuvant therapy. Amit et al. explicitly excluded patients that received adjuvant therapy for other reasons than inadequate resections and showed that of all patients that underwent defect-driven IOARM, 35% required adjuvant therapy while only 8% of all patients that underwent specimen-driven IOARM required adjuvant therapy¹⁹. Only Datta et al. has compared results of adjuvant therapy between patients who received IOARM and those who did not (i.e., control group). The authors demonstrated there was no significant reduction. This result can be explained by the fact that some patients receive adjuvant therapy for other reasons than an inadequate resection (e.g., extra-capsular spread and perineural involvement)³⁰. Future studies should be designed to study the impact of IOARM by also including the need for adjuvant therapy, next to other prognostic parameters (e.g., LR, RR, OS, DSS).

Of the 8 studies that investigated the performance of IOARM for bone tissue, 6 reported on the specimen-driven method and 2 on the defect-driven method. Cytological methods were developed for this. Nieberler et al. demonstrated that the 3 years disease-free survival and overall survival were higher for patients treated with

specimen-driven IOARM compared to the control group (DSS: 80% vs 40%; OS: 70% vs 20%). They have also demonstrated that based on specimen-driven IOARM of bone resection margins a number patients did not need to receive adjuvant radiotherapy¹¹.

When comparing specimen-driven IOARM with defect-driven IOARM we can conclude that for both, soft tissue and bone tissue, the SE and IE are higher for defect-driven IOARM, **Tables 2.3** and **2.6**. Consequently, the performance (e.g., average accuracy, sensitivity, specificity, PPV and NPV) of specimen-driven IOARM is better (**Tables 2.3** and **2.6**). However, it is important to stress that this conclusion is limited by the low number of available studies reporting performance results for defect-driven IOARM.

Another interesting finding was the discrepancy in the reported rate of initially adequate resections for soft tissue specimens. Some recent studies, report adequate resections in only a small minority (15%-26%) of the cases^{5, 7, 10}. Other studies have shown much higher rates of adequate resections, varying from 48.7% to 81.2%^{23, 25-28, 30, 31}.

Differences in oral subsite of the tumor might be a reason for this discrepancy. While in Asian countries, a large proportion of the patients have buccal SCC, in Europe and North-America, patients are more often treated for tongue SCC. It has been shown that tongue SCC is significantly more aggressive (more often poorly differentiated) compared to buccal SCC³⁸. It is harder to achieve a complete resection in poorly differentiated SCC³⁹. Moreover, differences in surgical approach may play a role; i.e., a difference in balancing the need to remove the tumor, while sparing healthy tissue. However, this information is not available in the papers that were studied.

This literature review shows that there is a low number of studies on the performance of IOARM available. This is the main limitation of this study. However, we firmly believe that with upcoming awareness on the need for IOARM there will be enough evidence in the literature to perform a thorough systematic review/meta-analysis, in the near future. Another limitation of this review is that the studies included performed IOARM according to different protocols. Moreover, the outcome was often evaluated according to different criteria. This makes a comparison of the studies unreliable.

Nevertheless, some conclusions can be drawn: IOARM improves patient outcome and the performance of specimen-driven IOARM is superior to the performance of defect-driven IOARM.

There can be no doubt that IOARM reduces the rate of inadequate margins (average IR Rev. for soft tissue: 47.8%; average IR Rev. for bone tissue: 78.4%), but it still shows

low sensitivity (average Sens. for soft tissue: 62.1%; average Sens. for bone tissue: 71.7%) caused by a high SE (average SE for soft tissue: 42.6%; average SE for bone tissue: 24.3%), **Tables 2.3** and **2.6**. The best-performing method; specimen-driven IO-ARM, is logistically demanding and time-consuming. In addition, grossing fresh tissue is counterintuitive to most pathologists for fear of interfering with final pathologic assessment. This will continue to stand in the way of IOARM widespread adoption, despite the significant improvement in OCSCC resection results, unless standard protocols and educational programs exist. At our institute we have a comprehensive IOARM protocol including a relocation protocol.

The development of objective technology is needed to address these practical hurdles and key to facilitating specimen-driven IOARM in OCSCC. An example of such technology is Raman spectroscopy; an optical technique which has been shown to discriminate between OCSCC and surrounding healthy tissue with high sensitivity and specificity (soft and bone tissue)⁴¹⁻⁴³. A dedicated instrument employing a fiber optic needle probe for rapid assessment of resection margins on OCSCC specimen is currently under development⁴⁴.

REFERENCES

- 1. Ferlay J, Colombet M, Soerjomataram I, Mathers C, Parkin DM, Piñeros M, et al. Estimating the global cancer incidence and mortality in 2018: GLOBOCAN sources and methods. Int J Cancer. 2019;144(8):1941@53. doi:10.1002/ijc.31937
- Sharma SM, Prasad BR, Pushparaj S, Poojary D. Accuracy of intraoperative frozen section in assessing margins in oral cancer resection. J Maxillofac Oral Surg. 2009;8(4):357-61. doi:10.1007/s12663-009-0085-9
- van der Ploeg T, Datema F, Baatenburg de Jong R, Steyerberg EW. Prediction of survival with alternative modeling techniques using pseudo values. PLoS One. 2014;9(6):e100234. doi:10.1371/journal.pone.0100234
- Chen SW, Zhang Q, Guo ZM, Chen WK, Liu WW, Chen YF, et al. Trends in clinical features and survival of oral cavity cancer: Fifty years of experience with 3,362 consecutive cases from a single institution. Cancer Manag Res. 2018;10:4523-35. doi:10.2147/CMAR.S171251
- 5. Varvares MA, Poti S, Kenyon B, Christopher K, Walker RJ. Surgical margins and primary site resection in achieving local control in oral cancer resections. Laryngoscope. 2015;125(10):2298-307. doi:10.1002/lary.25397
- Aaboubout Y, ten Hove I, Smits RWH, Hardillo JA, Puppels GJ, Koljenovic S. Specimendriven intraoperative assessment of resection margins should be standard of care for oral cancer patients. Oral Dis. 2020;27(1):111-6. doi:10.1111/odi.13619
- 7. Smits RWH, Koljenović S, Hardillo JA, ten Hove I, Meeuwis CA, Sewnaik A, et al. Resection margins in oral cancer surgery: Room for improvement. Head Neck. 2016;38(S1):E2197-203. doi:10.1002/hed.24075
- 8. Baddour HM, Magliocca KR, Chen AY. The importance of margins in head and neck cancer. J Surg Oncol. 2016;113(3):248-55. doi:10.1002/jso.24134
- 9. Lin A. Radiation therapy for oral cavity and oropharyngeal cancers. Dent Clin North Am. 2018;62(1):99-109. doi:10.1016/j.cden.2017.08.007
- Dik EA, Willems SM, Ipenburg NA, Adriaansens SO, Rosenberg AJWP, van Es RJJ. Resection of early oral squamous cell carcinoma with positive or close margins: Relevance of adjuvant treatment in relation to local recurrence: Margins of 3 mm as safe as 5 mm. Oral Oncol. 2014;50(6):611-5. doi:10.1016/j.oraloncology.2014.02.014
- Nieberler M, Häußler P, Kesting MR, Kolk A, Deppe H, Weirich G, et al. Clinical Impact of Intraoperative Cytological Assessment of Bone Resection Margins in Patients with Head and Neck Carcinoma. Ann Surg Oncol. 2016;23(11):3579-3586. doi:10.1245/s10434-016-5208-1
- 12. Nieberler M, Häußler P, Kesting MR, Kolk A, Stimmer H, Nentwig K, et al. Intraoperative cell isolation for a cytological assessment of bone resection margins in patients with head and neck cancer. Br J Oral Maxillofac Surg. 2017;55(5):510-516. doi:10.1016/j. bjoms.2017.02.006
- Smits RWH, ten Hove I, Dronkers EAC, Bakker Schut TC, Mast H, Baatenburg de Jong RJ, et al. Evaluation of bone resection margins of segmental mandibulectomy for oral squamous cell carcinoma. Int J Oral Maxillofac Surg. 2018;47(8):959-964. doi:10.1016/j. ijom.2018.03.006

- 14. Murphy J, Isaiah A, Wolf JS, Lubek JE. The influence of intraoperative frozen section analysis in patients with total or extended maxillectomy. Oral Surg Oral Med Oral Pathol Oral Radiol. 2016;121(1):17-21. doi:10.1016/j.oooo.2015.07.014
- 15. Petrovic I, Montero PH, Migliacci JC, Palmer FL, Ganly I, Patel SG, et al. Influence of bone invasion on outcomes after marginal mandibulectomy in squamous cell carcinoma of the oral cavity. J Craniomaxillofac Surg. 2017;45(2):252-257. doi:10.1016/j.jcms.2016.11.017
- Kraeima J, Dorgelo B, Gulbitti HA, Steenbakkers RJHM, Schepman KP, Roodenburg JLN, et al. Multi-modality 3D mandibular resection planning in head and neck cancer using CT and MRI data fusion: A clinical series. Oral Oncol. 2018;81:22-28. doi:10.1016/j.oraloncology.2018.03.013
- 17. Meier JD, Oliver DA, Varvares MA. Surgical margin determination in head and neck oncology: Current clinical practice. The results of an International American Head and Neck Society member survey. Head Neck. 2005;27(11):952-958. doi:10.1002/hed.20269
- Maxwell JH, Thompson LDR, Brandwein-Gensler MS, Weiss BG, Canis M, Purgina B, et al. Early Oral Tongue Squamous Cell Carcinoma. JAMA Otolaryngol Head Neck Surg. 2015;141(12):1104. doi:10.1001/jamaoto.2015.1351
- Amit M, Na'ara S, Leider-Trejo L, Akrish S, Cohen JT, Billan S, et al. Improving the rate of negative margins after surgery for oral cavity squamous cell carcinoma: A prospective randomized controlled study. Head Neck. 2016;38(S1):E1803-E1809. doi:10.1002/ hed.24320
- Tirelli G, Hinni ML, Fernández-Fernández MM, Bussani R, Gatto A, Bonini P, et al. Frozen sections and complete resection in oral cancer surgery. Oral Dis. 2019;25(5):1309-1317. doi:10.1111/odi.13101
- 21. Kain JJ, Birkeland AC, Udayakumar N, Morlandt AB, Stevens TM, Carroll WR, et al. Surgical margins in oral cavity squamous cell carcinoma: Current practices and future directions. Laryngoscope. 2020;130(1):128-138. doi:10.1002/lary.27943
- 22. Lydiatt WM, Patel SG, O'Sullivan B, Brandwein MS, Ridge JA, Migliacci JC, et al. Head and neck cancers-major changes in the American Joint Committee on cancer eighth edition cancer staging manual. CA Cancer J Clin. 2017;67(2):122-137. doi:10.3322/caac.21389
- 23. Ord RA, Aisner S. Accuracy of frozen sections in assessing margins in oral cancer resection. J Oral Maxillofac Surg. 1997;55(7):663-669. doi:10.1016/S0278-2391(97)90570-X
- 24. Pathak KA, Nason RW, Penner C, Viallet NR, Sutherland D, Kerr PD. Impact of use of frozen section assessment of operative margins on survival in oral cancer. Oral Surg Oral Med Oral Pathol Oral Radiol Endodontol. 2009;107(2):235-239. doi:10.1016/j.tripleo.2008.09.028
- 25. Chaturvedi P, Datta S, Nair S, Nair D, Pawar P, Vaishampayan S, et al. Gross examination by the surgeon as an alternative to frozen section for assessment of adequacy of surgical margin in head and neck squamous cell carcinoma. Head Neck. 2014;36(4):557-563. doi:10.1002/hed.23313
- 26. Ettl T, El-Gindi A, Hautmann M, Gosau M, Weber F, Rohrmeier C, et al. Positive frozen section margins predict local recurrence in R0-resected squamous cell carcinoma of the head and neck. Oral Oncol. 2016;55:17-23. doi:10.1016/j.oraloncology.2016.02.012
- 27. Buchakjian MR, Tasche KK, Robinson RA, Pagedar NA, Sperry SM. Association of main specimen and tumor bed margin status with local recurrence and survival in oral cancer

- surgery. JAMA Otolaryngol Head Neck Surg. 2016;142(12):1191-1198. doi:10.1001/jamaoto.2016.2329
- 28. Mair M, Nair D, Nair S, Dutta S, Garg A, Malik A, et al. Intraoperative gross examination vs frozen section for achievement of adequate margin in oral cancer surgery. Oral Surg Oral Med Oral Pathol Oral Radiol. 2017;123(5):544-549. doi:10.1016/j.oooo.2016.11.018
- 29. Abbas SA, Ikram M, Tariq MU, Raheem A, Saeed J. Accuracy of frozen sections in oral cancer resections, an experience of a tertiary care hospital. J Pak Med Assoc. 2017;67(5):806-809.
- 30. Datta S, Mishra A, Chaturvedi P, Bal M, Nair D, More Y, et al. Frozen section is not cost beneficial for the assessment of margins in oral cancer. Indian J Cancer. 2019;56(1):19-23. doi:10.4103/ijc.IJC_41_18
- 31. Chaturvedi P, Singh B, Nair S, Nair D, Kane SV, D'cruz A, et al. Utility of frozen section in assessment of margins and neck node metastases in patients undergoing surgery for carcinoma of the tongue. J Cancer Res Ther. 2012;8(Suppl 1):S100-5. doi:10.4103/0973-1482.92222
- 32. Arick Forrest L, Schuller DE, Sullivan MJ, Lucas JG. Rapid analysis of mandibular margins. Laryngoscope. 1995;105(5):475-477. doi:10.1288/00005537-199505000-00004
- 33. Wysluch A, Stricker I, Hölzle F, Wolff K-D, Maurer P. Intraoperative evaluation of bone margins with frozen-section analysis and trephine drill extraction technique: A preliminary study. Head Neck. 2010;32(11):1473-1478. doi:10.1002/hed.21350
- 34. Bilodeau EA, Chiosea S. Oral Squamous Cell Carcinoma with Mandibular Bone Invasion: Intraoperative Evaluation of Bone Margins by Routine Frozen Section. Head Neck Pathol. 2011;5(3):216-220. doi:10.1007/s12105-011-0264-0
- 35. Nieberler M, Häußler P, Drecoll E, Stoeckelhuber M, Deppe H, Hölzle F, et al. Evaluation of intraoperative cytological assessment of bone resection margins in patients with oral squamous cell carcinoma. Cancer Cytopathol. 2014;122(9):646-656. doi:10.1002/cncy.21428
- 36. Namin AW, Bruggers SD, Panuganti BA, Christopher KM, Walker RJ, Varvares MA. Efficacy of bone marrow cytologic evaluations in detecting occult cancellous invasion. Laryngoscope. 2015;125(5):E173-E179. doi:10.1002/lary.25063
- 37. Cariati P, Cabello Serrano A, Fernandez Solis J, Ferrari S, Torné Poyatos P, Martinez Lara I. Intraoperative cytological examination of bone medullary. A useful technique to predict the extension of bone invasion in segmental mandibulectomy. Am J Otolaryngol - Head Neck Med Surg. 2019;40(5):743-746. doi:10.1016/j.amjoto.2019.07.005
- 38. Nair S, Singh B, Pawar PV, Datta S, Nair D, Kane S, et al. Squamous cell carcinoma of tongue and buccal mucosa: clinico-pathologically different entities. Eur Arch Oto-Rhino-Laryngol. 2016;273(11):3921-3928. doi:10.1007/s00405-016-4051-0
- 39. Brinkman JN, Hajder E, Van Der Holt B, Den Bakker MA, Hovius SER, Mureau MAM. The effect of differentiation grade of cutaneous squamous cell carcinoma on excision margins, local recurrence, metastasis, and patient survival: A retrospective follow-up study. Ann Plast Surg. 2015;75(3):323-326. doi:10.1097/SAP.000000000000110

- 40. van Lanschot CGF, Mast H, Hardillo JA, Monserez D, ten Hove I, Barroso EM, et al. Relocation of inadequate resection margins in the wound bed during oral cavity oncological surgery: A feasibility study. Head Neck. 2019;41(7):2159-2166. doi:10.1002/hed.25690
- 41. Barroso EM, Smits RWH, Schut TCB, Ten Hove I, Hardillo JA, Wolvius EB, et al. Discrimination between Oral Cancer and Healthy Tissue Based on Water Content Determined by Raman Spectroscopy. Anal Chem. 2015;87(4):2419-2426. doi:10.1021/ac504362y
- 42. Barroso EM, Smits RWH, Van Lanschot CGF, Caspers PJ, Ten Hove I, Mast H, et al. Water concentration analysis by Raman spectroscopy to determine the location of the tumor border in oral cancer surgery. Cancer Res. 2016;76(20):5945-5953. doi:10.1158/0008-5472.CAN-16-1227
- 43. Barroso EM, ten Hove I, Bakker Schut TC, Mast H, van Lanschot CGF, Smits RWH, et al. Raman spectroscopy for assessment of bone resection margins in mandibulectomy for oral cavity squamous cell carcinoma. Eur J Cancer. 2018;92:77-87. doi:10.1016/j.ejca.2018.01.068
- 44. Puppels GJ, Barroso EML, Aaboubout Y, Nunes Soares MR, Artyushenko VG, Bocharnikov A, et al. Intra-operative assessment of tumor resection margins by Raman spectroscopy to guide oral cancer surgery (conference presentation). In: Petrich W, Huang Z, editors. Biomedical Vibrational Spectroscopy 2020. Advances in Research and Industry [Internet]. San Francisco (CA): SPIE; 2020. p. 1. Available from: https://www.spiedigitallibrary.org/conference-proceedings-of-spie/11252/1125206/



3 INTRAOPERATIVE ASSESSMENT OF RESECTION MARGINS IN ORAL CAVITY CANCER: THIS IS THE WAY

Yassine Aaboubout, Elisa M Barroso, Mahesh Algoe, Patricia C Ewing-Graham, Ivo Ten Hove, Hetty Mast, José A Hardillo, Aniel Sewnaik, Dominiek A Monserez, Stijn Keereweer, Brend P Jonker, Cornelia G F van Lanschot, Roeland W H Smits, Maria R Nunes Soares, Lars Ottevanger, Sanne E Matlung, Paul A Seegers, Vera van Dis, Robert M Verdijk, Eppo B Wolvius, Peter J Caspers, Tom C Bakker Schut, Robert J Baatenburg de Jong, Gerwin J Puppels, Senada Koljenović

J Vis Exp. 2021 May 10;(171).



ABSTRACT

The goal of head and neck oncological surgery is complete tumor resection with adequate resection margins while preserving acceptable function and appearance. For oral cavity squamous cell carcinoma (OCSCC), different studies showed that only 15%-26% of all resections are adequate. A major reason for the low number of adequate resections is the lack of information during surgery; the margin status is only available after the final histopathologic assessment, days after surgery.

The surgeons and pathologists at the Erasmus MC, University Medical Center in Rotterdam started the implementation of specimen-driven intraoperative assessment of resection margins (IOARM) in 2013, which became the standard of care in 2015. This method enables the surgeon to turn an inadequate resection into an adequate resection by performing an additional resection during the initial surgery. Intraoperative assessment is supported by a relocation method procedure that allows accurate identification of inadequate margins (found on the specimen) in the wound bed.

The implementation of this protocol resulted in an improvement of adequate resections from 15%-40%. However, the specimen-driven IOARM is not widely adopted because grossing fresh tissue is counter-intuitive for pathologists. The fear exists that grossing fresh tissue will deteriorate the anatomical orientation, shape, and size of the specimen and therefore will affect the final histopathologic assessment. These possible negative effects are countered by the described protocol. Here, the protocol for specimen-driven IOARM is presented in detail, as performed at the institute.

VIDEO QR-CODE



INTRODUCTION

Every year, around 350,000 new patients are diagnosed worldwide with cancer in the oral cavity; 90% of cases are squamous cell carcinoma¹. The mortality rate is 175,000 worldwide per year and the 5-year survival is 50% to $64.8\%^{1-4}$.

The primary treatment of oral cavity squamous cell carcinoma (OCSCC) is surgery⁵. The goal of the surgery is the complete removal of the tumor with adequate margins, according to the Royal College of Pathologists⁶. Margins >5 mm (clear) are regarded as adequate, whereas margins from 0-5 mm are regarded as inadequate.

Adequate resection margins lead to higher survival and a reduction in local recurrencerates of OCSCC⁷⁻⁹. Tumor resections with inadequate margins result in the need for adjuvant therapy (postoperative radiotherapy and/or chemotherapy). This brings an additional burden for the patient, increasing morbidity and reducing the quality of life¹⁰. The resection margin is the only oncological prognostic factor that the surgeon and pathologist can influence.

Recent reports have shown that adequate resections are only achieved in 15%-26% of cases^{7,8,11}. These poor results are caused by the complex anatomy of the oral cavity and the lack of intraoperative guidance. During surgery, the surgeon can only rely on inspection, palpation, and preoperative imaging.

The final margin status follows only several days after the operation. If an inadequate margin is encountered at the final pathologic assessment, a second operation is usually not an option, because the wound bed reconstruction has usually healed by that time. Moreover, a second operation is mostly not effective, because the relocation of the inadequate margin is even more difficult in the postoperative setting.

To overcome the lack of intraoperative information about margin status, specimendriven intraoperative assessment of resection margins (IOARM) was implemented in 20139. It became the standard of care in the institute in 2015. Described here is the IOARM method in detail to enable colleagues at other institutes to implement this protocol.

PROTOCOL

This study was approved by the institutional Medical Ethics Committee (MEC-2015-150).

NOTE: All the patient and personnel information in the figures or examples are fictional (i.e., XXXXX and YYYYY).

1. Before surgery

- 1. Surgery department: Request for IOARM during the planning of surgery.
- 2. Pathology department: Ensure logistics/equipment (see Table of Materials) and the availability of personnel (pathologist/pathology resident and assistant).

2. During surgery

- 1. Operation room (OR)
 - 1. Ensure that all involved personnel are familiar with the relocation proto-
 - 2. Follow the relocation protocol.
 - 3. Submerge the tags in chlorhexidine for at least 30 min before the start of the surgery.
 - 4. Place the tags paired on either side of the intended line of resection (both superficial and deep), so that one tag is on the resection specimen and the other remains at the corresponding spot in the wound bed (Figure 3.1A) as described by Van Lanschot et al.¹².
 - 5. Cut between each pair of tags.
 - 6. Remove the specimen with the tumor (one tag from each pair remains in the wound bed, Figure 3.1B).
 - 7. Fill out the pathology request form with a clear indication of the anatomical location of the tags (e.g., tag 1 = anterior, tag 2 = superior).
 - 8. Record the surgical procedure-related defects of the specimen and their location in relation to the tags, on the pathology request form.

NOTE: Procedure-related defects create false resection surfaces and can lead to incorrect allocation of inadequate margins during both IOARM and final pathology.

9. Bring the specimen to the pathology department.

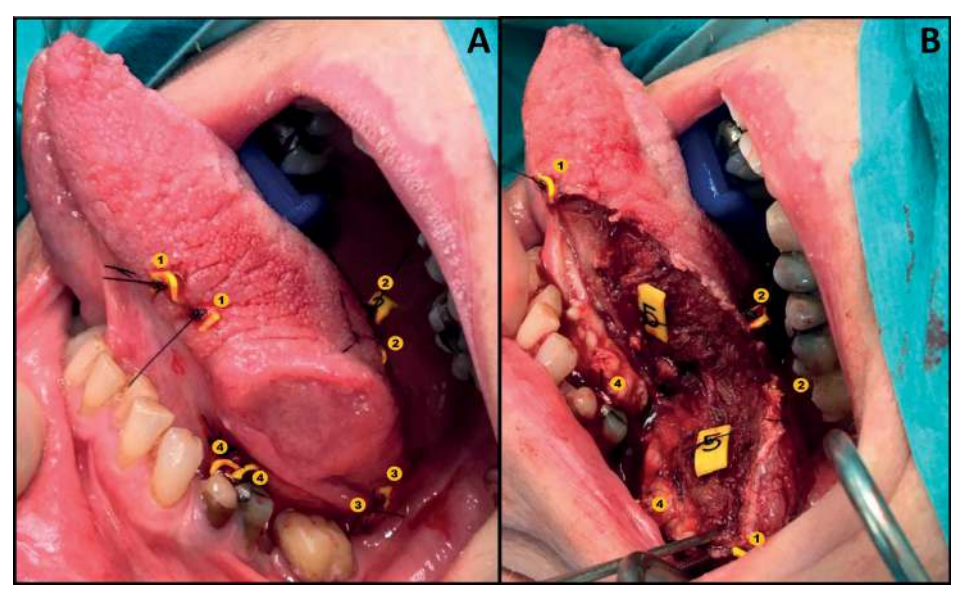


Figure 3.1. Illustration of the relocation protocol. (A) Application of tags in a pair-wise manner. (B) Wound bed and specimen both with one tag of each pair.

- 2. IOARM Grossing room (GR), pathology department
 - 1. Rinse the specimen with water and gently pat it dry with gauze or paper.

NOTE: Register every next step with photographs and store them in the Electronic Patient File (EPF).

- 2. Record the general information (date, patient id, pathology number, surgeon, pathologist, type of specimen, and tags used) on the anatomical template.
- 3. Indicate the locations of the tags on the anatomical template (Figure 3.2).
- 4. Place the specimen on the anatomical template.
- 5. Ink the resection surface according to standard protocol (e.g., superior blue and inferior green).
- 6. Inspect the specimen visually and by palpation (pathologist and surgeon).
- 7. Indicate the location of any suspicious region (i.e., margin <5 mm) on the anatomical template and relate it to the numbered tags (section Result of IOARM, Figure 3.2).
- 8. Perform an incision perpendicular to the resection surface at the suspicious region (Figure 3.3A). Depending on the size of the specimen and/or suspicious regions, make one or more incisions with a distance of about 5 mm. In case of more than one incision, number the incisions as IOA1, IOA2, etc.

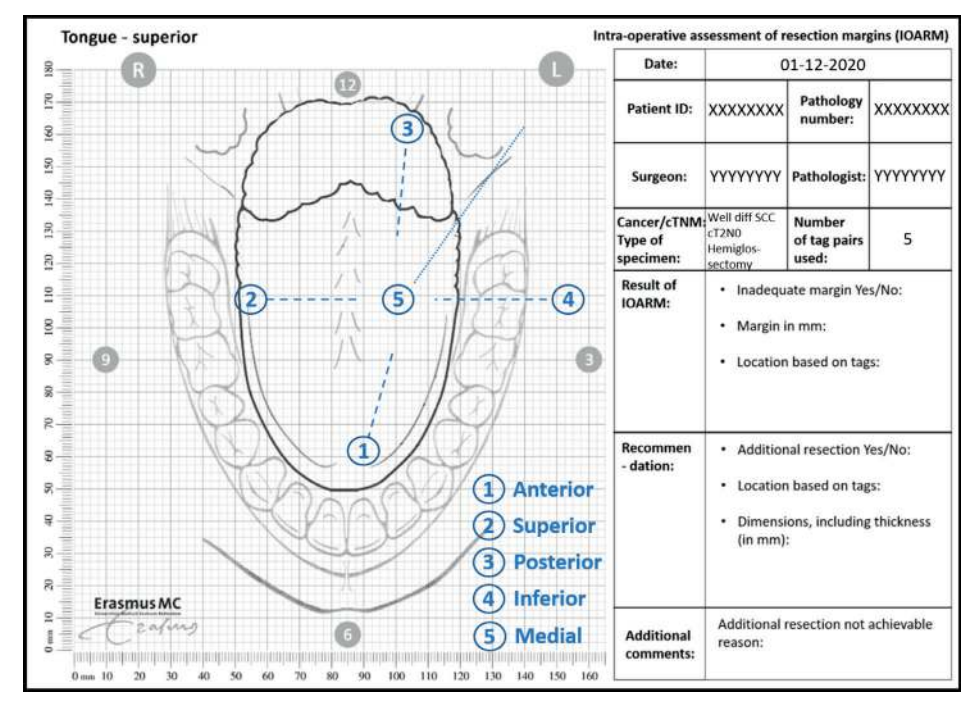


Figure 3.2. Example of anatomical template for IOARM.

 Measure the margins (i.e., the distance between resection surface and tumor border) on the tissue sections (Figure 3.3B) and record the exact values in mm on the anatomical template (section Result of IOARM, Figure 3.3C).

NOTE: If the tumor border is macroscopically not distinguishable (e.g., the tumor cannot be distinguished from surrounding fibrotic or salivary gland tissue), microscopic analysis by frozen section is indicated.

- 10. Proceed with the completion of the operation, step 2.2.19. If an adequate margin is detected (i.e., additional resection is not needed).
- 11. Indicate the exact location based on the tags if an inadequate margin is detected and record it on the template. Proceed with an additional resection if surgically/technically achievable, step 2.2.13.
- 12. Annotate the reason on the template, if an additional resection is not achievable (section Additional comments, Figure 3.2).

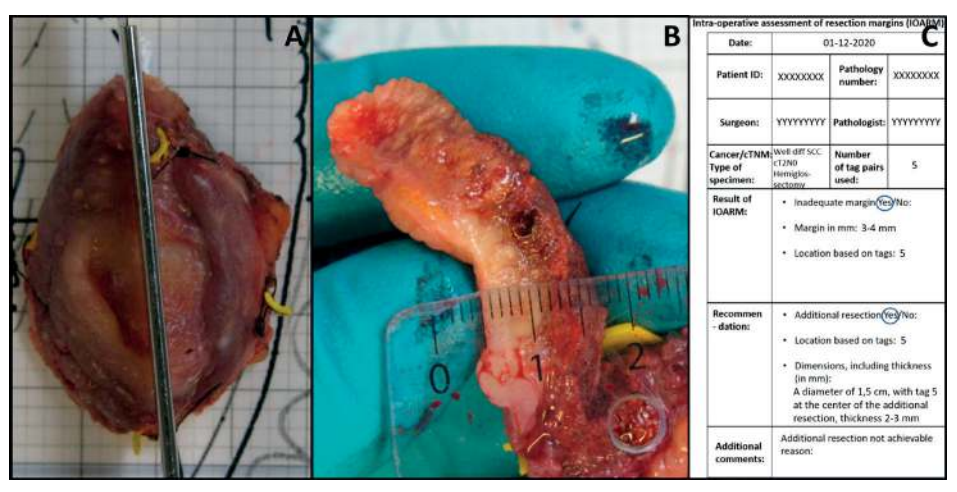


Figure 3.3. Illustration of IOARM. (A) Perpendicular incision performed after identification of suspicious region by palpation. (B) The margin is measured. (C) The result of IOARM and the recommendation are recorded.

13. Recommend (pathologist/surgeon) the additional resection based on the exact location and indicate the thickness needed to achieve an adequate resection (Figure 3.3C).

NOTE: If the inadequate margin concerns a positive margin, a minimal thickness of 6 mm should be recommended for the additional resection.

- 14. Keep (pathologist) the main resection specimen in the refrigerator until the additional resection is received.
- 15. Relocate (surgeon) the area of additional resection in relation to the tags, in the wound bed, based on the record of IOARM (Figure 3.3C).
- 16. Perform the additional resection.
- 17. Send the additional resection to the GR.
- 18. Verify (pathologist) the accuracy of the additional resection regarding its location (based on tags) and its size.

NOTE: The above steps are applicable in the case of a close margin. In the case of a positive margin, an IOARM of the additional resection is necessary (pathologist). The surgeon waits for the result of the second IOARM before completing the operation.

- 19. Remove (surgeon) the remaining tags from the wound bed and complete the operation.
- 20. Copy (pathologist) all data from the anatomical template to the EPF.

3. After IOARM - Grossing room (GR), pathology department

NOTE: To preserve the anatomical orientation and shape of the specimen the following steps are performed.

 Reassemble the specimen by the correct orientation of all tissue sections (cross-sections and the polar ends) based on the tags and the photographs recorded during IOARM.

NOTE: Cross-sections are in the middle of the specimen and the polar ends are the outer parts of the specimen.

- 2. Cut the pieces of cork slightly larger than the tissue sections.
- 3. Place each tissue section on a piece of cork.
- 4. Draw a line on the cork around the tissue section with a permanent marker and take a photograph (Figure 3.4A).
- 5. Place another piece of cork on top of all tissue sections except the polar ends (Figure 3.4B).
- Keep the upper and lower cork together, with the tissue section in between, by placing pins through both corks next to the edge of the tissue section, but not through the tissue section (Figure 3.4B).
- 7. Place the polar ends on a separate piece of cork (Figure 3.4A).
- 8. Keep the polar ends attached to the cork by obliquely placing pins over the tissue and piercing the cork just beside the edge of the tissue (**Figure 3.4B**).

CAUTION: Do not puncture the specimen with the pins.

- 9. Reassemble the whole specimen: put all the tissue sections including the polar ends together in the correct anatomical orientation.
- 10. Keep all the tissue sections together by puncturing the adjacent corks (Figure 3.4C).
- 11. Position the specimen with the correct orientation on the anatomical template and take a photograph.
- 12. Place the specimen in formaldehyde solution (formalin 4%).

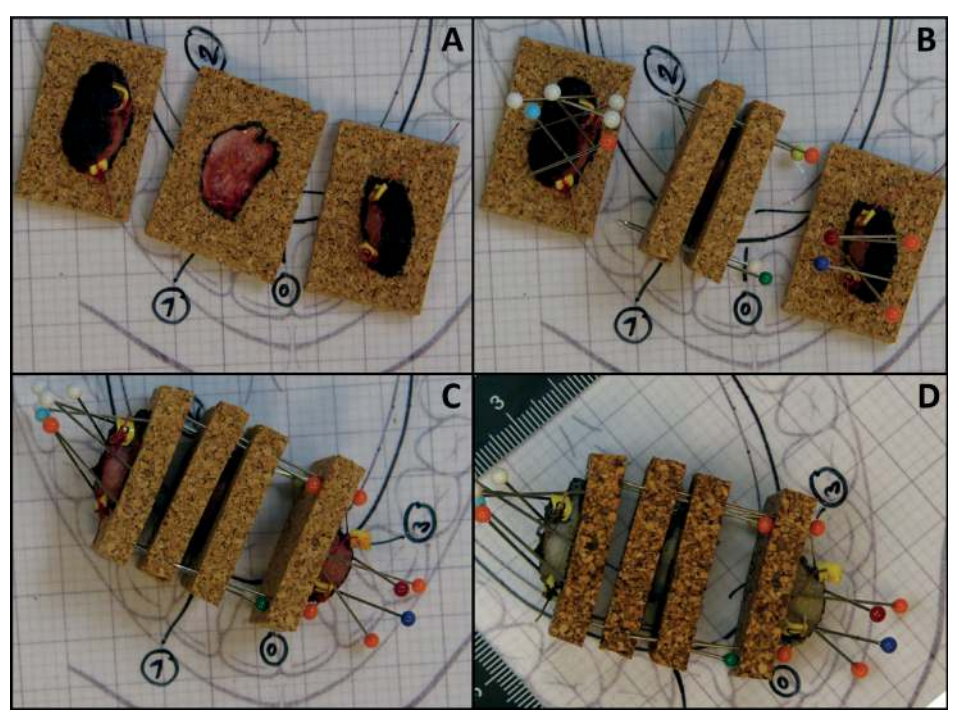


Figure 3.4. Illustration of the method to preserve the anatomical orientation and shape of tissue sections. (A) Tissue sections are placed on a piece of cork with a line drawn on the cork around the tissue section with a permanent marker. (B) Pins are obliquely placed over the polar ends and another piece of cork is placed over the tissue section. (C) Illustration of a reassembled fresh specimen kept together with pins that puncture the adjacent corks. (D) Illustration of a reassembled fixed specimen kept together with pins that puncture adjacent corks.

NOTE: For proper fixation, pieces of paper can be placed on top of the specimen to keep it submerged in formalin.

- 13. Make a clear and visible warning note on the container with the specimen (e.g., caution needles/pins), to avoid accidents.
- 14. Store the container with the specimen for further processing, according to the standard pathology protocol.

4. Grossing of the fixed specimen after IOARM

NOTE: After formalin fixation, the specimen should be grossed preferably by the pathologist/resident/assistant, who performed the IOARM.

CAUTION: Be careful with the needles/pins when removing the specimen from the container.

1. Follow the institutional grossing protocol.

NOTE: Take additional measures to ensure the correct orientation and to facilitate the comparison of the margin status between IOARM and final pathologic assessment.

- 1. Consult the pictures of the IOARM.
- 2. Take the specimen out of the container.
- 3. Check whether all the tissue sections are present.
- 4. Position the specimen with the correct orientation on the anatomical template and take a photograph (Figure 3.4D).
- 5. Remove the pins.
- 6. Separate the individual tissue sections with corresponding cork.
- 7. Take photographs of each tissue section with their corresponding corks, focusing on the lines that were drawn around the tissue section to assess possible shrinkage of tissue after fixation (Figure 3.5).
- 8. Detach all tissue sections systematically from the cork (e.g., start from anterior to posterior or left to right).
- 9. Gross the IOARM-tissue sections to the standard final tissue sections (2-3 mm thick).
- 10. Place all final tissue sections, in the correct anatomical orientation (e.g., from anterior to posterior), on a paper on the grossing table.
- 11. Number all the final tissue sections consecutively with a permanent marker on the paper (Figure 3.6).
- 12. Annotate the location of IOARM with a permanent marker (Figure 3.6).
- 13. Take photographs, including all final tissue sections and store them in the EPF (Figure 3.6).
- 14. Select the relevant final tissue sections and IOARM sections to be further processed for final pathologic assessment.

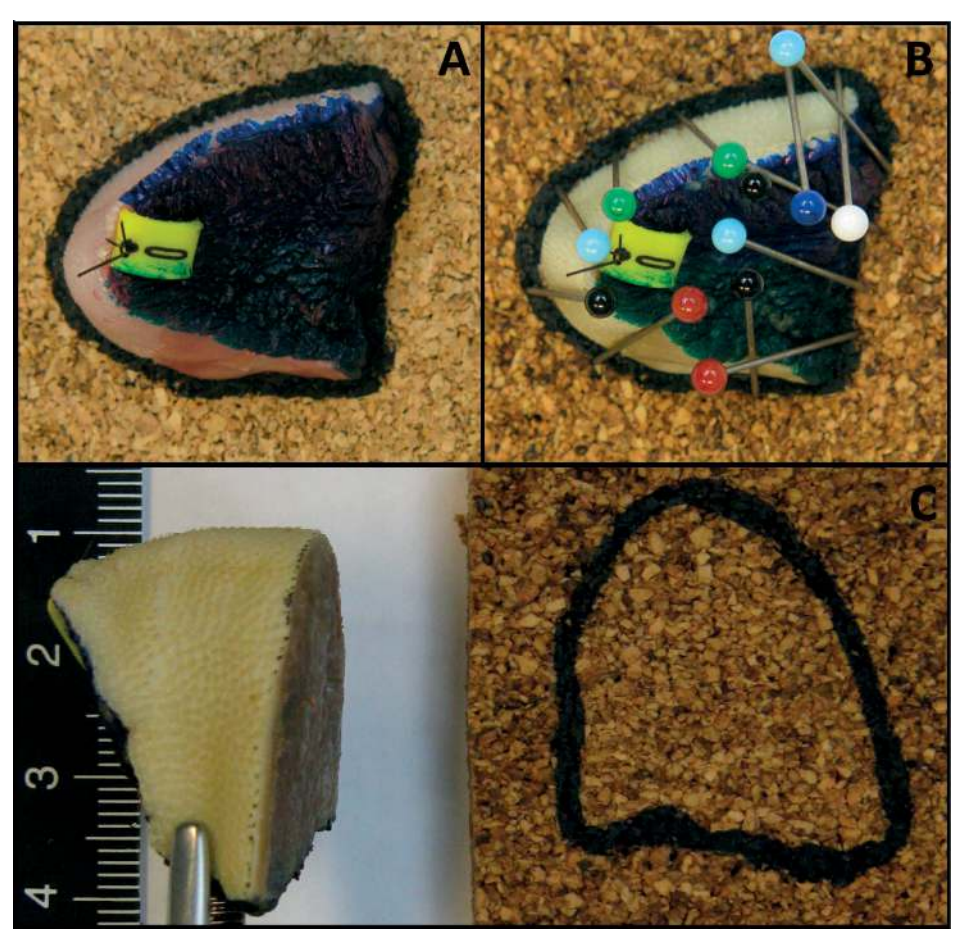


Figure 3.5. Illustration of a polar end with the cut surface facing the cork, held against the cork by tilted pins. (A) Fresh specimen. (B) After fixation. (C) The cut surface of the polar end is flat after fixation.

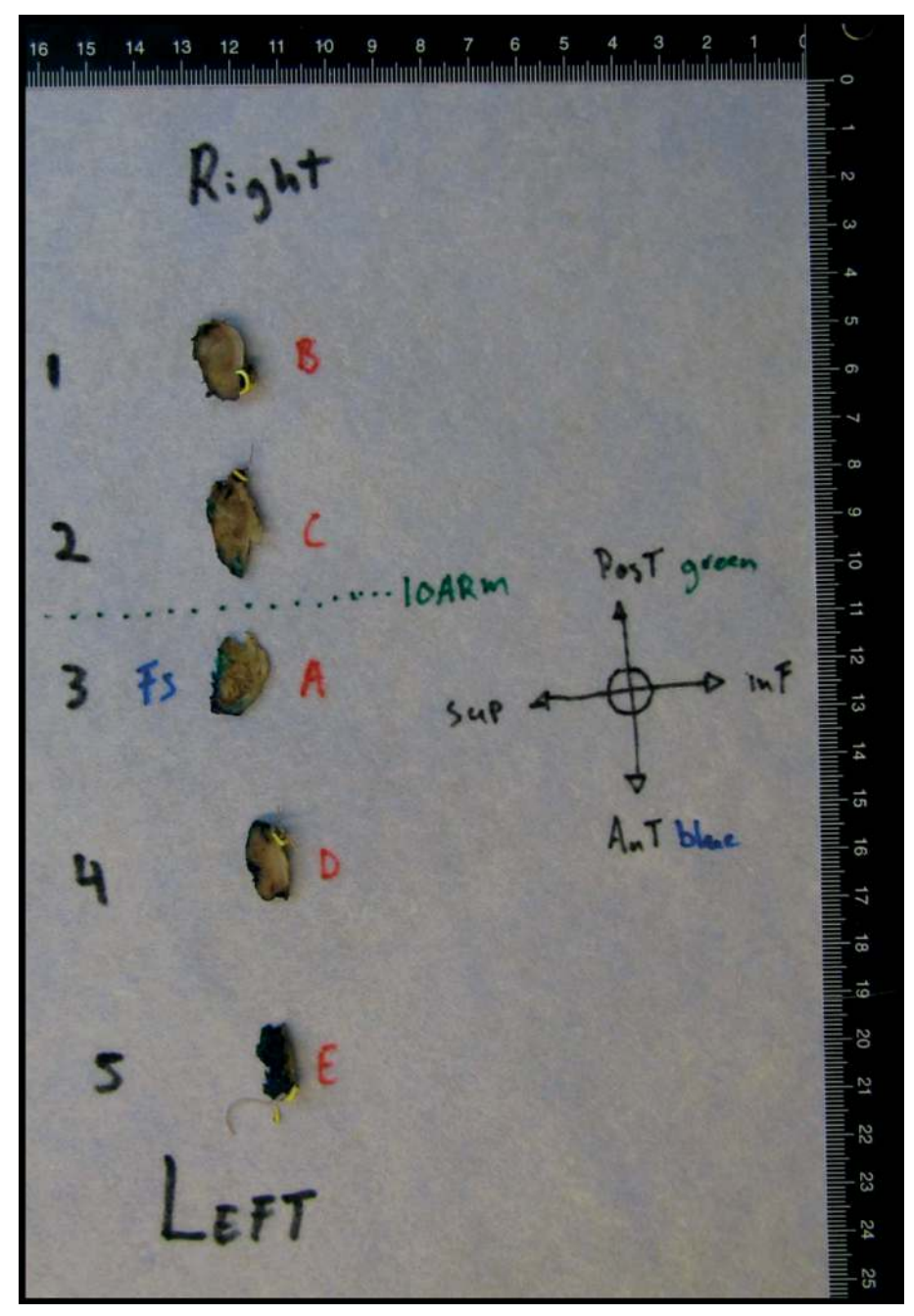


Figure 3.6. Grossed specimen with the location of the IOARM marked. Corresponding numbers 1-5 refer to tissue sections from left to right. A-E corresponds with tissue sections included for histopathologic evaluation. Note that the remaining piece of tissue that was evaluated by frozen section (FS) is indicated to enable direct comparison with the permanent HE-stained section.

- 5. The final pathologic assessment Impact of IOARM on final margin status
- 1. Follow the local standardized protocol. The protocol followed here is the PALGA (Pathologisch-Anatomisch Landelijk Geautomatiseerd Archief, the nationwide network and registry of histo- and cytopathology in the Netherlands) national Head-Neck protocol for the final standardized structured pathology report.

NOTE: This protocol is based on the up-to-date standards of the American Joint Committee on Cancer (AJCC), Union for International Cancer Control (UICC), and the World Health Organisation (WHO).

- 1. Assess all the margins in millimeters, including mucosa, submucosa, and bone.
- 2. If an inadequate margin is found, annotate its extent (e.g., submucosal margin anterior is 3.5 mm, extending over a trajectory of 6 mm).
- 3. Assess the presence of dysplasia and its grade for mucosal resection margins.
- 4. Indicate the final margin by adding the dimensions of the additional resection (if performed) to the margin measured on the main specimen.
- 5. Record the unique pathology number of the additional resection in the pathology report of the main specimen (e.g., Margins: anterior 6 mm, posterior 8 mm, superior 6 mm (including 3mm of the additional resection, H20-2021), inferior 7 mm, medial 5.3 mm).
- 6. Verify the margins found during IOARM.
- 7. Annotate the result of this verification (e.g., NB Margins found during the intraoperative assessment are in concordance with margins based on the final pathology).

NOTE: The time needed for IOARM should be limited in order to not interfere with the surgical workflow. At the institute, the IOARM takes about 10 min. The surgeon and pathologist perform the IOARM together. For the relocation method (placing the tags during surgery) an additional time of 5 min is needed. This will differ for each institute depending on the logistics.

REPRESENTATIVE RESULTS

Example of IOARM resulting in an adequate resection

The patient presents with a cT2N0M0 SCC of the left side of the tongue with no medical history. The patient undergoes hemiglossectomy supported by IOARM. The specimen is inspected and palpated; the mucosal margins are measured as >5 mm. One area in the submucosal resection surface is suspicious for an inadequate margin, located around tag 5. The submucosal margin is 3-4 mm at tag 5. All the information is recorded on the template and copied to the EPF (Figure 3.7A).

Date:	0	1-12-2020		В	Date:	0	1-12-2020	
Patient ID:	xxxxxxx	Pathology number:	xxxxxxx		Patient ID:	xxxxxxx	Pathology number:	xxxxxxx
Surgeon:	YYYYYYYY	Pathologist:	YYYYYYYY		Surgeon:	YYYYYYYY	Pathologist:	YYYYYYYY
Cancer/cTNM: Type of specimen:	Mod diff SCC cT2N0M0 Hemiglos- sectomy	Number of tag pairs used:	5		Cancer/cTNM Type of specimen:	Well diff SCC cT1N0M0 Hemiglos- sectomy	Number of tag pairs used:	5
Result of IOARM:	Margin i	ate margin(e n mm: 3-4 m n based on tag	m		Result of IOARM:	Margin	ate margin Ye in mm: >5 mr n based on tag	m
Recommen - dation:	 Location Dimensi (in mm) A diame at the ce 	nal resection on tag ons, including teter of 1,5 cm enter of the a n, thickness 2	s: 5 thickness , with tag 5 dditional		Recommen - dation:	Location	nal resection Y n based on tag ions, including :	ıs:
Additional comments:	Additional reason:	resection not	achievable		Additional comments:	Additional reason:	resection not	achievable

Figure 3.7. Examples of two different IOARMs recorded on the anatomical template. (A) IOARM resulting in an adequate resection. (B) IOARM not resulting in an adequate resection.

The surgeon returns to the OR and performs the additional resection. The pathologist verifies the accuracy and dimensions, including the thickness of the additional resection.

The final pathology report shows the presence of moderately differentiated pT2 squamous cell carcinoma on the left side of tongue. The tumor diameter is 2.5 cm and the depth of invasion is 6.0 mm. The worst pattern of invasion (WPOI) is category 3. Perineural invasion (PNI) is not present and the lymphovascular invasion (LVI) is present. The minimal margins (mucosal and submucosal) at the inferior, superior, anterior, and posterior location are 5.8 mm (including additional resection (PA number: XXXXXX) of 3 mm thickness), 6.2 mm (including additional resection (PA number: XXXXXX) of 3 mm thickness), 5.2 mm, and 5.5 mm, respectively (Table 3.1). IOARM is in concordance with final pathology.

Table 3.1. Example of resection margins during IOARM resulting in an adequate resection at final pathology, after additional resection.

Margins (m	m)		
Location	Based on IOARM	After additional resection	Based on Final pathology
Inferior	3-4	6-7	5.8
Superior	3-4	6-7	6.2
Anterior	>5		5.2
Posterior	>5		5.5

Example of IOARM not resulting in an adequate resection

The patient presents with a cT1NOMO SCC of the right side of the tongue with no medical history. The patient underwent a resection supported by IOARM. The surgeon takes the specimen to the pathologist at the pathology department. The mucosa is visually inspected, and the mucosal margins are measured with a transparent ruler, all mucosal margins are >5 mm. The submucosal margins are visually inspected and palpated and all margins seem >5 mm. A suspicious area is found at tag 1 (anterior resection surface) and tag 3 (posterior resection surface). A grossing knife is placed perpendicular to the resection surface from anterior to posterior (tag 1 to tag 3) and an incision is made. The pathologist measures the margin on the cross-section and the margins are >5 mm. All the information is recorded on the template and copied to the EPF (Figure 3.7B).

The final pathology report shows a well-differentiated pT1 squamous cell carcinoma on the right side of the tongue. The diameter of the tumor is 1.8 cm, and the depth of invasion is 3.8 mm. The worst pattern of invasion (WPOI) is category 2. Perineural invasion (PNI), lymphovascular invasion (LVI), and dysplasia are not present. The minimal margins (mucosal and submucosal) at the inferior, superior, anterior, and

posterior locations are 4.0 mm, 6.1 mm, 6.4 mm, and 7.8 mm, respectively (**Table 3.2**). IOARM is not in concordance with final pathology, margin inferior was missed.

Table 3.2. Example of resection margins during IOARM not resulting in an adequate resection at final pathology.

Margins (n	nm)		
Location	Based on IOARM	After additional resection	Based on Final pathology
Inferior	>5		4.0
Superior	>5	Not recommend all margins > E mm	6.1
Anterior	6	Not recommend all margins > 5 mm	6.4
Posterior	8		7.8

DISCUSSION

The goal of surgical treatment of OCSCC patients is the complete removal of the tumor with adequate margins. This is too often not achieved, which inspired to design an adjusted approach to oral cancer surgery with a focus on intraoperative assessment of resection margins. Aside from resection margins, other adverse tumor factors such as the pattern of invasion, perineural invasion, and lymphovascular invasion also affect the local recurrence. However, of all adverse tumor factors, surgeons and pathologists can only influence the resection margins^{7,8,11}.

The specimen-driven IOARM method was implemented in 2013; this was eventually supported by the evidence that specimen-driven IOARM is superior to defect-driven IOARM^{7,13-17}. This resulted in its recommendation by AJCC in 2017¹⁸. Noteworthy, the specimen-driven IOARM method became the standard of care in the institute in 2015. From 2013 until 2020 the IOARM was performed in 304 cases with a steep increase from 2018.

It is important to realize that developing and implementing an IOARM method involves many personnel (pathologists/surgeons/assistants/trainees/researchers), in order to make it standard of care. Many professionals were involved, during many years, in the development of this protocol, which is actually the strength of the method. The development of this method started in 2013 and reached a consensus in 2015. This was achieved based on the two-weekly meetings during which discussions regarding all the patients treated with surgery, including IOARM, took place. In this way, it was possible to timely adjust and refine the procedure. Besides, the two-weekly meetings enabled prospective data collection, which provides the basis for the performance and follow-up studies. Moreover, for every case, the team ensured that the final

pathology was not compromised due to IOARM. Finally, it is important to realize that this kind of assessment is a dynamic process and will always undergo changes toward improvement.

With the specimen-driven IOARM method, the margins are assessed by inspection, palpation, and perpendicular incisions (grossing). This approach provides an as accurate as possible estimation of margins in millimeters and enables feedback on whether an additional resection is needed and what the dimensions should be. Kubik et al. described several reasons (e.g., additional resection at an incorrect location, the incorrect orientation of the additional resection, incorrect dimensions of the additional resection) for additional resections to be inadequate¹⁷. The IOARM is a valuable method but only when accompanied by an as accurate as possible relocation method of inadequate margins to enable the surgeon to perform an adequate additional resection. The spatial relationship between the additional resection and the main specimen is the key factor. Therefore, a simple but elegant relocation method as shown in Figure 3.1 was developed and described in detail by Van Lanschot et al. 12. This method allows the surgeon to perform an additional resection based on the relocation of the inadequate margin defined by the tags in the wound bed. For example, a margin of 2 mm is found between tags 1-2-3, the surgeon performs an additional resection around tags 1-2-3 with a thickness of 4 mm. This relocation method is shown to be effective by the results of Smits et al.9.

This IOARM method is supported by frozen section procedure only if the tumor cannot be distinguished macroscopically from surrounding tissue (e.g., fibrosis of tissue after radiotherapy or scar formation after previous surgery, or salivary gland tissue). Some institutes use another approach, in which frozen sections are taken from the specimen from all quadrants^{13,19}. This method enables a more standardized protocol. However, the comprehensiveness of this method might not be always efficient. Moreover, multiple frozen sections are needed which is costly, time-consuming, and not accessible for all institutes. The described method is more efficient because the region of interest is preselected (i.e., region of suspicious inadequate margin) and is therefore cheaper, faster, and available for every institute. This is in accordance with previous findings that frozen section analysis does not improve the accuracy of specimen-driven IOARM based on grossing in most cases and is not cost-effective²⁰⁻²².

According to the literature >93% of all inadequate margins are found at the submucosal resection margins²³. This is in line with the findings of the institute. Mucosal alterations with high-grade dysplasia/CIS are often easy to detect during IOARM, only in a few cases, a frozen section is recommended. Until now in the IOARM cohort, any

mucosal positive margins regarding cancer or high-grade dysplasia/CIS have not been encountered.

Even though specimen-driven IOARM significantly improves the rate of adequate resections in OCSCC patients and consequently improves patient outcome^{7,9,21,22}, its wide implementation is lagging. The main cause of this is the fact that the grossing of fresh tissue is counter-intuitive for pathologists. The pathologists are fearful that grossing fresh tissue will deteriorate the anatomical orientation, shape, and size of the specimen, and therefore will affect the final histopathologic assessment^{24,25}. However, the measures prescribed in the protocol prevent these possible negative effects. Since the implementation of this protocol, the anatomical orientation, shape, and size of the specimen have never been altered nor was the final pathologic assessment ever compromised (manuscript in preparation).

Although little additional time is required to perform IOARM, it is clear that no real obstacles exist to implement IOARM, but there must be a willingness to go through a learning curve, regarding the grossing of fresh tissue and identifying inadequate margins. The most important prerequisite is a dedicated and cooperative team of surgeons and pathologists. In this study, an IOARM method for head and neck cancer surgery has been described, that can easily be implemented in every institute and during any other cancer surgery. This protocol significantly improves the rate of adequate resections while concomitantly reducing the need for postoperative radiotherapy and improving the patient outcome. The specimen-driven IOARM method will help surgeons to achieve first-time-right surgery and patients will benefit.

REFERENCES

- 1. Bray F, Ferlay J, Soerjomataram I, Siegel RL, Torre LA, Jemal A. Global cancer statistics 2018: GLOBOCAN estimates of incidence and mortality worldwide for 36 cancers in 185 countries. *CA Cancer J Clin*. 2018;68(6):394-424. doi:10.3322/caac.21492
- 2. Sharma SM, Prasad BR, Pushparaj S, Poojary D. Accuracy of intraoperative frozen section in assessing margins in oral cancer resection. *J Maxillofac Oral Surg.* 2009;8(4):357-61. doi:10.1007/s12663-009-0085-9
- van der Ploeg T, Datema F, Baatenburg de Jong R, Steyerberg EW. Prediction of survival with alternative modeling techniques using pseudo values. *PLoS One*. 2014;9(6):e100234. doi:10.1371/journal.pone.0100234
- 4. Chen SW, Yang SN, Liang JA, Lin FJ, Liao CT, Yen TC. Trends in clinical features and survival of oral cavity cancer: fifty years of experience with 3,362 consecutive cases from a single institution. *Cancer Manag Res.* 2018;10:4523-35. doi:10.2147/CMAR.S171251
- 5. Shah JP, Gil Z. Current concepts in management of oral cancer—surgery. *Oral Oncol*. 2009;45(4-5):394-401. doi:10.1016/j.oraloncology.2008.05.013
- Helliwell T, Woolgar J. Dataset for histopathology reporting of mucosal malignancies of the oral cavity. London, UK: Royal College of Pathologists; 2013.
- 7. Varvares MA, Poti S, Kenyon B, Christopher K, Walker RJ. Surgical margins and primary site resection in achieving local control in oral cancer resections. *Laryngoscope*. 2015;125(10):2298-307. doi:10.1002/lary.25397
- 8. Smits RW, Koljenović S, Hardillo JA, ten Hove I, Meeuwis CA, Sewnaik A, et al. Resection margins in oral cancer surgery: room for improvement. *Head Neck*. 2016;38(S1):E2197-203. doi:10.1002/hed.24075
- Smits RWH, Koljenović S, Hardillo JA, ten Hove I, Meeuwis CA, Sewnaik A, et al. Intraoperative assessment of the resection specimen facilitates achievement of adequate margins in oral carcinoma. Front Oncol. 2020;10:614593. doi:10.3389/fonc.2020.614593
- 10. Lin A. Radiation therapy for oral cavity and oropharyngeal cancers. *Dent Clin North Am*. 2018;62(1):99-109. doi:10.1016/j.cden.2017.08.007
- 11. Dik EA, Willems SM, Ipenburg NA, van Es RJ. Resection of early oral squamous cell carcinoma with positive or close margins: relevance of adjuvant treatment in relation to local recurrence: margins of 3 mm as safe as 5 mm. *Oral Oncol*. 2014;50(6):611-5. doi:10.1016/j.oraloncology.2014.02.014
- 12. van Lanschot CGF, van Baar J, van Es RJJ, Willems SM. Relocation of inadequate resection margins in the wound bed during oral cavity oncological surgery: a feasibility study. *Head Neck*. 2019;41(7):2159-66. doi:10.1002/hed.25690
- 13. Amit M, Binenbaum Y, Sharma K, Ramer N, Ramer I, Agbetoba A, et al. Improving the rate of negative margins after surgery for oral cavity squamous cell carcinoma: a prospective randomized controlled study. *Head Neck*. 2016;38(S1):E1803-9. doi:10.1002/hed.24320
- 14. Maxwell JH, Thompson LD, Brandwein-Gensler M, Urken ML. Early oral tongue squamous cell carcinoma: sampling of margins from tumor bed and worse local control. *JAMA Otolaryngol Head Neck Surg.* 2015;141(12):1104-10. doi:10.1001/jamaoto.2015.1351

- 15. Hinni ML, Zarka MA, Hoxworth JM. Margin mapping in transoral surgery for head and neck cancer. *Laryngoscope*. 2013;123(5):1190-8. doi:10.1002/lary.23860
- Kain JJ, Birkeland AC, Udayakumar N, Brenner JC, Swiecicki PL, Mierzwa M, et al. Surgical margins in oral cavity squamous cell carcinoma: current practices and future directions. *Laryngoscope*. 2020;130(1):128-38. doi:10.1002/lary.27943
- 17. Kubik MW, Hinni ML, Weaver AL, Moore EJ, Price DL, Garcia JJ. Intraoperative margin assessment in head and neck cancer: a case of misuse and abuse. *Head Neck Pathol*. 2020;14(2):291-302. doi:10.1007/s12105-019-01041-0
- 18. Amin MB, Edge SB, Greene FL, Byrd DR, Brookland RK, Washington MK, et al. The eighth edition AJCC cancer staging manual: continuing to build a bridge from a population-based to a more "personalized" approach to cancer staging. *CA Cancer J Clin*. 2017;67(2):93-9. doi:10.3322/caac.21388
- Gokavarapu S, Rao GV, Ganly I, Panda NK, Das AK, Kataria T, et al. Revision of margins under frozen section in oral cancer: a retrospective study of involved margins in pT1 and pT2 oral cancers. Br J Oral Maxillofac Surg. 2015;53(9):875-9. doi:10.1016/j. bjoms.2015.06.008
- Chaturvedi P, Pai PS, Nair D, Chaturvedi M, Chaukar D, D'Cruz A. Gross examination by the surgeon as an alternative to frozen section for assessment of adequacy of surgical margin in head and neck squamous cell carcinoma. *Head Neck*. 2014;36(4):557-63. doi:10.1002/ hed.23313
- 21. Mair M, Nair D, Pramesh CS, D'Cruz AK. Intraoperative gross examination vs frozen section for achievement of adequate margin in oral cancer surgery. *Oral Surg Oral Med Oral Pathol Oral Radiol*. 2017;123(5):544-9. doi:10.1016/j.oooo.2016.11.018
- 22. Datta S, Mair M, Nair D, Pramesh CS, Chaturvedi P, D'Cruz AK. Frozen section is not cost beneficial for the assessment of margins in oral cancer. *Indian J Cancer*. 2019;56(1):19-23. doi:10.4103/ijc.IJC_41_18
- 23. Woolgar JA, Triantafyllou A. A histopathological appraisal of surgical margins in oral and oropharyngeal cancer resection specimens. *Oral Oncol*. 2005;41(10):1034-43. doi:10.1016/j.oraloncology.2005.05.004
- Umstattd LA, Mills JC, Critchlow WA, Renner GJ, Zitsch RP. Shrinkage in oral squamous cell carcinoma: an analysis of tumor and margin measurements in vivo, post-resection, and post-formalin fixation. *Am J Otolaryngol*. 2017;38(6):660-2. doi:10.1016/j.amjoto.2017.08.002
- 25. Pangare TB, Jain A, Jain R, Das SN, Kar M, Alam S. Effect of formalin fixation on surgical margins in patients with oral squamous cell carcinoma. *J Oral Maxillofac Surg*. 2017;75(6):1293-8. doi:10.1016/j.joms.2017.01.013

MATERIALS LIST

Name	Company	Catalog Number	Comments
Anatomical templates			https://www.palga.nl/assets/uploads/ Protocollen/HoofdHalstumoren.pdf
Anatomical tweezers			
Brush			to apply the inc to the tissue
Bucket for formalin fixation			Size of the container depends on the size fo the tissue
Buffered formalin 4%			
Camera			
Computer			
Cork			Thin plates of cork
Ethanol 70%			
Examination gloves			
Gauze or Paper			That won't leave particles on the specimen
Grossing knife 15cm			
Grossing knife 30cm			
Grossing tabel			
Inc for tissue			3 or more different colors
Labcoat			
Long pins/Sewing pins			
Paper			To place the tissue sections on during the grossing
Permanent markers			Different colors (black/blue/red/green)
Relocation tags	Premier Farnell Limited BV, Utrecht, The Netherlands		Numbered from 0-9, cut to a size of 5 mm x 7 mm x 2 mm
Scalpel			
Surgical tweezers			
Sutures	Ethicon	Ethilon 3.0	To suture in the tags
Tap water			
Transparant ruler 30 cm			2 rulers needed



ASSESSMENT OF RESECTION MARGINS BY RAMAN SPECTROSCOPY TO GUIDE ORAL CANCER SURGERY

Yassine Aaboubout, Maria R. Nunes Soares, Tom C. Bakker Schut, Elisa M. Barroso, Martin van der Wolf, Elena Sokolova, Viacheslav Artyushenko, Alexey Bocharnikov, Iskander Usenov, Cornelia G. F. van Lanschot, Lars Ottevanger, Hetty Mast, Ivo ten Hove, Brend P. Jonker, Stijn Keereweer, Dominiek A. Monserez, Aniel Sewnaik, Jose A. Hardillo, Rob J. Baatenburg de Jong, Senada Koljenović* and Gerwin J. Puppels*

Analyst. 2023 Aug 21;148(17):4116-4126



ABSTRACT

Patients with oral cavity cancer are almost always treated with surgery. The goal is to remove the tumor with a margin of more than 5 mm of surrounding healthy tissue. Unfortunately, this is only achieved in about 15% to 26% of cases. Intraoperative assessment of tumor resection margins (IOARM) can dramatically improve surgical results. However, current methods are laborious, subjective, and logistically demanding. This hinders broad adoption of IOARM, to the detriment of patients. Here we present the development and validation of a high-wavenumber Raman spectroscopic technology, for quick and objective intraoperative measurement of resection margins on fresh specimens. It employs a thin fiberoptic needle probe, which is inserted into the tissue, to measure the distance between a resection surface and the tumor. A tissue classification model was developed to discriminate oral cavity squamous cell carcinoma (OCSCC) from healthy oral tissue, with a sensitivity of 0.85 and a specificity of 0.92. The tissue classification model was then used to develop a margin length prediction model, showing a mean difference between margin length predicted by Raman spectroscopy and histopathology of -0.17 mm.

INTRODUCTION

Worldwide, 350 000 patients per year are diagnosed with oral cavity cancer, of which about 90% is squamous cell carcinoma (OCSCC)¹.

Surgery is the primary form of treatment. In an adequate tumor resection, the whole tumor is removed with a histopathological margin of more than 5 mm of healthy tissue. At the same time, it is important to spare healthy tissue to limit the loss of function (e.g., speaking, mastication, and swallowing) and facial disfigurement²⁻⁴.

Five-year disease-specific survival of oral cancer patients currently stands at 84% for adequate tumor resections, but only 68% for inadequate resections, despite the much more frequent use of adjuvant therapy in these cases (mostly postoperative radiotherapy)⁵.

Unfortunately, with surgeons having to rely on visual inspection, palpation, and preoperative imaging, adequate resection margins are rarely achieved (15%-26%) in oral cancer surgery²⁻⁶.

This can be improved by intraoperative assessment of resection margins (IOARM), enabling the surgeon to excise additional tissue when needed to turn an initially inadequate resection into an adequate resection. A recently introduced IOARM-method for inspection of a fresh specimen, by a dedicated pathologist and the surgeon, has led to a dramatic improvement in the rate of adequate tumor resections from 15% to 58%^{4,5}.

However, the method is laborious, logistically very demanding, and subjective, which hinders its widespread adoption. IOARM works, but there is a need for an objective and easy-to-use technology to allow more patients to benefit from it. A range of techniques, among which fluorescence imaging, ultrasound-guided resection, and magnetic resonance imaging of tongue cancer specimens is currently being explored for application in objective IOARM⁷⁻¹².

Raman spectroscopy is a non-destructive, label-free, optical technique, that provides information about the overall molecular composition of tissues. The development of medical applications of this technique is rapidly gaining momentum¹³⁻¹⁹. Here, we report on the development and validation of a Raman spectroscopy-based objective IOARM-device (RIOARM-device), which uses the high-wavenumber (HWVN) part of the Raman spectrum. A thin fiber-optic needle probe is inserted into the specimen to

rapidly determine the distance between the resection surface and the tumor border (margin length).

MATERIALS AND METHODS

Patient selection and resection specimen handling

This study was approved by the Medical Ethics Committee of Erasmus Medical Center (Erasmus MC) (protocol MEC-2015-150). OCSCC patients who underwent surgical treatment between May 2019 and September 2021 were included, after informed consent.

In total 71 patients were included, 40 patients for the tissue classification model (see below "Development of a tissue classification model") and 31 for the margin length prediction model (see below "Development of a margin length prediction model").

The experiments on fresh resection specimens were performed within 30 minutes after arrival from the operating room, after which they underwent routine pathology processing.

RIOARM-device

The RIOARM-device is shown in **Figure 4.1** and is described in more detail in the ESI (S1: RIOARM-device).

It employs disposable HWVN single fiber-optic needle probes. The proximal end of the single fiber of the disposable fiber-optic needle probe is butt-coupled to a fiber patch cord in the RIOARM-device positioning arm, which at the other end is connected to a Raman module. The Raman module launches laser light (671 nm, 65 mW) into the fiber and receives Raman scattered light from the fiber. Because the RIOARM-device records high-wavenumber Raman spectra in the 2600-4000 cm⁻¹ region, where the background signal of the optical fibers is very low, a single fiber can be used to guide laser light to the tissue and to collect Raman scattered light from the tissue^{20,21}. The spectral resolution of the system is <12.5 cm⁻¹ over the entire spectral interval. The depth resolution of the system is <0.35 mm (details described in the ESI, S2: Experimental determination of the depth resolution). The experiments were performed in a room with ceiling lighting comprised of LED-lamps having no emission above 700 nm. Because Raman spectra were collected above 800 nm, experiments could be carried out with room lighting on without any interference with the collection of Raman spectra.

The fiber-optic needle probe is connected to the motorized translation stage of the RIOARM-device positioning arm and a vacuum system. The motorized translation stage is used to drive the fiber-optic needle into the tissue under investigation. The vacuum system serves to create an under pressure that prevents tissue deformation during the insertion of the fiber-optic needle.

In operation, the fiber-optic needle probe was positioned perpendicular to the tissue surface and then inserted with a velocity of 1.8 mm s⁻¹, over a distance of 7 mm. Raman spectra were recorded every 0.14 seconds, resulting in 4 Raman spectra per mm.

Data preprocessing

All data preprocessing and data analysis software routines were built in-house using MATLAB (version 2020a, Mathworks, Natick, MA, USA).

All spectra were intensity and wavenumber calibrated as described earlier²². Cosmic ray events were removed, and any background signal generated in the systems optical path was subtracted. Autofluorescence (AF) contributes in varying degrees to the tissue spectra. This AF background signal was fitted with a 3rd-order polynomial and was subtracted from the measured spectrum to obtain the Raman signal. The polynomial fit was optimized for the 2600-2800 cm⁻¹ and 3800-4000 cm⁻¹ spectral regions, which do not contain significant Raman signal contributions. The subtracted polynomial was used to quantify the autofluorescence background signal.

The following criteria were used to exclude low-quality spectra from the data set:

- Saturation of the CCD detector by very high tissue AF.
- Raman signal-to-noise ratio (RSNR) <0.1. The RSNR is defined as the mean of the ratios between the Raman signal and the square root of the total acquired signal (Raman signal + AF + device background) in the spectral region between 2600-4000 cm⁻¹.

RSNR 2600-4000 cm - 1 =
$$\frac{Raman \ signal}{\sqrt{Raman \ signa + AF \ signal + device \ backgr}}$$

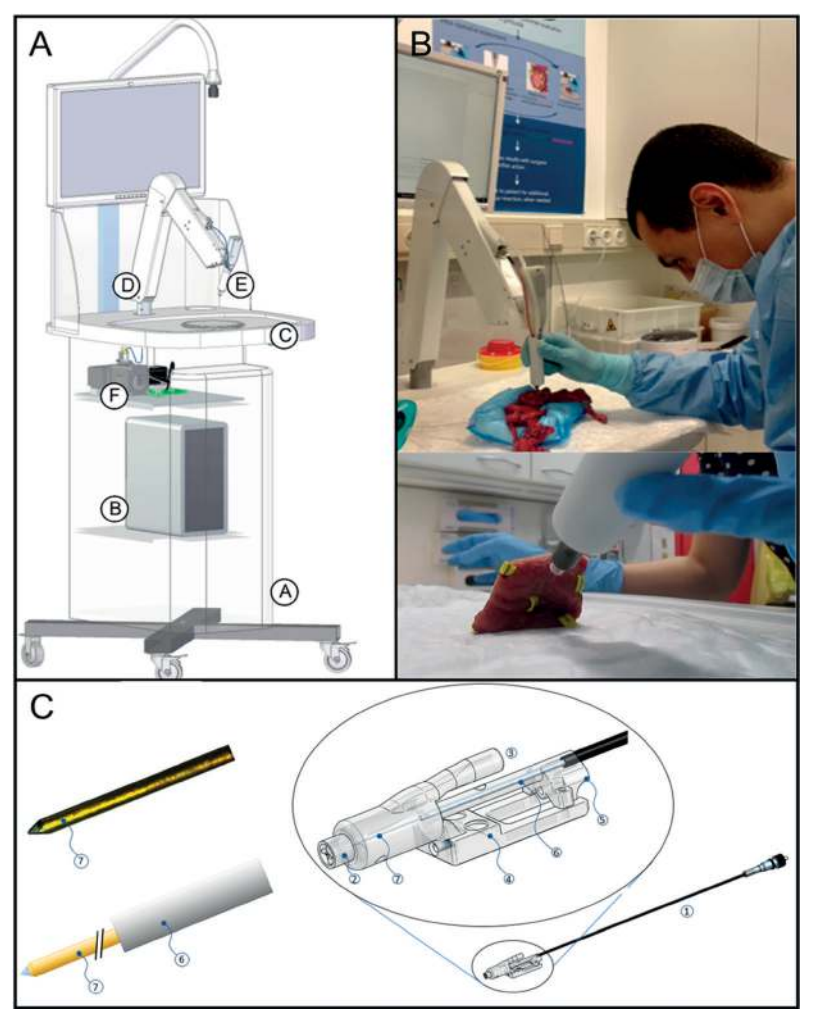


Figure 4.1. RIOARM-device. Panel A: Main components of the RIOARMdevice: (A): custom-built cart, (B): personal computer (Windows 10, Hewlett-Packard prodesk), (C): workspace for specimen positioning, (D): positioning arm, for positioning the fiber-optic needle probe, (E): the disposable fiber-optic needle probe (illustrated in panels (B) and (C)), which is fiber-optically coupled to (F): a custom-built raman spectroscopy module. Panel B: positioning of the fiber-optic needle probe on a specimen. Panel C: Disposable fiber-optic needle probe, comprised of: - a single copper-coated multimode fused silica fiber (core/cladding/coating diameter: 105/125/150 μm) in a thin (300 μm outer diameter) metal tube (6), covered by protective braided pebax/polyamide tubing. - an Fc/ Pc-connector at its proximal end, butt-coupling the probe to the internal fiber patch cord of the raman-RIOARM-device (panel A). - a port 3, connected to a vacuum system. It maintains an under pressure in chamber 2, around the fiber-optic probe end, when the chamber is placed on the tissue. This fixes the tissue in place against tip 2, preventing surface deformation when the fiberoptic needle is inserted into the tissue. - Part 4, used to fasten the fiber-optic needle probe to the positioning arm of the Raman-RIOARM-device. - Part 5, connecting the fiber-optic probe to the linear translation stage in the positioning arm, enabling the insertion of the fiber-optic needle into thetissue at a set speed. - The distal end 7 of the needle which penetrates the tissue measures 150 μm in diameter and has a conically polished tip. (Further details in the ESI, S1 RIOARM device†).

Data analysis

Three Raman spectral tissue markers were used as discriminators between OCSCC and healthy tissue:

- 1. The water concentration [H2O] defined as water mass percentage (expressed in grams of water per 100 grams of wet tissue) was calculated using the method developed by Caspers et al.²³ and described in detail in previous studies²⁴⁻²⁶.
- 2. The Raman signal intensity ratio of two wavenumber regions ($I_{2852-2884 \text{ cm}}^{-1}$: $I_{2910-2966 \text{ cm}}^{-1}$) of the CH-stretching region was determined, indicative of the lipid-to-protein ratio (Lipid/Protein)^{27,28}.
- 3. The Raman signal to AF signal ratio (Raman/AF) was calculated for the 3350-3550 wavenumber region ($I_{Raman3350-3550 \text{ cm}}^{-1}$: $I_{AF 3350-3550 \text{ cm}}^{-1}$).

Development of a tissue classification model

For the development of the tissue classification model, Raman measurements were performed on fresh specimen cross-sections containing both tumor and healthy tissue. For these measurements, the RIOARM-device was slightly modified. The positioning arm was replaced by a manual X-Y positioning stage (with a better than 100 µm positioning precision) to which the fiber-optic needle probe was attached (**Figure 4.2A** and **B**). This enabled precise positioning of the fiber-optic needle probe on the specimen and retrieval of measurement locations needed for histopathological annotation of Raman spectra. To prevent dehydration of the cross-section tissue surface, the tissue was shielded from ambient air with plastic foil wrapped around the X-Y positioning stage (**Figure 4.2C**).

For the measurements, due care was taken to maintain anatomical orientation, as required for final histopathology, which is the gold standard for diagnosis and prognostication.

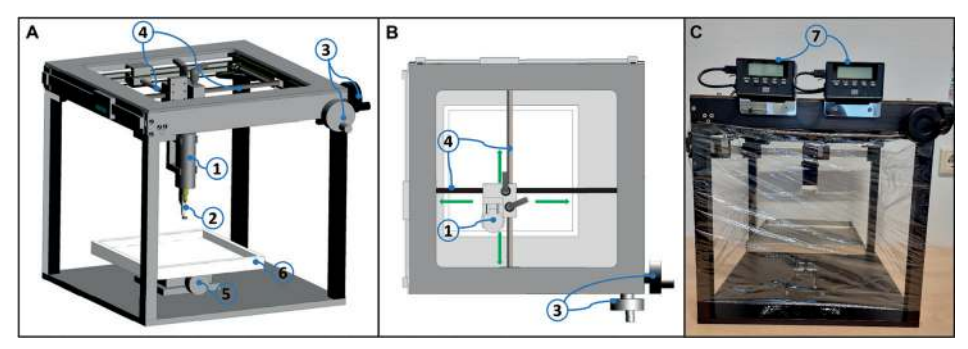


Figure 4.2. Manual X-Y positioning stage. (A). A front-side view showing the fiber -optic needle probe 1 and needle 2; the two actuators 3 are used to move the fiber-optic needle probe in the X and Y directions along the guiding rods 4; the specimen is placed on the plate 6 and is moved towards needle 2 by means of actuator 5. (B). Top view of the stage. The X-Y movements of the fiber-optic needle probe 1 along the 2 guiding rods 4 are indicated by the green arrows. (C). Picture of the stage showing two monitors 7 to read the X-Y position of the fiber-optic needle probe. The stage is wrapped in plastic foil to prevent tissue dehydration during the measurements.

The specimen cross-section was fixed onto a cork substrate and placed under an X-Y positioning stage, to which the fiber optic probe of the RIOARM-device was attached (Figure 4.3A).

Raman experiments were performed as follows:

- a. A series of Raman measurements were performed along a straight line, using the Y-axis of the X-Y stage (white lines, **Figure 4.3A**), moving from the resection surface towards and into the tumor with a step size of 1 mm.
- b. The X-position of the first line measurement was demarcated by a pin (black pin, Figure 4.3A) inserted into the cork. The location of this pin served as the reference point for histological annotation after the experiment (Figure 4.3A).
- c. At each measurement location, the fiber-optic needle was driven into the tissue, with a velocity of 3.6 mm s⁻¹, while collecting Raman spectra from the tissue cross-section surface to 3 mm below the surface. Raman spectra were recorded every 0.14 seconds, resulting in 2 Raman spectra per mm. A laser power of 65 mW was used.
- d. Depending on the size of the specimen cross-section, a number of line measurements were performed, spaced 1 mm apart along the X-axis. After the experiment, a photograph was taken and the cross-section was formalin-fixed for further processing (Figure 4.3B).

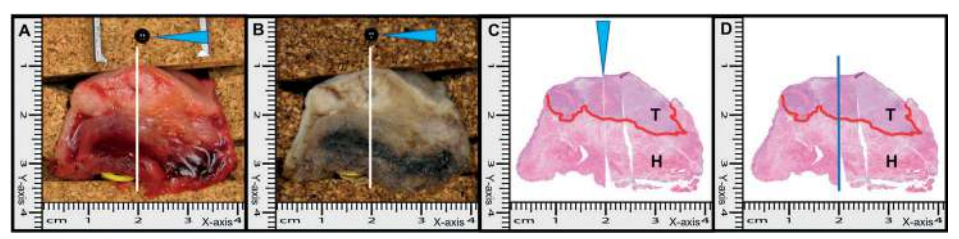


Figure 4.3. Illustration of the procedure for histopathological annotation of Raman measurements on specimen cross-sections. (A) and (B). Cross-section of a resection specimen before and after formalin fixation. The black pin (blue arrow) demarcates the X-position of the first line of Raman measurements (white line). (C) and (D). H&E slide obtained from the cross-section surface. The reference incision that was used for identifying the first Raman line measurement is clearly visible (blue arrowhead). The red line marks the tumor border. T: Tumor, H: Healthy Tissue. The first Raman line measurement is indicated by the blue line (D).

Each measurement location was histologically annotated and labeled "healthy" or "tumor". For the histological annotation, a superficial straight incision was made in the cross-section surface, at the position of the first Raman line measurement, starting at the black demarcation pin (Figure 4.3B). This was also done on the opposite side of the cross-section. From both sides, hematoxylin and eosin (H&E) stained thin tissue sections were made (Figure 4.3C), using the reference incisions for annotation of Raman measurement locations as healthy or tumor (Figure 4.3D). Raman measurement locations were excluded from further analysis if the histological annotation was not the same for both H&E slides.

In our estimation, the relocation of Raman measurement locations for histopathological annotation has an uncertainty of 1 mm in both X and Y directions. For this reason, measurements within 2 mm of the tumor border were excluded from further analysis.

The tissue classification model was developed using a support vector machine (SVM) method with a fine Gaussian kernel (Machine Learning Toolbox, MATLAB 2020a). The values for [H2O], Lipid/Protein, and Raman/AF obtained from the tissue spectra were used as input, together with the histological classification of the tissue (binary classifier: tumor or healthy).

For each [H2O], Lipid/Protein, Raman/AF input set, the model yields a tumor probability. The model was trained using k-fold cross-validation (k = number of patients). A receiver operating characteristic (ROC) curve was calculated as internal validation. The discriminative power of the model was determined by calculating the area under the curve (AUC) obtained for different tumor-probability thresholds. The accuracy, sensitivity, and specificity of this model were determined at a tumor-probability threshold of 0.5. The model was validated on an independent data set.

Development of a margin length prediction model

The RIOARM-device was used on intact fresh specimens, to obtain Raman spectra from the resection surface to 7 mm below the resection surface (Raman profiles). Depending on the size of the specimen, up to six measurement locations were selected. The intact specimens were kept in a closed container until the Raman measurements were performed which lasted between 5 and 10 minutes.

Two considerations are at the heart of the experimental design described below. We estimate that the relocation of the position of Raman measurements on resection specimens, in H&E slides is only precise to about 1 mm. This can lead to an error in the histological margin length annotation of the measurement, because the border between tumor and healthy tissue is neither regular nor parallel to the resection surface.

To minimize the effect on the development of the margin length prediction model, an approach was chosen in which up to 6 RIOARM-device profile measurements were performed within a resection surface area of about 2 mm × 2 mm, each yielding a margin length. The center of the measurement area was demarcated by a numbered needle, inserted perpendicularly to the resection surface. After tissue processing, the histological margin lengths were determined at up to 6 locations less than 1 mm from the numbered relocation needle. The mean margin length prediction of the RIOARM-device was then compared to the mean histological margin length. A measurement location was excluded if individual histological margin lengths differed by more than 2 mm.

After the experiment, a picture was taken (Figure 4.4A). The intact specimen with the numbered needles was then formalin-fixed for further processing. After fixation, another photograph was taken (Figure 4.4B). The specimen was grossed, following the standard pathology procedure, without the removal of the numbered needles (Figure 4.4C and D). This resulted in specimen cross-sections of 2 to 3 mm in thickness. Along the length of a numbered needle, superficial incisions were made on both sides of the specimen cross-sections. H&E slides were prepared from both sides of the cross-section, in which the incisions served as a reference for histological annotation of the profile measurements (Figure 4.4E and F).

Based on the tissue classification model, each spectrum of a Raman profile was converted into a tumor probability, resulting in tumor probability profiles, showing tumor probability as a function of distance to the resection surface.

Interpretation of tumor probability profiles.

A tumor probability profile of 7 mm is based on 29 Raman spectra (one for every 250 μ m). The tissue classification model that uses these spectra as input, will inevitably generate occasional false positives and false negatives. Decision rules were developed for the interpretation of tumor probability profiles, based on the occurrence of tumor probabilities >0.5.

- 1. When the whole 7 mm profile has a probability <0.5, no tumor is encountered and the margin length is ≥7 mm.
- 2. When the whole profile has a probability ≥0.5, the margin length is 0 mm.
- 3. When the probability profile has only one transition from low (<0.5) to high (≥0.5) tumor probability, the location of this transition demarcates the margin length.
- 4. Profiles with more than 4 crossings of the 0.5 threshold are considered inconclusive, and no margin length prediction is given.
- 5. For all other tumor probability profiles, a simple parametrized interpretation model was adopted for the prediction of the margin length.

In summary; 2 parameters, related to the length of low and high tumor probability segments in a tumor probability profile, were optimized; H_{min} and L_{max} :

- If a segment of a profile with a high tumor probability is longer than value H_{min} , the decision is that the tumor border is located at the start of that segment.
- If a segment of a profile with a high tumor probability is shorter than the value H_{min} , the decision rule depends on additional profile shape characteristics. For example, if 2 segments of high tumor probability are interrupted by a segment of low tumor probability, the decision rule for the location of the tumor border, depends on the length of that low probability segment.
 - If it is smaller than the value L_{max} the presence of that low probability segment is ignored.
 - If it is larger than value L_{max} the presence of the first high probability segment is ignored.

The margin length determined at final pathology was used as gold standard. ESI **Table** 4 shows the different tumor probability profiles and the decision rules for predicting the margin length. Using the development data set, both H_{min} and L_{max} were varied from 1 to 6 mm with a step size of 1 mm.

The difference between the histological margin lengths and the predicted margin lengths was calculated for each combination of H_{min} and L_{max} for all tumor probability profiles. In this way, the combination of H_{min} and L_{max} that yielded the lowest mean error was determined.

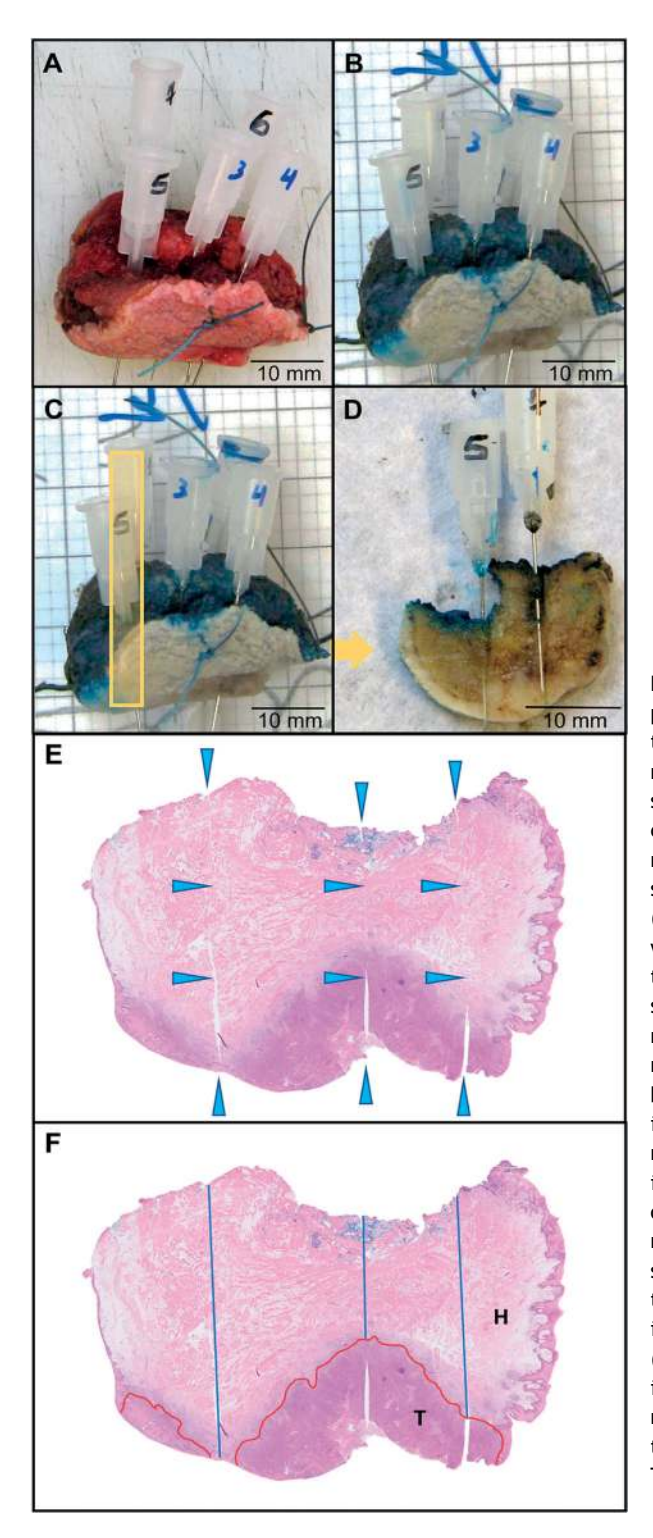


Figure 4.4. Illustration of the procedure for histological annotation of Raman profile measurements. (A). Intact fresh resection specimen with numbered needles demarcating the Raman profile measurement areas. (B). The specimen after formalin fixation. (C). The specimen of figure B with the yellow square indicating the location of the cross-section shown in figure (D). (D). Specimen cross-section containing measurement locations marked by needles 5 and 7. Superficial incisions were made along the numbered needles, to enable identification of the trajectory of the Raman profile measurements in H&E-slides. (E). H&Eslide showing the trajectories of the Raman profile measurements indicated by needles 5 and 7. (F). The H&E-slide of figure (E), illustrates the histological annotation. The red line marks the tumor border. H: Healthy Tissue, T: Tumor.

Data obtained from a specimen were either used for the development of the margin length prediction model, or for the validation of the model. Allocation of specimens to either the model development dataset or the model validation dataset was based on balancing anatomical tumor locations (tongue, floor of mouth, buccal mucosa, gingiva maxilla, and gingiva mandible) and the number of adequate/inadequate margins in both groups.

Valid tumor probability profiles were used to calculate a mean margin length prediction for a measurement location. Profiles were considered invalid if, during a profile measurement the vacuum broke, which leads to tissue surface deformation during needle insertion. A profile was also considered invalid if it contained more than 2 consecutive points for which no tumor probability could be calculated. Finally, profiles that gave an inconclusive margin length prediction (ESI **Table 5**;† profile shape 10), were excluded.

Measurement locations with 2 or more valid tumor probability profiles were used to test the margin length prediction model, for both the development data set and the validation data set.

The mean error in margin length prediction was calculated to investigate a potential bias of the RIOARM-device. The mean absolute error in margin length prediction was calculated to determine the error in the margin length determination by the RIOARM-device.

RESULTS

Tissue classification model

Raman measurements were performed on fresh specimen cross-sections from 40 OCSCC patients. Patient and tumor characteristics are shown in ESI **Table 2**. Data from 25 patients were used to develop the tissue classification model and data from 15 patients were used for its validation.

The development of the tissue classification model wasbased on 1347 tumor spectra and 1784 healthy tissue spectra. Typical Raman spectra of tumor and healthy tissue are shown in **Figure 4.5A**, **B**, **and C**. Each spectrum was analyzed to yield values for 3 Raman spectral tissue markers: [H2O], Lipid/ Protein, and Raman/AF. **Figure 4.5D**, **E**, **and F** compare the distribution of values of these 3 markers for healthy tissue (green) and tumor (red), for all spectra in the development data set. A wide range

of [H2O]-values are found for healthy tissue. Tumor is characterized by a narrow range of [H2O]-values, overlapping with the highest [H2O]-values found in healthy tissue. Similarly, healthy tissue shows a wide range of Lipid/Proteinvalues. Tumor is characterized by a narrow range of values, overlapping with the lowest Lipid/Proteinvalues found in healthy tissue. Finally, many healthy tissue spectra are characterized by an intense AF background, resulting in low Raman/AF-values. This is only rarely encountered in tumor spectra.

The calculated values of [H2O], Lipid/Protein, and Raman/AF, and the respective histological annotation of each spectrum were used as input for the development of the tissue classification mode (see Materials and Methods). The tissue classification model showed a discriminative power of 0.93 (based on the area under the ROCcurve, **Figure 4.6A**), an accuracy of 0.89, a sensitivity of 0.87, and a specificity of 0.91 at the tumor probability threshold value of 0.5.

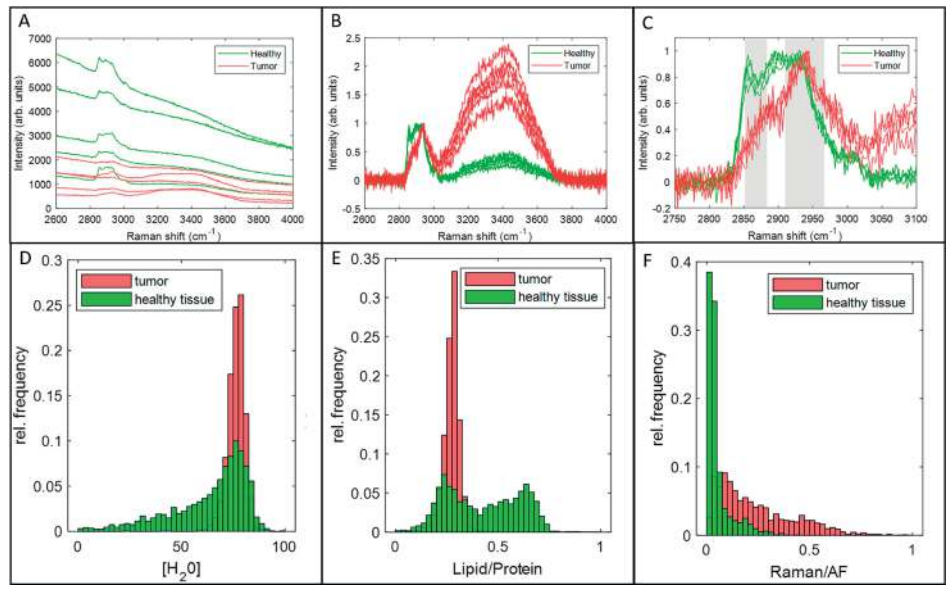


Figure 4.5. Examples of Raman spectra of tumor and healthy tissue. (A). Raman spectra after pre-processing (Materials and methods, section Data preprocessing), illustrating the higher tissue autofluorescence (AF) background in most healthy tissue spectra. (B). Raman spectra of figure A after subtraction of the AF background and intensity normalization on the CH-stretching region (2910-2966 cm⁻¹), illustrating the higher intensity in the OH-stretching region (3350-3550 cm⁻¹) in tumor spectra due to the higher water concentration in tumor^{19,20}. (C). Close-up of the 2750-3100 cm⁻¹ CH-stretching region of the spectra of figure B, illustrating the higher lipid-to-protein band ratio in healthy tissue. (D). Histogram of [H2O] values. (E). Histogram of Lipid/Protein values. (F). Histogram of Raman/AF values.

The developed classification model was validated on an independent data set obtained from specimens of 15 patients, made up of 426 tumor spectra and 1240 healthy tissue spectra. A discriminative power of 0.92, an accuracy of 0.90, a sensitivity of 0.85, and a specificity of 0.92 were found.

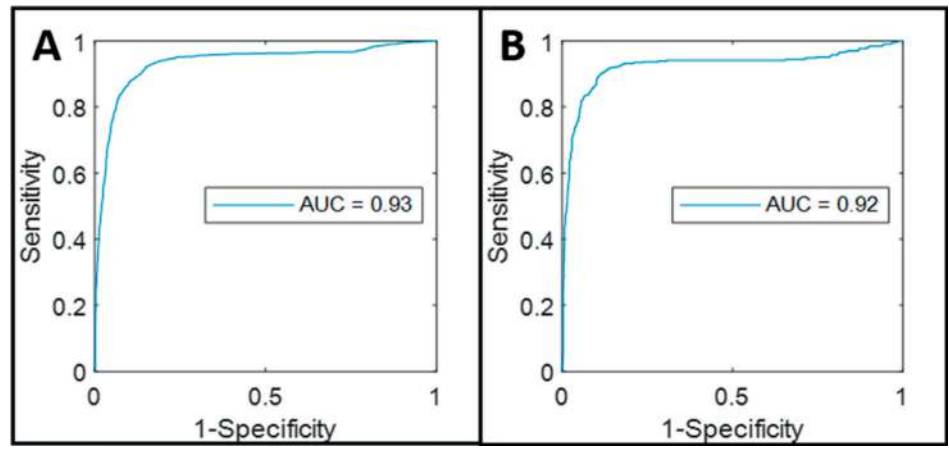


Figure 4.6. ROC-curves for the development and validation data sets of the tissue classification model. (A). ROC-curve of the leave-one-patient-out internal validation of the tissue classification model. (B). ROC-curve of the validation of the tissue classification model on the independent data set.

Margin length prediction model

Raman profile measurements were performed on fresh intact specimens of 31 OCSCC patients, to obtain tumor probability profiles from the resection surface to a depth of 7 mm. Patient and tumor characteristics are shown in ESI **Table 3**.

Data from fourteen specimens were used for the development of the margin length prediction model. Raman and histology data were obtained at 44 resection surface locations (28 adequate margins and 16 inadequate margins) yielding a total of 217 tumor probability profiles (examples are shown in **Figure 4.7**).

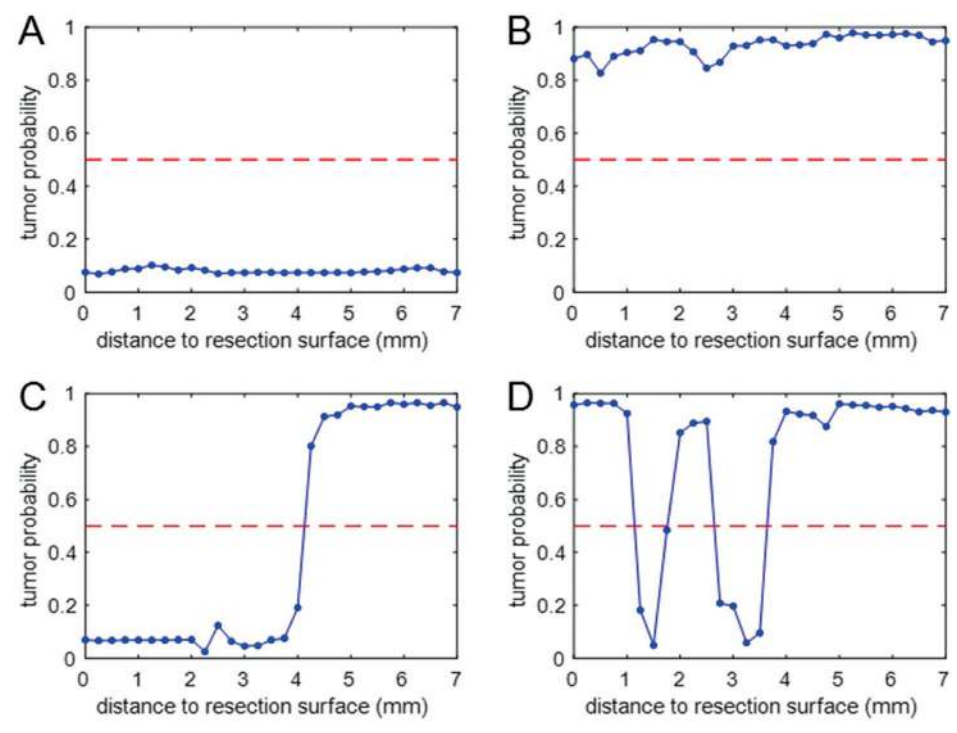


Figure 4.7. Examples of tumor probability profiles. (A): Tumor probability <0.5 over the entire length of the profile. (B): Tumor probability ≥ 0.5 over the entire length of the profile. (C): Starting segment with tumor probability <0.5 followed by a segment with tumor probability ≥ 0.5 . (D): Multiple alternating segments of high (≥ 0.5) and low (<0.5) tumor probability.

The data set contained 86 profiles with a tumor probability <0.5 over the entire length of the profile, 22 profiles with a starting segment of tumor probability <0.5 after which tumor probability changed and remained \geq 0.5, and 9 profiles with tumor probability \geq 0.5 over their entire length. Interpretation of these profiles in terms of margin length prediction is straightforward (Materials and methods and ESI **Table 5**†).

One hundred profiles had more complex shapes with alternating segments of high $(\ge 0.5; H)$ and low (< 0.5; L) tumor probability.

The combination of the H_{min} and L_{max} values (see Materials and Methods) that yielded the lowest mean error between margin length prediction and histology was: H_{min} = 4 mm and L_{max} = 2 mm, leading to the decision rules shown in ESI **Table 5.**†

Using these decision rules, the mean margin length prediction by Raman spectroscopy was compared to the mean histo-logical margin length, for each measurement location. Five of the 44 measurement locations were excluded because insufficient valid tumor probability profiles were available for the calculation of a mean margin length prediction.

Figure 4.8A shows the histogram of the error in margin length prediction for the development data set. The mean difference between margin length prediction by the RIOARM-device and histology was -0.15 mm, showing an absence of significant bias. The mean absolute difference in the margin length prediction was 0.69 mm, which is within the estimated error margin of the gold standard histological margin length.

An independent data set, obtained from 17 specimens (44 measurement locations; 29 adequate margins and 15 inadequate margins, and a total of 211 tumor probability profiles) was used for the validation of the margin length prediction model. Four measurement locations were excluded because insufficient valid tumor probability profiles were available for the calculation of a mean margin length prediction.

Figure 4.8B shows the histogramof the error in themargin length prediction. The mean difference between margin length prediction by the RIOARM-device and histopathology was -0.17 mm. The mean absolute difference in the margin length prediction was 0.76 mm.

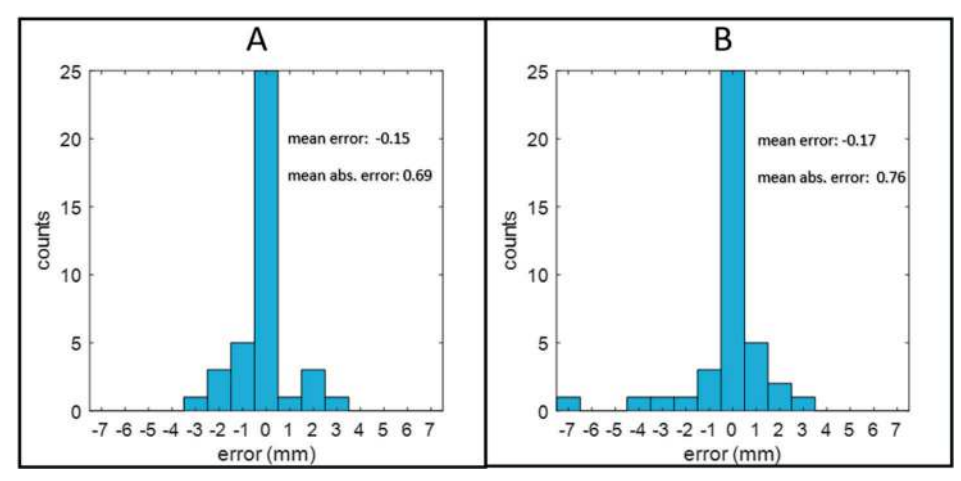


Figure 4.8. Histograms of margin length prediction errors (RIOARM-device margin length prediction minus gold standard histological margin length). (A): Results for the model data set on which the model parameters were optimized. (B): Results for the independent validation data set.

Figure 4.9 shows the confusion matrix of RIOARM-device adequate/inadequate margin predictions based on individual Raman profiles against histology. In 166 cases the RIOARMdevice prediction is correct. There are 9 false negatives (i.e., missed inadequate margins) and 2 false positives. Based on these numbers, sensitivity and specificity for inadequate margins are 78% and 98%, respectively.

The RIOARM-device returned a margin length between 4 and 6 mm for 13 profiles. Given the mean absolute error in the margin length prediction (0.76 mm) we classify such a result as "potentially inadequate margin (PIM)".

Of the 211 profiles in the validation data set, 31 belonged to the inconclusive category of ESI **Table 5**,† for which currently no margin length prediction is rendered. These are separately mentioned in **Figure 4.9**.

inconclusive: 31

PIM: 13

histopathology adequate inadequate 125 9 2 31

Figure 4.9 Confusion matrix of RIOARM-device adequate/inadequate margin predictions against histology. The acronym PIM stands for potentially inadequate margin.

DISCUSSION

The clinical relevance of adequate resection margins in OCSCC surgery is evident. Patients with adequate resection margins have higher survival rates and fewer patients need adjuvant (radio)therapy; a well-known cause of additional morbidity^{4,5,29}.

This study demonstrates the feasibility of an easy-to-use device for the objective assessment of tumor resection margins on fresh resection specimens. A measurement at a single location takes about 5 seconds and in principle, data analysis can take place in real-time, although for this paper it was carried out off-line. This allows for the assessment of the resection margins at many locations of a specimen, within a short period of time, while the patient is still in the operating room. Moreover, the measurements could be carried out in, or close to, the operating room and would not necessarily be carried out by a pathologist.

The mean absolute error in the margin length prediction by the RIOARM-device was <1 mm. This is within the estimated 1 mm uncertainty in our gold standard histological margin length assessment. Moreover, the RIOARM-device showed no positive or negative bias in margin length with respect to histology.

Therefore, it may be expected that the RIOARM-device will indicate adequate and inadequate margins with high accuracy. This is confirmed by a test on the profiles of the margin length prediction validation data set. If a "PIM"- or an "inconclusive"-

result would be obtained, additional measurements close to that location could be performed for a definitive result.

Despite the very high specificity, inevitably some false positives will occur. If an isolated measurement shows an "inadequate margin"-result, additional measurements can be performed in the vicinity of that location, to either confirm or reject that result.

The combination of high specificity (98%) and short measurement time can partly compensate for the lower 78% sensitivity, because it enables measurements at many locations, without the risk of introducing high numbers of false positive results. Moreover, both the tissue classification model and the margin length prediction model, although validated on independent data sets, are still based on data sets of limited sizes. Therefore, it is expected that they can be further improved.

The next step towards implementation of the technology, is the development of a measurement protocol for systematic IOARM and result reporting, that takes the above considerations into account. It appears feasible to determine the resection margins on a specimen at up to 100 locations within an acceptable time frame of 15 minutes, which is currently not achievable in any other way. Intraoperative detection of inadequate margins can be combined with the recently introduced paired-tagging technique for accurate relocation of such inadequate margins in the wound bed³⁰. This provides the surgeon with the opportunity to return to the patient and remove additional tissue at the exact location of the inadequate margin, to achieve an adequate tumor resection.

CONCLUSIONS

We have presented the development and technical validation of a Raman spectroscopic technology for quick and accurate assessment of oral cavity tumor resection margins.

We expect that the intraoperative assessment of resection margins based on Raman spectroscopy will lead to at least the same dramatic improvement in the rate of adequate resections, that was obtained with the IOARM-method based on visual inspection and palpation of the specimen. However, RIOARM is much more conducive to widespread adoption⁵.

Margin status is an important prognostic factor, and one of the few that can be brought under the control of the surgeon. Especially in oral cancer surgery, there is immense room for improvement. RIOARM has the potential to play an important role in addressing this need.

We have developed our technology with a focus on oral cancer surgery, but its application is by no means limited to that. The ability to locate the closest resection margin intraoperatively provides the surgeon with actionable information that facilitates the further improvement of many other tumor resection procedures³¹.

REFERENCES

- Ferlay J, Soerjomataram I, Dikshit R, et al. Cancer incidence and mortality worldwide: sources, methods and major patterns in GLOBOCAN 2012. *Int J Cancer*. 2015;136(5):E359-86. doi:10.1002/jjc.29210
- Varvares MA, Poti S, Kenyon B, Christopher K, Walker RJ. Surgical margins and primary site resection in achieving local control in oral cancer resections. *Laryngoscope*. 2015;125(10):2298-307. doi:10.1002/lary.25397
- 3. Aaboubout Y, ten Hove I, Smits RWH, Hardillo JA, Puppels GJ, Koljenovic S. Specimendriven intraoperative assessment of resection margins should be standard of care for oral cancer patients. *Oral Dis.* 2021;27(1):111-6. doi:10.1111/odi.13619
- Smits RWH, Koljenovic S, Hardillo JA, et al. Resection margins in oral cancer surgery: room for improvement. Head Neck. 2016;38(Suppl 1):E2197-203. doi:10.1002/hed.24075
- Smits RWH, van Lanschot CGF, Aaboubout Y, et al. Intraoperative assessment of the resection specimen facilitates achievement of adequate margins in oral carcinoma. Front Oncol. 2020;10:614593. doi:10.3389/fonc.2020.614593
- Dik EA, Willems SM, Ipenburg NA, Adriaansens SO, Rosenberg AJWP, van Es RJJ. Resection of early oral squamous cell carcinoma with positive or close margins: relevance of adjuvant treatment in relation to local recurrence: margins of 3 mm as safe as 5 mm. *Oral Oncol*. 2014;50(10):958-63. doi:10.1016/j.oraloncology.2014.02.014
- 7. Voskuil FJ, Vonk J, van der Vegt B, et al. Intraoperative imaging in pathology-assisted surgery. *Nat Biomed Eng.* 2021;6(5):503-14. doi:10.1038/s41551-021-00808-8
- 8. de Koning KJ, Koppes SA, de Bree R, et al. Feasibility study of ultrasound-guided resection of tongue cancer with immediate specimen examination to improve margin control—comparison with conventional treatment. *Oral Oncol*. 2021;116:105249. doi:10.1016/j. oraloncology.2021.105249
- 9. Heidkamp J, Weijs WLJ, Engen-van Grunsven ACH, et al. Assessment of surgical tumor-free resection margins in fresh squamous-cell carcinoma resection specimens of the tongue using a clinical MRI system. *Head Neck*. 2020;42(8):2039-49. doi:10.1002/hed.26125
- 10. Heidkamp J, Scholte M, Rosman C, Manohar S, Fütterer JJ, Rovers MM. Novel imaging techniques for intraoperative margin assessment in surgical oncology: a systematic review. *Int J Cancer*. 2021;149(3):635-45. doi:10.1002/ijc.33570
- 11. Kain JJ, Birkeland AC, Udayakumar N, et al. Surgical margins in oral cavity squamous cell carcinoma: current practices and future directions. *Laryngoscope*. 2020;130(1):128-38. doi:10.1002/lary.27943
- Noorlag R, de Bree R, Witjes MJH. Image-guided surgery in oral cancer: toward improved margin control. Curr Opin Oncol. 2022;34(3):170-6. doi:10.1097/CCO.0000000000000824
- 13. Faur CI, Falamas A, Chirila M, et al. Raman spectroscopy in oral cavity and oropharyngeal cancer: a systematic review. *Int J Oral Maxillofac Surg.* 2022;51(11):1373-81. doi:10.1016/j.ijom.2022.02.015
- 14. Heng HPS, Shu C, Zheng W, Lin K, Huang Z. Advances in real-time fiber-optic Raman spectroscopy for early cancer diagnosis: pushing the frontier into clinical endoscopic applications. *Transl Biophotonics*. 2021;3(1):e202000018. doi:10.1002/tbio.202000018

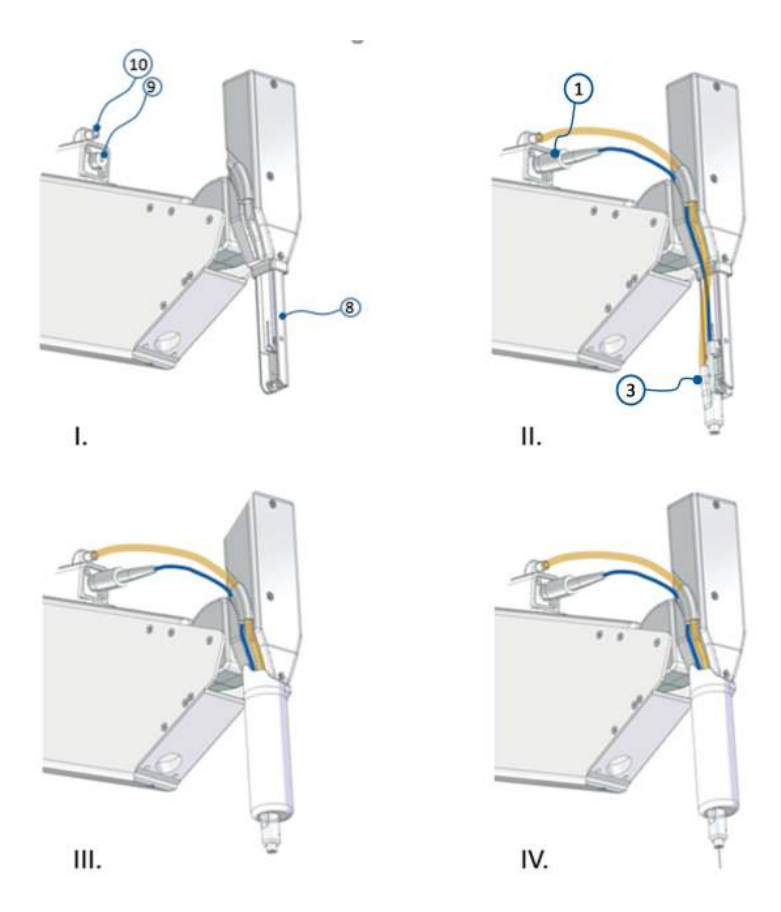
- Lizio MG, Boitor R, Notingher I. Selective-sampling Raman imaging techniques for ex vivo assessment of surgical margins in cancer surgery. *Analyst*. 2021;146(12):3799-809. doi:10.1039/D1AN00296A
- 16. Byrne HJ, Behl I, Calado G, et al. Biomedical applications of vibrational spectroscopy: oral cancer diagnostics. *Spectrochim Acta A Mol Biomol Spectrosc.* 2021;252:119470. doi:10.1016/j.saa.2021.119470
- 17. Azemtsop Matanfack G, Rüger J, Stiebing C, Schmitt M, Popp J. Imaging the invisible—bioorthogonal Raman probes for imaging of cells and tissues. *J Biophotonics*. 2020;13(9):e202000129. doi:10.1002/jbio.202000129
- 18. Hubbard TJE, Shore A, Stone N. Raman spectroscopy for rapid intra-operative margin analysis of surgically excised tumour specimens. *Analyst*. 2019;144(22):6479-96. doi:10.1039/C9AN01163C
- 19. Bury D, Morais C, Ashton K, Dawson T, Martin F. Ex vivo Raman spectrochemical analysis using a handheld probe demonstrates high predictive capability of brain tumour status. *Biosensors*. 2019;9(2):49. doi:10.3390/bios9020049
- 20. Koljenovic S, Bakker Schut TC, Wolthuis R, et al. Tissue characterization using high wave number Raman spectroscopy. *J Biomed Opt.* 2005;10(3):031116. doi:10.1117/1.1922307
- Santos IP, Caspers PJ, Bakker Schut TC, et al. Raman spectroscopic characterization of melanoma and benign melanocytic lesions suspected of melanoma using high-wavenumber Raman spectroscopy. *Anal Chem.* 2016;88(15):7683-8. doi:10.1021/acs.analchem.6b01592
- 22. Wolthuis R, Schut TCB, Caspers PJ, et al. Raman spectroscopic methods for in vitro and in vivo tissue characterization. In: *Fluorescent and Luminescent Probes for Biological Activity*. Elsevier; 1999:433-55. doi:10.1016/B978-012447836-7/50034-8
- 23. Caspers PJ, Bruining HA, Puppels GJ, Lucassen GW, Carter EA. In vivo confocal Raman microspectroscopy of the skin: noninvasive determination of molecular concentration profiles. *J Invest Dermatol*. 2001;116(3):434-42. doi:10.1046/j.1523-1747.2001.01258.x
- 24. Barroso EM, Smits RWH, Bakker Schut TC, et al. Discrimination between oral cancer and healthy tissue based on water content determined by Raman spectroscopy. *Anal Chem*. 2015;87(4):2419-26. doi:10.1021/ac504362y
- 25. Barroso EM, Smits RWH, van Lanschot CGF, et al. Water concentration analysis by Raman spectroscopy to determine the location of the tumor border in oral cancer surgery. *Cancer Res.* 2016;76(20):5945-53. doi:10.1158/0008-5472.CAN-16-1227
- 26. Barroso EM, ten Hove I, Bakker Schut TC, et al. Raman spectroscopy for assessment of bone resection margins in mandibulectomy for oral cavity squamous cell carcinoma. *Eur J Cancer*. 2018;92:77-87. doi:10.1016/j.ejca.2018.01.068
- 27. Choe C, Lademann J, Darvin ME. Confocal Raman microscopy for investigating the penetration of various oils into the human skin in vivo. *J Dermatol Sci.* 2015;79(2):176-8. doi:10.1016/j.jdermsci.2015.05.004
- 28. Czamara K, Majka Z, Sternak M, et al. Distinct chemical changes in abdominal but not in thoracic aorta upon atherosclerosis studied using fiber optic Raman spectroscopy. *Int J Mol Sci.* 2020;21(14):4838. doi:10.3390/ijms21144838

- 29. Kang CJ, Wen YW, Lee SR, et al. Surgical margins status and prognosis after resection of oral cavity squamous cell carcinoma: results from a Taiwanese nationwide registry-based study. *Cancers* (*Basel*). 2021;14(1):15. doi:10.3390/cancers14010015
- 30. van Lanschot CGF, Mast H, Hardillo JA, et al. Relocation of inadequate resection margins in the wound bed during oral cavity oncological surgery: a feasibility study. *Head Neck*. 2019;41(7):2159-66. doi:10.1002/hed.25690
- 31. Santos IP, Barroso EM, Bakker Schut TC, et al. Raman spectroscopy for cancer detection and cancer surgery guidance: translation to the clinics. *Analyst*. 2017;142(17):3025-47. doi:10.1039/C7AN00957G

SUPPLEMENTARY INFORMATION

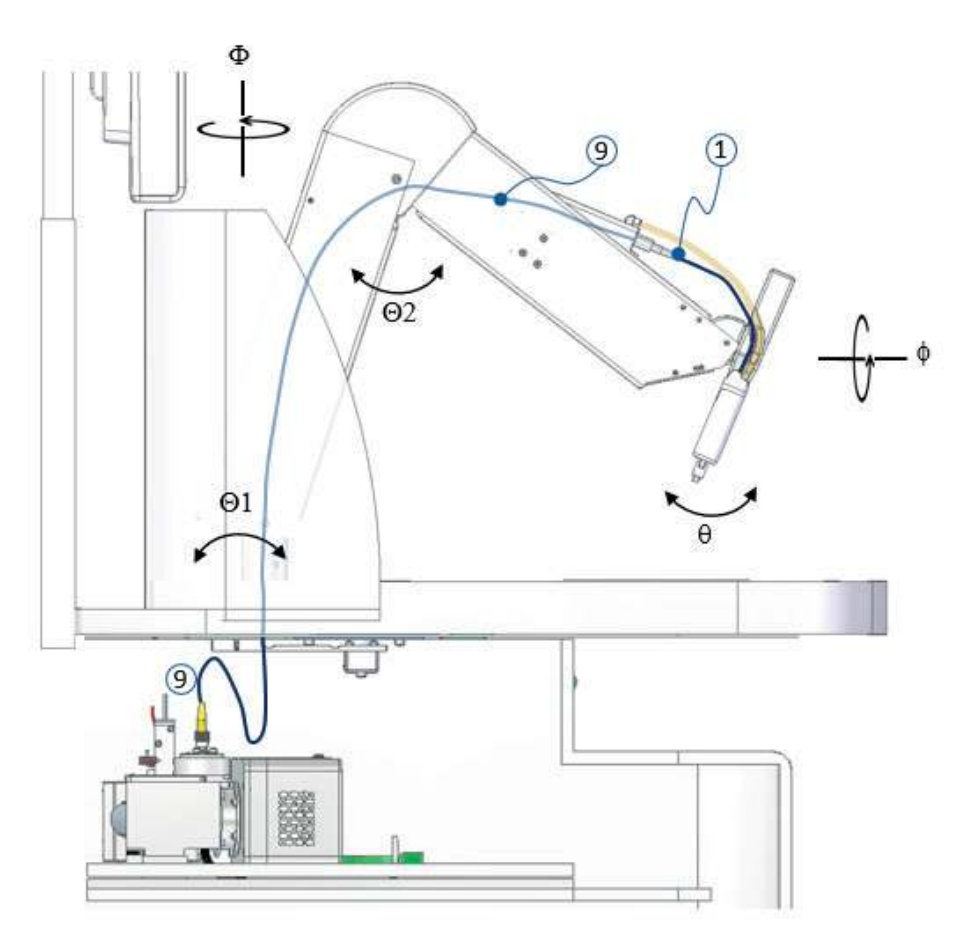
S1 RIOARM-device

The technical details of the RIOARM-device are illustrated in Supplementary Figure. 1 to 3. Supplementary Figure. 1 shows the connection of the fiber-optic needle probe and the vacuum tubing to the position arm of the device. Supplementary Figure. 2 illustrates the 5 degrees of freedom for positioning the fiber-optic probe perpendicular to the tissue. Supplementary Figure. 3 shows the connection of fiber-optic needle probe to Raman module and illustrates the technical details of Raman module.

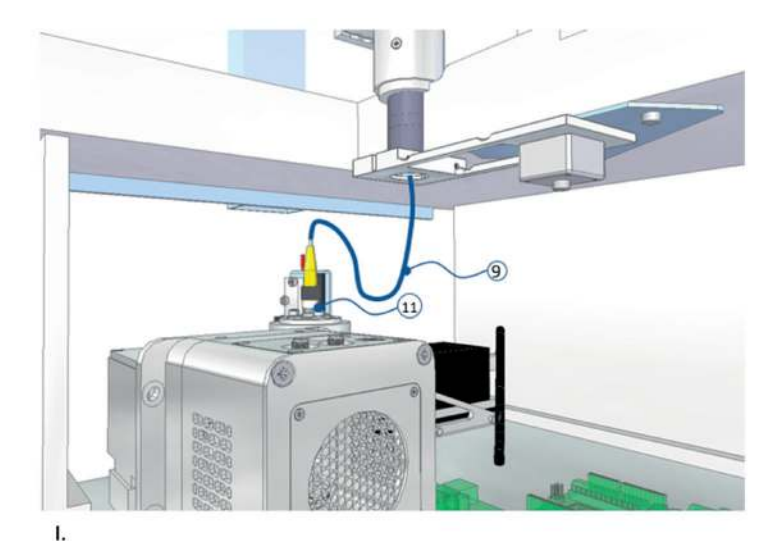


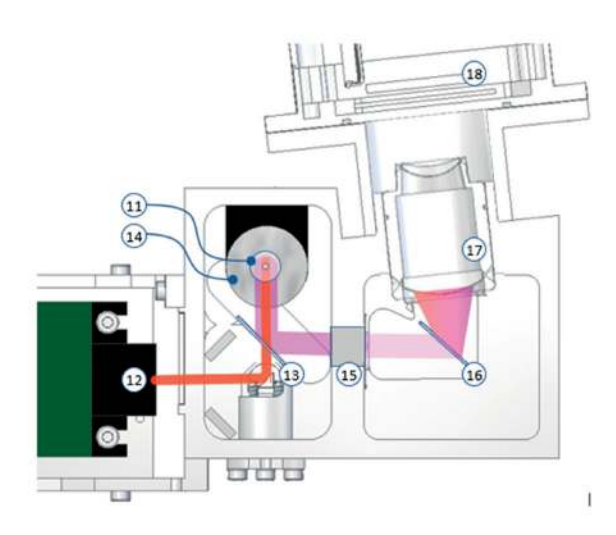
Supplementary Figure.1 | Connection of the fiber-optic needle probe to the positioning arm Panels I. and II: The disposable fiber-optic needle probe is fixed to part 8 of the device positioning arm. The FC/PC connector 1 at its proximal end connects to the positioning arm, by means of which the probe optical fiber (blue) is butt-coupled to the fiber optic patch cord 9 running inside the positioning arm. Vacuum tubing (yellow) connects vacuum port 10 of the positioning arm to vacuum port 3 of the fiber-optic needle probe. Vacuum port 10 is connected to a vacuum pump (not shown).

Panel III.: a protective housing is placed over the fiber-optic needle probe after fixation to the positioning arm. Panel IV.: fiber-optic needle probe with the needle fully extended.



Supplementary Figure.2| Positioning arm. The positioning arm of the Raman-RIOARM-device has 5 degrees of rotational freedom. This enables XYZ-positioning of the tip of the fiber-optic needle probe, perpendicular to the tissue surface.





Supplementary Figure.3 | Raman module

II.

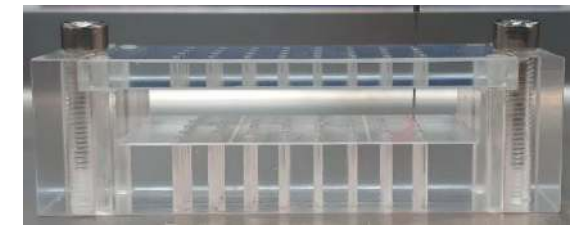
Panel I. Connection of fiber-optic needle probe to Raman module. Fiber patch cord 9 runs through the positioning arm and is connected to the fiber port 11 of the Raman module of the RIOARM-device.

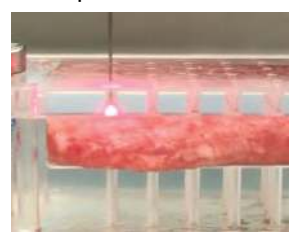
Panel II. Top view of the custom-designed Raman Module of the RIOARM-device (RiverD International, The Netherlands). 671 nm laser light from a diode-pumped solid state laser 12 (Gem671, 50 mW-250 mW, Laser Quantum, UK) is focused by a parabolic mirror 14 (Thorlabs MPD129-P01) into the core of fiber patch cord 9 (Panel I.), passing through dichroic mirror 13 (Semrock FF750-SiDiO2). Raman scattered light is received from patch cord 9, collimated by parabolic mirror 14 and reflected by dichroic mirror 13. A color glass filter 15 (Schott RG715-10-SAR) is used to suppress laser light intensity, before the Raman scattered light enters the spectrometer part of the Raman module. A fused silica transmission diffraction grating 16 (LightSmyth Technologies Inc. T-1702-895) is used to disperse the Raman scattered light. A custom designed projection lens assembly 17 is used to project the 2600-4000 cm⁻¹ spectral interval onto back-illuminated deep depletion charge coupled device (CCD) chip of a cooled CCD-camera 18 (Andor iVac, 316 LDC-DD, Andor Technology Ltd., UK).

S2 Experimental determination of depth resolution

The depth resolution of the fiber-optic needle probe was experimentally determined by measuring the Raman signal intensity of calf tongue tissue while the needle crossed the tissue-air interface.

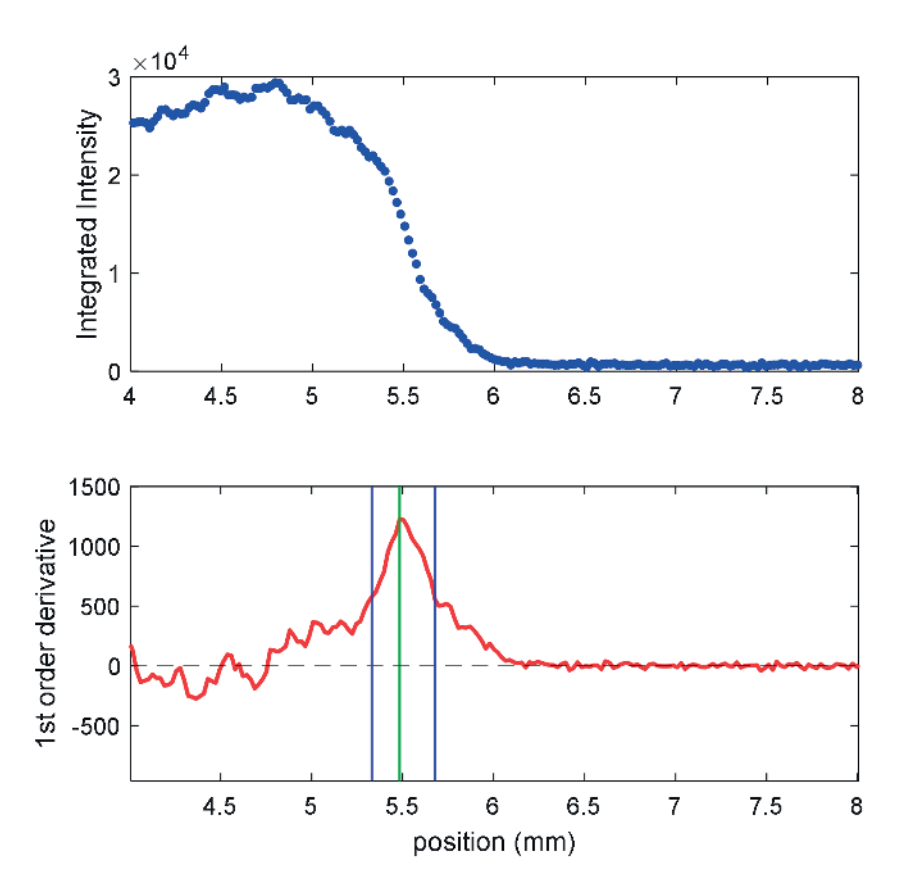
The setup for these measurements is shown in Supplementary **Figure. 4**, left panel. A 5 mm-slice of tissue was fixed between two horizontal PMMA (polymethylmetacrylate)-plates, both with an array of through-holes of 1 mm in diameter. For each measurement, the fiber-optic needle was aligned with one of the holes in the top plate and moved to the tissue surface (Supplementary **Figure. 4**, right panel). Raman spectra were acquired while the needle was moved through the tissue in 20 μ m steps, with an exposure time of 0.1 s.





Supplementary Figure.4| Experimental setup for determination of the depth resolution of the fiber-optic needle

A response curve was obtained by plotting the integrated Raman signal intensity in the 2710 to 3800 cm⁻¹ spectral interval (after subtraction of autofluorescence background (as described in the Method section) as a function of needle position (Supplementary **Figure. 5** top panel). The first order derivative of the response curve shows a maximum (Supplementary **Figure. 5** bottom panel). The full width at half maximum (FWHM) was used as measure of depth resolution.



Supplementary Figure.5 | Example of a measurement result for determination of fiber-optic needle depth resolution: Top: Response curve: Raman signal intensity as function fiber-optic needle position. Bottom: first order derivative of the response curve. Green line demarcates the position of the maximum; Blue lines mark the FWHM-positions Response curves were obtained at 8 different positions. A mean depth resolution of 0.34 mm was found, as shown in Supplementary Table 1.

S3 Supplementary Tables

Supplementary Table 1 | Determination of the depth resolution.

FWHM (mm)
0.28
0.39
0.31
0.39
0.28
0.34
0.38
0.32
0.34

Supplementary Table 2 | Tissue classification model: patient and tumor characteristics.

	Times lesstion	
Data set	Tumor location	pTNM
Development	Buccal mucosa	T3N3b
Development	Tongue	T3N2b
Development	Tongue	T2
Development	Floor of the mouth	T1
Development	Floor of the mouth	T2N0
Development	Tongue	T3
Development	Tongue	T3N0
Development	Buccal mucosa	T2
Development	Tongue	T2
Development	Buccal mucosa	T4aN0
Development	Tongue	T2N2b
Development	Tongue	T3N0
Development	Tongue	T4a
Development	Tongue	T1
Development	Tongue	T3N1
Development	Floor of the mouth	T2N2b
Development	Tongue	T3N2b
Development	Tongue	T3N0
Development	Tongue	T3N1
Development	Buccal mucosa	T2N1
Development	Tongue	T2N0
Development	Tongue	T4aN0
Development	Tongue	T2N1
Development	Tongue/Floor of mouth	T2N0
Development	Floor of mouth/Tongue	T2N1
Validation	Tongue	T1
Validation	Floor of mouth/Tongue	T3N3b
Validation	Floor of the mouth	T1
Validation	Tongue	T1
Validation	Buccal mucosa	T4aN2b
Validation	Floor of the mouth	T4aN0
Validation	Tongue	T3N3b
Validation	Tongue	T2
Validation	Tongue	Т3
Validation	Tongue	T2
Validation	Tongue	T2
Validation	Tongue	T3N3b
Validation	Floor of the mouth	T4aN0
Validation	Tongue	T2
Validation	Tongue	T2N0

Supplementary Table 3 | Margin length prediction model: patient and tumor characteristics.

Development Tongue T1 Development Tongue T1N3b Development Tongue T2N0 Development Tongue T2N0 Development Tongue T4AN0 Development Tongue T4AN0 Development Tongue T4AN0 Development Floor of mouth T1N0 Development Floor of mouth T2N0 Development Floor of mouth T2N0 Development Floor of mouth T2 Development Floor of mouth T3 Development Floor of mouth T3 Development Floor of mouth T4AN1 Development Gingiva maxilla T2N1 Development Gingiva maxilla T2N1 Development Buccal mucosa T2N1 Development Buccal mucosa T1N1 Development Buccal mucosa T1 Valdiation Tongue T2 Validation Tongue T2N1 Validation Tongue T2N3b Validation Floor of mouth T1 Validation Floor of mouth T1 Validation Floor of mouth T2 Validation Floor of mouth T1 Validation Floor of mouth T2 Validation Floor of mouth T4AN0 Validation Gingiva mandible T1 Validation Gingiva mandible T2N0 Validation Buccal mucosa T4AN0 Validation Buccal mucosa T1N0	Data set	Tumor location	рТИМ
Development Tongue T1N3b Development Tongue T2N0 Development Tongue T4AN0 Development Floor of mouth T1N0 Development Floor of mouth T2N0 Development Floor of mouth T2N0 Development Floor of mouth T2N0 Development Floor of mouth T3 Development Floor of mouth T3 Development Floor of mouth T4AN1 Development Gingiva maxilla T2N1 Development Gingiva mandible T4a Development Buccal mucosa T2N1 Development Buccal mucosa T1 Valdiation Tongue T2 Validation Tongue T3N0 Validation Tongue T3N0 Validation Tongue T2N1 Validation Tongue T2N3b Validation Floor of mouth T1 Validation Floor of mouth T1 Validation Floor of mouth T2 Validation Floor of mouth T4AN0 Validation Gingiva mandible T1 Validation Gingiva mandible T2N0 Validation Gingiva mandible T2N0	Development	Tongue	T1
Development Tongue T2NO Development Tongue T4aNO Development Floor of mouth T1NO Development Floor of mouth T2NO Development Floor of mouth T2NO Development Floor of mouth T2NO Development Floor of mouth T3 Development Floor of mouth T4aN1 Development Gingiva maxilla T2N1 Development Gingiva mandible T4a Development Buccal mucosa T2N1 Development Buccal mucosa T1 Valdiation Tongue T2 Validation Tongue T3NO Validation Tongue T2N3b Validation Floor of mouth T1 Validation Floor of mouth T1 Validation Floor of mouth T1 Validation Floor of mouth T2 Validation Floor of mouth T4aNO Validation Gingiva mandible T1 Validation Gingiva mandible T2NO Validation Buccal mucosa T4aNO	Development	Tongue	T1
Development Floor of mouth T1NO Development Floor of mouth T2NO Development Floor of mouth T2NO Development Floor of mouth T2 Development Floor of mouth T3 Development Floor of mouth T3 Development Floor of mouth T4AN1 Development Gingiva maxilla T2N1 Development Gingiva mandible T4a Development Buccal mucosa T2N1 Development Buccal mucosa T1 Valdiation Tongue T2 Validation Tongue T3NO Validation Tongue T2N3b Validation Floor of mouth T1 Validation Floor of mouth T1 Validation Floor of mouth T2 Validation Floor of mouth T4aNO Validation Gingiva mandible T1 Validation Gingiva mandible T2NO Validation Buccal mucosa T4aNO	Development	Tongue	T1N3b
Development Floor of mouth T1N0 Development Floor of mouth T2N0 Development Floor of mouth T2 Development Floor of mouth T3 Development Floor of mouth T3 Development Floor of mouth T4aN1 Development Gingiva maxilla T2N1 Development Gingiva mandible T4a Development Buccal mucosa T2N1 Development Buccal mucosa T1 Valdiation Tongue T2 Validation Tongue T3N0 Validation Tongue T3N0 Validation Tongue T2N3b Validation Floor of mouth T1 Validation Floor of mouth T1 Validation Floor of mouth T1 Validation Floor of mouth T2 Validation Floor of mouth T4aN0 Validation Gingiva mandible T1 Validation Gingiva mandible T2N0 Validation Gingiva mandible T2N0 Validation Gingiva mandible T2N0 Validation Gingiva mandible T2N0	Development	Tongue	T2N0
Development Floor of mouth T2NO Development Floor of mouth T2 Development Floor of mouth T3 Development Floor of mouth T4aN1 Development Gingiva maxilla T2N1 Development Gingiva mandible T4a Development Buccal mucosa T2N1 Development Buccal mucosa T1 Valdiation Tongue T2 Validation Tongue T3NO Validation Tongue T2N1 Validation Tongue T2N3b Validation Floor of mouth T1 Validation Floor of mouth T2 Validation Floor of mouth T1 Validation Floor of mouth T2 Validation Floor of mouth T4aNO Validation Gingiva mandible T1 Validation Gingiva mandible T2NO Validation Gingiva mandible T2NO Validation Gingiva mandible T2NO	Development	Tongue	T4aN0
Development Floor of mouth T2 Development Floor of mouth T3 Development Floor of mouth T4aN1 Development Gingiva maxilla T2N1 Development Gingiva mandible T4a Development Buccal mucosa T2N1 Development Buccal mucosa T1 Valdiation Tongue T2 Validation Tongue T3N0 Validation Tongue T2N1 Validation Tongue T2N3b Validation Tongue T2N3b Validation Floor of mouth T1 Validation Floor of mouth T2 Validation Floor of mouth T2 Validation Floor of mouth T1 Validation Floor of mouth T2 Validation Floor of mouth T4aN0 Validation Gingiva mandible T1 Validation Gingiva mandible T2N0 Validation Gingiva mandible T2N0 Validation Buccal mucosa T4aN0	Development	Floor of mouth	T1N0
Development Floor of mouth T3 Development Floor of mouth T4aN1 Development Gingiva maxilla T2N1 Development Gingiva maxilla T2N1 Development Buccal mucosa T2N1 Development Buccal mucosa T1 Valdiation Tongue T2 Validation Tongue T3N0 Validation Tongue T2N3b Validation Floor of mouth T1 Validation Floor of mouth T1 Validation Floor of mouth T1 Validation Floor of mouth T2 Validation Floor of mouth T4aN0 Validation Gingiva mandible T1 Validation Gingiva mandible T2N0 Validation Buccal mucosa T4aN0	Development	Floor of mouth	T2N0
Development Floor of mouth T4aN1 Development Gingiva maxilla T2N1 Development Gingiva mandible T4a Development Buccal mucosa T2N1 Development Buccal mucosa T1 Valdiation Tongue T2 Validation Tongue T3N0 Validation Tongue T3N0 Validation Tongue T2N3b Validation Tongue T2N3b Validation Floor of mouth T1 Validation Floor of mouth T2 Validation Floor of mouth T1 Validation Floor of mouth T1 Validation Floor of mouth T2 Validation Floor of mouth T4aN0 Validation Gingiva mandible T1 Validation Gingiva mandible T2N0 Validation Buccal mucosa T4aN0	Development	Floor of mouth	T2
DevelopmentGingiva maxillaT2N1DevelopmentBuccal mucosaT2N1DevelopmentBuccal mucosaT1ValdiationTongueT2ValidationTongueT2ValidationTongueT2N1ValidationTongueT2ValidationTongueT2ValidationTongueT2ValidationTongueT3N0ValidationTongueT2N3bValidationFloor of mouthT1ValidationFloor of mouthT2ValidationFloor of mouthT1ValidationFloor of mouthT2N2bValidationFloor of mouthT2ValidationFloor of mouthT2ValidationFloor of mouthT2ValidationFloor of mouthT2ValidationFloor of mouthT4aN0ValidationGingiva mandibleT1ValidationGingiva mandibleT2N0ValidationBuccal mucosaT4aN0	Development	Floor of mouth	T3
Development Gingiva mandible T4a Development Buccal mucosa T2N1 Development Buccal mucosa T1 Valdiation Tongue T2 Validation Tongue T3N0 Validation Tongue T2N3b Validation Tongue T2N3b Validation Floor of mouth T1 Validation Floor of mouth T2 Validation Floor of mouth T1 Validation Floor of mouth T2 Validation Floor of mouth T4aN0 Validation Gingiva mandible T1 Validation Gingiva mandible T2N0 Validation Buccal mucosa T4aN0	Development	Floor of mouth	T4aN1
Development Buccal mucosa T2N1 Development Buccal mucosa T1 Valdiation Tongue T2 Validation Tongue T2 Validation Tongue T2N1 Validation Tongue T2N1 Validation Tongue T2 Validation Tongue T2 Validation Tongue T3N0 Validation Tongue T2N3b Validation Tongue T2N3b Validation Floor of mouth T1 Validation Floor of mouth T2 Validation Floor of mouth T1 Validation Floor of mouth T2 Validation Floor of mouth T4aN0 Validation Gingiva mandible T1 Validation Gingiva mandible T2N0 Validation Buccal mucosa T4aN0	Development	Gingiva maxilla	T2N1
Development Buccal mucosa T1 Valdiation Tongue T2 Validation Tongue T2 Validation Tongue T2N1 Validation Tongue T2 Validation Tongue T2 Validation Tongue T3N0 Validation Tongue T3N0 Validation Tongue T2N3b Validation Tongue T2N3b Validation Floor of mouth T1 Validation Floor of mouth T2 Validation Floor of mouth T1 Validation Floor of mouth T1 Validation Floor of mouth T2 Validation Floor of mouth T4aN0 Validation Gingiva mandible T1 Validation Gingiva mandible T2N0 Validation Buccal mucosa T4aN0	Development	Gingiva mandible	T4a
ValdiationTongueT2ValidationTongueT2ValidationTongueT2N1ValidationTongueT2ValidationTongueT3N0ValidationTongueT2N3bValidationFloor of mouthT1ValidationFloor of mouthT2ValidationFloor of mouthT1ValidationFloor of mouthT2ValidationFloor of mouthT2ValidationFloor of mouthT2ValidationFloor of mouthT2ValidationFloor of mouthT4aN0ValidationGingiva mandibleT1ValidationGingiva mandibleT2N0ValidationBuccal mucosaT4aN0	Development	Buccal mucosa	T2N1
Validation Tongue T2 Validation Tongue T2N1 Validation Tongue T2 Validation Tongue T3N0 Validation Tongue T2N3b Validation Tongue T2N3b Validation Floor of mouth T1 Validation Floor of mouth T2 Validation Floor of mouth T1 Validation Floor of mouth T1 Validation Floor of mouth T2 Validation Floor of mouth T2N2b Validation Floor of mouth T2 Validation Floor of mouth T4aN0 Validation Gingiva mandible T1 Validation Gingiva mandible T2N0 Validation Buccal mucosa T4aN0	Development	Buccal mucosa	T1
Validation Tongue T2N1 Validation Tongue T2 Validation Tongue T3N0 Validation Tongue T2N3b Validation Floor of mouth T1 Validation Floor of mouth T2 Validation Floor of mouth T1 Validation Floor of mouth T1 Validation Floor of mouth T2 Validation Floor of mouth T2N2b Validation Floor of mouth T2 Validation Floor of mouth T4aN0 Validation Gingiva mandible T1 Validation Gingiva mandible T2N0 Validation Buccal mucosa T4aN0	Valdiation	Tongue	T2
Validation Tongue T2 Validation Tongue T3N0 Validation Tongue T2N3b Validation Floor of mouth T1 Validation Floor of mouth T2 Validation Floor of mouth T1 Validation Floor of mouth T2 Validation Floor of mouth T2N2b Validation Floor of mouth T2 Validation Floor of mouth T4aN0 Validation Gingiva mandible T1 Validation Gingiva mandible T2N0 Validation Buccal mucosa T4aN0	Validation	Tongue	T2
Validation Tongue T3N0 Validation Tongue T2N3b Validation Floor of mouth T1 Validation Floor of mouth T2 Validation Floor of mouth T1 Validation Floor of mouth T2N2b Validation Floor of mouth T2N2b Validation Floor of mouth T2 Validation Floor of mouth T4aN0 Validation Gingiva mandible T1 Validation Gingiva mandible T2N0 Validation Buccal mucosa T4aN0	Validation	Tongue	T2N1
ValidationTongueT2N3bValidationFloor of mouthT1ValidationFloor of mouthT2ValidationFloor of mouthT1ValidationFloor of mouthT2N2bValidationFloor of mouthT2ValidationFloor of mouthT2ValidationFloor of mouthT2ValidationFloor of mouthT4aN0ValidationGingiva mandibleT1ValidationGingiva mandibleT2N0ValidationBuccal mucosaT4aN0	Validation	Tongue	T2
Validation Floor of mouth T1 Validation Floor of mouth T2 Validation Floor of mouth T1 Validation Floor of mouth T2N2b Validation Floor of mouth T2 Validation Floor of mouth T4aN0 Validation Gingiva mandible T1 Validation Gingiva mandible T2N0 Validation Buccal mucosa T4aN0	Validation	Tongue	T3N0
Validation Floor of mouth T2 Validation Floor of mouth T1 Validation Floor of mouth T2N2b Validation Floor of mouth T2 Validation Floor of mouth T2 Validation Floor of mouth T2 Validation Floor of mouth T4aN0 Validation Gingiva mandible T1 Validation Gingiva mandible T2N0 Validation Buccal mucosa T4aN0	Validation	Tongue	T2N3b
ValidationFloor of mouthT1ValidationFloor of mouthT2N2bValidationFloor of mouthT2ValidationFloor of mouthT2ValidationFloor of mouthT4aN0ValidationGingiva mandibleT1ValidationGingiva mandibleT2N0ValidationBuccal mucosaT4aN0	Validation	Floor of mouth	T1
Validation Floor of mouth T2N2b Validation Floor of mouth T2 Validation Floor of mouth T2 Validation Floor of mouth T4aN0 Validation Gingiva mandible T1 Validation Gingiva mandible T2N0 Validation Buccal mucosa T4aN0	Validation	Floor of mouth	T2
ValidationFloor of mouthT2ValidationFloor of mouthT2ValidationFloor of mouthT4aN0ValidationGingiva mandibleT1ValidationGingiva mandibleT2N0ValidationBuccal mucosaT4aN0	Validation	Floor of mouth	T1
ValidationFloor of mouthT2ValidationFloor of mouthT4aN0ValidationGingiva mandibleT1ValidationGingiva mandibleT2N0ValidationBuccal mucosaT4aN0	Validation	Floor of mouth	T2N2b
ValidationFloor of mouthT4aN0ValidationGingiva mandibleT1ValidationGingiva mandibleT2N0ValidationBuccal mucosaT4aN0	Validation	Floor of mouth	T2
ValidationGingiva mandibleT1ValidationGingiva mandibleT2N0ValidationBuccal mucosaT4aN0	Validation	Floor of mouth	T2
ValidationGingiva mandibleT2N0ValidationBuccal mucosaT4aN0	Validation	Floor of mouth	T4aN0
Validation Buccal mucosa T4aN0	Validation	Gingiva mandible	T1
	Validation	Gingiva mandible	T2N0
Validation Buccal mucosa T1N0	Validation	Buccal mucosa	T4aN0
	Validation	Buccal mucosa	T1N0

Supplementary Table 4 | Tumor probability profile shapes and decision rules for prediction of tumor border location (indicated by the position of the blue hatched line).

H1, H2, and H3: profile segments with tumor probability \geq 0.5.

L1, L2, and L3: profile segments with tumor probability < 0.5.

 H_{min} and L_{max} : threshold value parameters for optimization (see main text)

		Decision rules	
	Profile shape	Condition	Margin position
1 H	1 05 0 0 7	H1 = 7 mm	0
2	1 H1 U1	H1 ≥ H _{min} mm	0
HL	0 7	H1 < H _{min} mm	7
3 HLH	1 H1 H2 H2	$H1 \ge H_{min}$ mm $H1 < H_{min}$ mm & L1 < L _{max} mm	0
4	7	$H1 < H_{min}$ mm & $L1 \ge L_{max}$ mm $H1 \ge H_{min}$	start of H2 0
HLHL	1 H1 H2 L2	H1 < H_{min} mm & L1 < L_{max} mm & H2 $\geq H_{min}$ mm	0
	0 7	$H1 < H_{min}$ mm & $L1 \ge L_{max}$ mm & $H2 \ge H_{min}$ mm $H1 < H_{min}$ mm & $L1 \ge L_{max}$ mm & $H2 < H_{min}$ mm	start of H2 7
5		H1 > H _{min}	0
HLHLH	1 H1 H2 H3	H1 < H_{min} mm & L1 < L_{max} mm & H2 $\geq H_{min}$ mm H1 < H_{min} mm & L1 $\geq L_{max}$ mm & H2 $\geq H_{min}$ mm	0 start of H2
HEHEH	0.5 0 L1 L2 7	H1 < H_{min} mm & L1 \geq L_{max} mm & H2 < H_{min} mm & L2 \leq L_{max} mm & H2 < L_{min} mm & L2 < L_{max} mm	start of H2
		$\label{eq:hammon} \begin{array}{l} H1 < H_{min} \ mm \ \& \ L1 \geq L_{max} \ mm \ \& \ H2 < H_{min} \ mm \\ \& \ L2 \geq L_{max} \ mm \end{array}$	start of H3
6 L	0.5 0 L1	L1 = 7 mm	7
7	1 H1	H1 ≥ H _{min} mm	start of H1
LHL	0 12	H1 < H _{min} mm	7
8 LHLH	0.5 H1 H2	$H1 \ge H_{min}$ mm $H1 < H_{min}$ mm & L2 < L _{max} mm	start of H1 start of H1
LIILII	0 7	H1 < H_{min} mm & L2 $\geq L_{max}$ mm	start of H2
9	1	H1 ≥ H _{min}	start of H1
LHLHL	0.5 H1 H2 L3	$H1 < H_{min}$ mm & $L2 < L_{max}$ mm & $H2 \ge H_{min}$ mm	start of H1
40	0 7	$H1 < H_{min} \ mm \ \& \ L2 \ge L_{max} \ mm \ \& \ H2 \ge H_{min} \ mm$ $H1 < H_{min} \ mm \ \& \ L2 \ge L_{max} \ mm \ \& \ H2 < H_{min} \ mm$	start of H2 7
10 LHLHL+	1 H1 H2 H3 0.5 L1 L2 L3 L4	more than 4 transitions (more than 5 high/	inconclusive
HLHLH+	0 7	low segments)	conclusive

Supplementary Table 5 | Margin length decision rules for different tumor probability profiles, after optimization of H_{min} (4 mm) and L_{max} (2 mm).

	Profile	Interpretation	Drofile Interpretation Interpret	Profile	Interpretation
Profile shape	description	rule	Profile shape	description	rule
0.00	Ξ		14 0.5	НГНГН	H1 < 4 mm, L1 ≥ 2 mm, H2 < 4, L2 < 2
0.00	로	H1 ≥ 4 mm	15 0.5	НГНГН	H1 < 4 mm, L1 ≥ 2 mm, H2 < 4, L2 ≥ 2
0.00	보	H1 < 4 mm	16 0.5		
0.00	于	H1 ≥ 4 mm	17 0.5	5	
0.00	于	H1 < 4 mm, L1 < 2 mm	18 0.5	뉰	H1 ≥ 4 mm
000000000000000000000000000000000000000	무	H1 < 4 mm, L1 ≥ 2 mm	19 0.5	뉨	H1 < 4 mm
0.00	HLH	H1 ≥ 4 mm	20 05	HLH	H1 ≥ 4 mm
0.00	HLHL	H1 < 4 mm, L1 < 2 mm, H2 ≥ 4	21 0.5	HLH	H1 < 4 mm, L2 < 2 mm

Supplementary Table 5 | Margin length decision rules for different tumor probability profiles, after optimization of H_{min} (4 mm) and L_{max} (2 mm). (*continued*)

e Interpretation :ion rule	H1 < 4 mm, L2 ≥ 2 mm	L H1≥4 mm	L H1 < 4 mm, L2 < 2 mm, H2 ≥ 4 mm	L H1 < 4 mm, L2 ≥ 2 mm, H2 ≥ 4 mm	H1 < 4 mm, L2 ≥ 2 mm, H2 ≥ 4 mm
Profile description	ГНГН	LHLHL	CHLHL	LHLHL	ГНГНГ
Profile shape	2 mm, H2 ≥ 4 mm 2 00 1 2 3 4 5 6 7	2 mm, H2 < 4 mm 2 3 0.5 0.1 2 3 4 5 6 7	24 0.5	00 1 2 3 4 5 6 7	H1 < 4 mm, L1 ≥ 26 0.5 0.5 0.5 0.5 0.5 0.5 0.5 0.5 0.5 0.5
Interpretation rule	H1 < 4 mm, L1 ≥ 22 2 mm, H2 ≥ 4 mm	H1 < 4 mm, L1 ≥ 23 2 mm, H2 < 4 mm	H1 > 4 mm 24	H1 < 4 mm, L1 < 25 0.5	H1 < 4 mm, L1 ≥ 26 2 mm, H2 ≥ 4
Profile description	HH	HH	НГНГН	НГНГН	НГНГН
Profile shape	9 0.5	10 0.5	11 0.5	12 0.5	13 0.5



5 EXPERIMENTAL STUDY ON NEEDLE INSERTION FORCE TO MINIMIZE TISSUE DEFORMATION IN TONGUE TISSUE

Y. Aaboubout, M.R. Nunes Soares, E.M. Barroso, L.C. van der Sar, A. Bocharnikov, I. Usenov, V. Artyushenko, P.J. Caspers, S. Koljenovic, T.C. Bakker Schut, J.J. van den Dobbelsteen, G.J. Puppels.

Med Eng Phys. 2021 Nov;97:40-46



ABSTRACT

This study reports on the effects of insertion velocity, needle tip geometry and needle diameter on tissue deformation and maximum insertion force. Moreover, the effect of multiple insertions with the same needle on the maximum insertion force is reported. The tissue deformation and maximum insertion force strongly depend on the insertion velocity and the tip geometry. No correlation was found between the outer diameter and the maximum insertion force for small needles (30G - 32G). The endurance experiments showed no remarkable difference in the maximum insertion force during 100 insertions.

INTRODUCTION

Each year, more than 350.000 new cases of oral cavity cancer are diagnosed, with a mortality rate of >175.000 per year¹. Squamous cell carcinoma (SCC) counts for 90% of the cancers of the oral cavity². The primary treatment for this type of cancer is surgery. The goal of surgery is the complete removal of the tumor with an adequate resection margin (> 5 mm of healthy tissue surrounding the tumor). Resection margins are an important prognostic factor. Patients with adequate resections have less local recurrence of the tumor and improved overall survival³⁻⁹.

However, achieving adequate resections is often hard due to the complex anatomy of the oral cavity. The surgeon can only rely on visual inspection, palpation, and preoperative imaging during surgery. Recent studies showed that this approach led to adequate resections in only 15-26% of all cases¹⁰⁻¹².

The number of adequate resections can be increased by performing intraoperative assessment of the resection margins^{9,13}. At our institute, we perform intraoperative assessment based on visual inspection, palpation, and grossing of the freshly resected specimen, supported by frozen sections when needed¹⁴. However, this method is labor-intensive and subjective. Therefore, there is a need for an objective intraoperative tool to improve the rate of adequate resections in oral cavity squamous cell carcinoma (OCSCC) patients.

Healthy tissue and tumor have different molecular compositions that can be distinguished by Raman spectroscopy¹⁵. Raman spectroscopy is a non-destructive optical technique that may allow for (real-time) intraoperative assessment of the molecular composition of tissues. Therefore, we aim for the development of a device with a fiber-optic needle probe that can determine the resection margin based on Raman spectroscopy. The fiber-optic needle is driven into the resection specimen, from the resection surface towards the tumor, while the probe collects Raman signal continuously along the insertion path. By performing multiple insertions on the resection specimen, a complete assessment of all resection margins is possible.

With the Raman fiber-optic needle probe, we aim to determine the distance between the resection surface and the tumor border with a maximum error of 1 mm. Tissue deformation during needle insertion is one potential source of error, which we want to limit to ≤ 0.5 mm leaving 0.5 mm due to other potential sources of error. Moreover, for a complete assessment of all resection margins of a specimen, multiple insertions (up to 100 times) are required, which might lead to deterioration of the needle and

affect measurement accuracy. The main intent of this study is to gain insight into tissue deformation during needle insertion including the effect of multiple insertions. Needle-tissue interaction is well described in the literature 16-18.

The needle insertion is divided into 3 phases, namely boundary displacement, tip insertion, and tip and shaft insertion¹⁸. The boundary displacement phase starts with the needle making contact with the tissue boundary and ends with the puncturing event (breaching of the surface of the tissue). During this phase, the force and tissue deformation continues to grow until the end of the phase. The tip insertion phase starts with the breaching of the surface of the tissue and ends with the tissue surface sliding from the tip onto the shaft of the needle. This coincides in most cases with a drop of the force. The tip and shaft insertion phase starts after the tissue surface moved over the needle tip onto the shaft of the needle (the needle entered the tissue with the tip and first part of the shaft). This phase ends either with the needle being stopped or a new boundary is encountered internally in the tissue. These phases will be recurrent if different tissue properties or multiple internal structures are encountered during the needle insertion¹⁸.

The literature shows that force and tissue deformation are highly influenced by: (1) needle characteristics (diameter, tip geometry, coating, others), (2) insertion method (insertion velocity, drive mode, insertion process), and (3) tissue characteristics^{16,18}. All of these factors need to be taken into account when optimizing the proposed fiber-optic needle probe for intraoperative assessment. Specific studies on needle-tissue interaction in oral cavity tissue or phantoms/biologic materials that mimic the oral cavity are however lacking. In the current study, we therefore investigate the effect of needle velocity and needle characteristics on the deformation of tongue tissue during needle insertions. We also report on the effect of multiple insertions on the needle insertion force.

METHODS AND MATERIALS

Tested needles

Eight commercial needles (specified in **Table 5.1**), with different tip geometries and outer diameters, were selected for this study.

Tested materials

Calf tongue was used for testing, because of its similarity to the human tongue. The tongue is the most prevalent location for OCSCC 9,19,20 . Tissue blocks of 2 cm × 2 cm ×

2 cm were cut from a fresh calf tongue, to fit the transparent measurement container (Figure 5.1B). The tissue blocks always originated from the center of the tongue dorsum (Figure 5.1A).

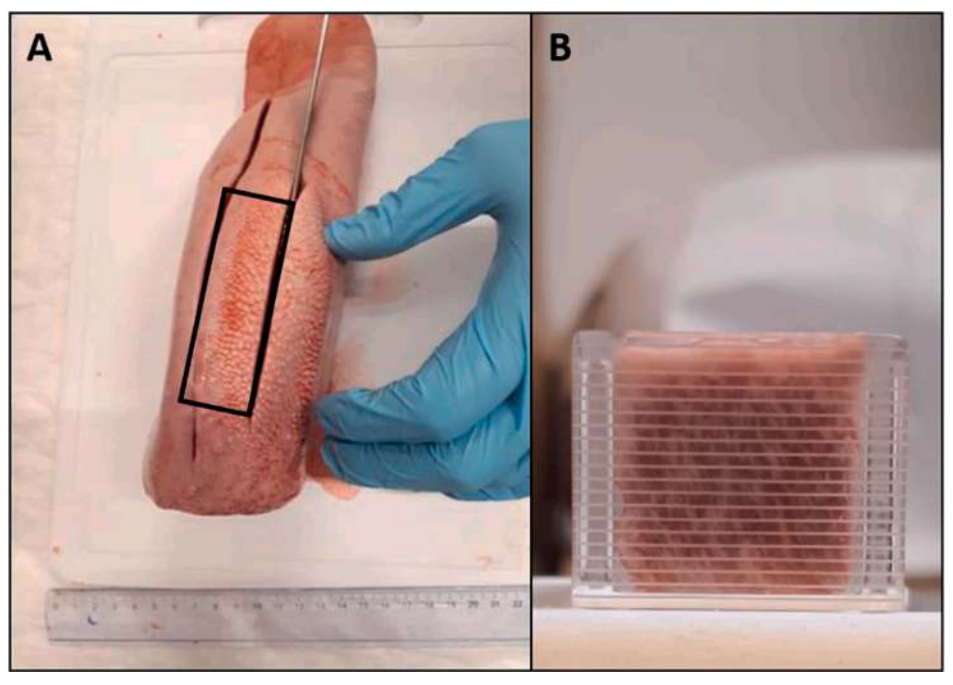


Figure 5.1. Calf tongue used for experiments. A. Cutting of the calf tongue, the black square indicates the area that was used for the experiments. B. Tissue blocks of $2 \text{ cm} \times 2 \text{ cm} \times 2 \text{ cm}$ in the transparent measurement container with engraved horizontal lines with a spacing of 1 mm.

Experimental setup

A force setup developed at the Faculty of Mechanical Engineering and Biomechanical Engineering at the Delft University of Technology was used to measure the maximum insertion force (**Figure 5.2**). The experimental setup consists of a linear stage (EGSL-BS-45-200-3P, Festo BV, Delft, The Netherlands) that moves in a vertical direction. Attached to the linear stage are a needle holder and an S-Beam Load Cell sensor (LSB200-FSH00104, FUTEK Advanced Sensor Technology Inc., Irvine, CA, USA). This sensor can register tension forces and compression forces. The sensor can read forces in the range of 0 to 10lbs (44.5 N). Four stage velocities (1 mm/s, 5 mm/s, 10 mm/s, and 20 mm/s) can be selected. The force sensor setup uses a MatLab interface for control and data acquisition.

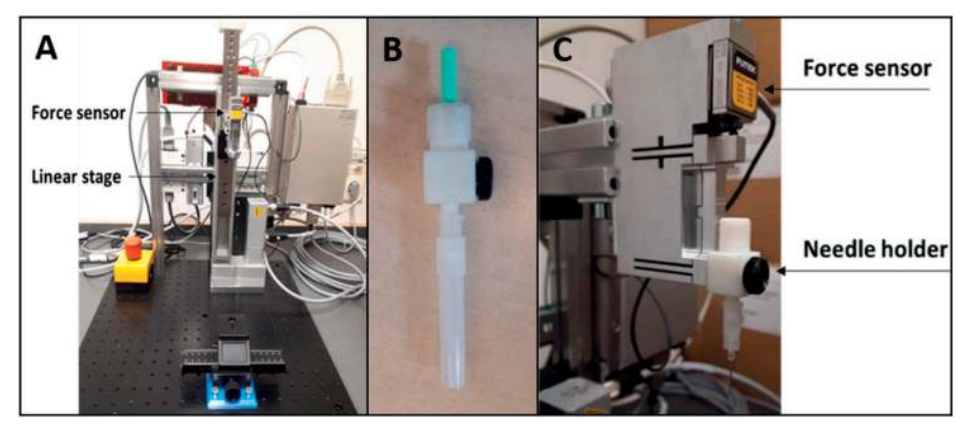


Figure 5.2. The setup to measure the insertion force. A. The force sensor is attached to a linear stage. B. The needle holder consisting of a Luer Lock (bottom part) and a 'Universal Lock' (top part). C. The needle holder is attached to the force sensor.

Table 5.1. List of needles

Label	Туре	Gauge	Ø(mm)	Tip shape	Material	Lubricant
3FB-Sterican 26G	Sterican*	26G	0.45	3 facet bevel	Stainless chromium nickels steel	Light silicone coating
3FB-Sterican 27G	Sterican*	27G	0.40	3 facet bevel	Stainless chromium nickels steel	Light silicone coating
3FB-Sterican 30G	Sterican*	30G	0.30	3 facet bevel	Stainless chromium nickels steel	Light silicone coating
Blunt- Sterican 27G	Sterican*	27G	0.40	Blunt (90 degrees)	Stainless chromium nickels steel	Light silicone coating
3FB-Omnican 30G	Omnican*	30G	0.30	3 facet bevel	Stainless chromium nickels steel	Light silicone coating
38B-Omnican 30G	Omnican**	30G	0.30	bevel 38 degrees	Stainless chromium nickels steel	Light silicone coating
Diamond- Clickfine 31 G	Clickfine***	31G	0.25	Diamond tip	Stainless steel	-
Diamond- Clickfine 32 G	Clickfine***	32G	0.23	Diamond tip	Stainless steel	-

^{*}Produced by B. Braun Holding GmbH & Co KG, Melsungen, Germany

 $^{^{\}star\star}$ Produced by B. Braun Holding GmbH & Co KG, Melsungen, Germany and adjusted to 38 degree bevel by art photonics GmbH, Berlin, Germany

^{***}Produced by Ypsomed AG, Burgdorf, Switzerland

Insertion protocol

Each needle was inserted into the tissue blocks at four different velocities: 1 mm/s, 5 mm/s, 10 mm/s, and 20 mm/s. To obtain a minimum required Raman signal quality the signal collection time should at least be 50-100 ms (based on other experiments). To achieve an accuracy of 1 mm for the determination of the margin a Raman measurement is needed every 0.5 mm (in accordance with the Nyquist theorem). This means that the maximum insertion velocity is 10 to 20 mm/s. We have also explored lower insertion velocities because this would allow longer Raman signal collection time and further improve Raman signal quality. For each velocity, five different insertions were performed. The needle was inserted perpendicularly to the tissue surface. To visualize tissue deformation, the insertions were performed close to the walls of the measurement containers. The needle was inserted each time at a different tissue location. For each needle, a new tissue block was used.

The measurement container has a scale that consists of engraved horizontal lines with a spacing of 1 mm. This scale was used to measure tissue deformation. A camera was placed next to the container and each insertion was video recorded to determine the deformation. Deformation was defined as the deepest point of tissue compression visible on the engraved raster on the measurement container. The average tissue deformation (mm) was calculated per needle and insertion velocity.

The needles with a deformation ≤ 0.5 mm were selected for the endurance experiments. Each selected needle was inserted into tongue tissue up to 100 times using the measurement container. The needle was inserted each time at a different tissue location. The maximum insertion force was collected for each insertion and plotted as a function of the number of insertions. The endurance experiments were performed with the best performing insertion velocities (10 mm/s and 20 mm/s) based on the first set of experiments.

Data processing

During needle insertion, the sensor signal (voltage) was recorded as a function of time. The voltage readings were converted into force (N) using a set of calibration measurements. Five calibration discs with known masses (93.8 g, 69.5 g, 43.3 g, 21.1 g, 0 g) were used. The voltage induced in the sensor by each disc was recorded while the disc was hanging from the needle holder and plotted as a function of the force exerted by the disk (**Figure 5.3**). A first-order polynomial regression of calibration data was used to convert the voltage to force (N): $V = 0.12 \times F - 4.87$ (**Figure 5.3**).

For this study, the maximum insertion force was considered to evaluate and compare the performance of the needles. The maximum force (N) of each needle insertion was determined by finding the maximum value in the force curve (**Figure 5.4**). The maximum forces of the 5 insertions performed with the same needle and with the same velocity were averaged.

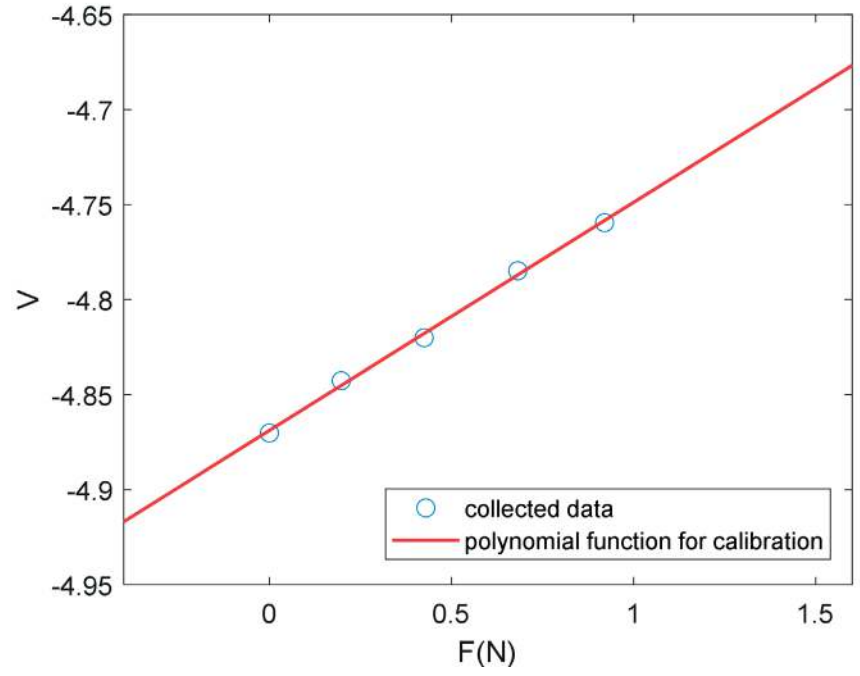


Figure 5.3. Graphical representation of voltage as a function of force (N) and polynomial approximation: V = 0.12*F - 4.87.

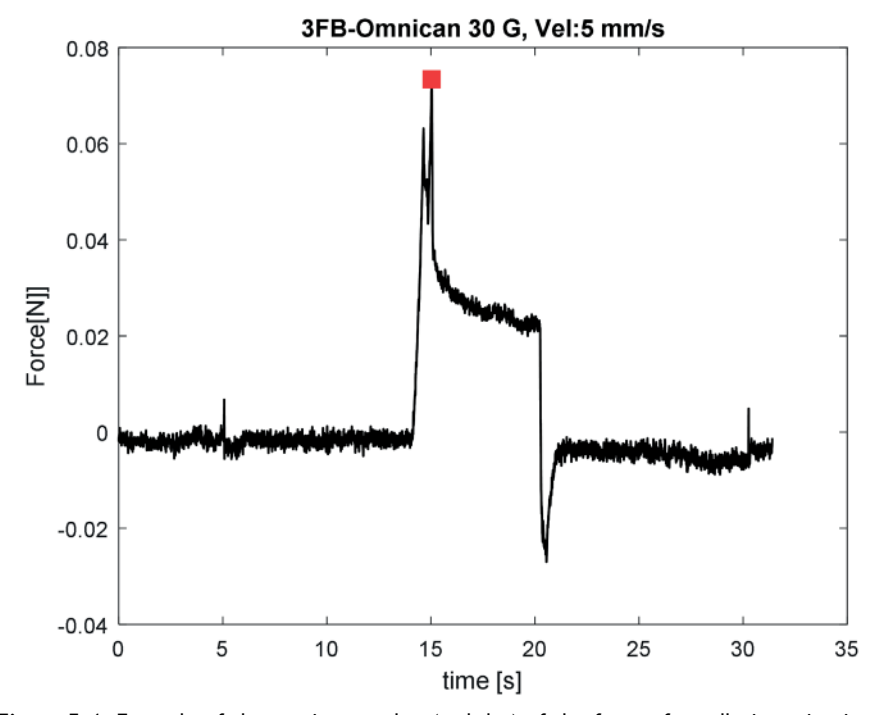


Figure 5.4. Example of the maximum value (red dot) of the force of needle insertion in tongue tissue.

RESULTS

Figure 5.5 shows the force profiles (insertion force as a function of time) on the needle during insertions in tongue tissue at a velocity of 5 mm/s. What can be observed is that, after the needle touches the tissue, there is an increase in the insertion force until the tissue surface is punctured. After the puncture, there is a decrease in the insertion force. For most of the tested needles, the insertion is accompanied by multiple puncture events that can be identified by several peaks in the force profile. Figure 5.6A shows tissue deformation and maximum insertion force for all tested needles, at different insertion velocities. The values of deformation and maximum force are averages of 5 insertions. The needle with blunt tip geometry (see also Figure 5.5D) showed a much higher insertion force and tissue deformation than other needles. Figure 5.6B zooms in on the other seven needle types.

The remaining needles (3FB-Omnican 30G, 38B-Omnican 30G, Diamond 31G, and Diamond 32G) show the lowest insertion force.

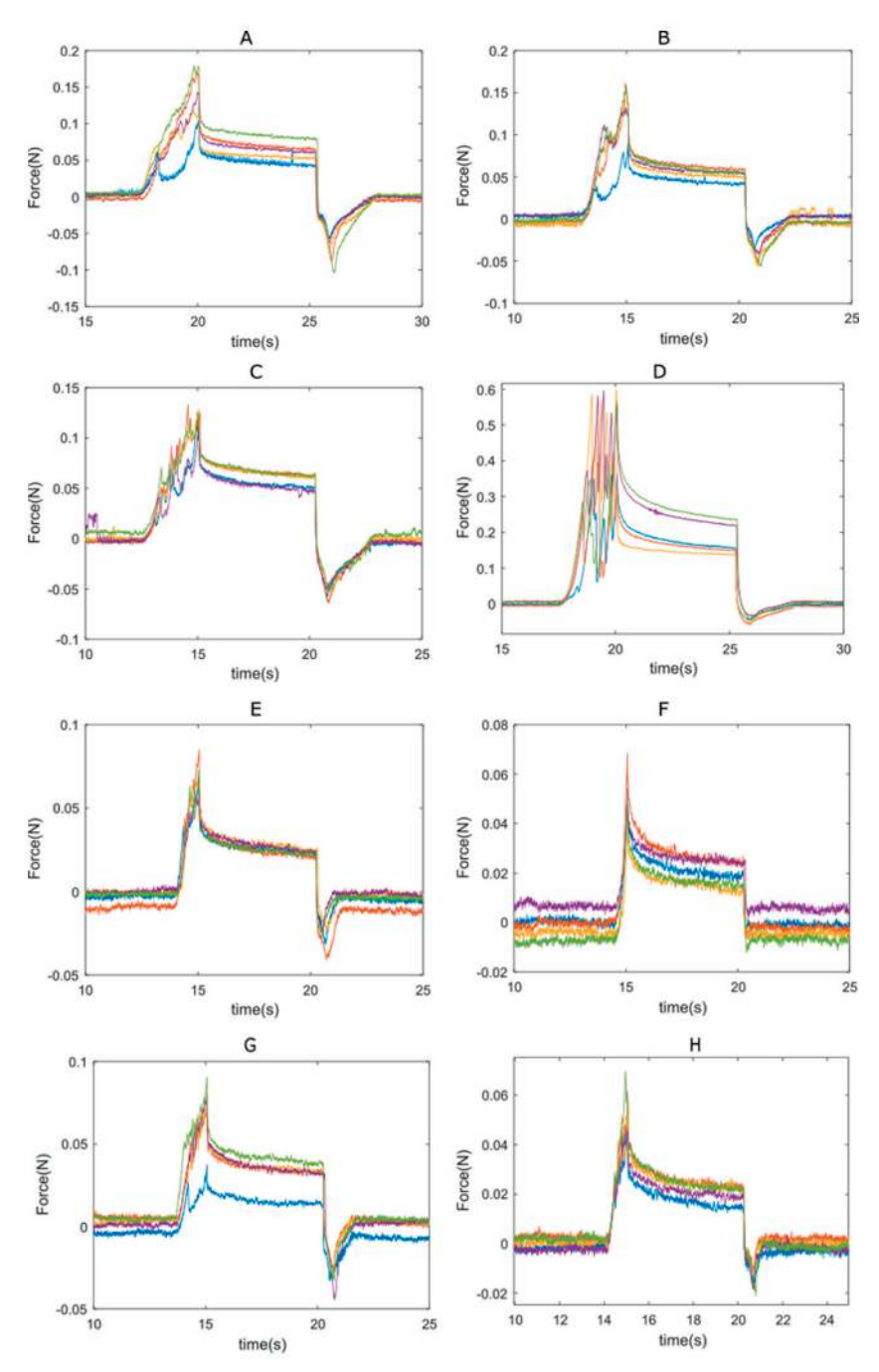


Figure 5.5. Typical insertion force profiles for each of the eight tested needle types, obtained for an insertion velocity of 5 mm/s. A. 3FB-Sterican 26G; B. 3FB-Sterican 27G; C. 3FB-Sterican 30G; D.Blunt 27G; E. 3FB-Omnican 30G; F. 38B-Omnican 30G; G. Diamond-Clickfine 31G; H Diamond-Clickfine 32G

The effect of increasing insertion velocity on the tissue deformation for these four needles is illustrated in **Figure 5.6C**. Clearly, a higher insertion velocity results in a decrease in tissue deformation.

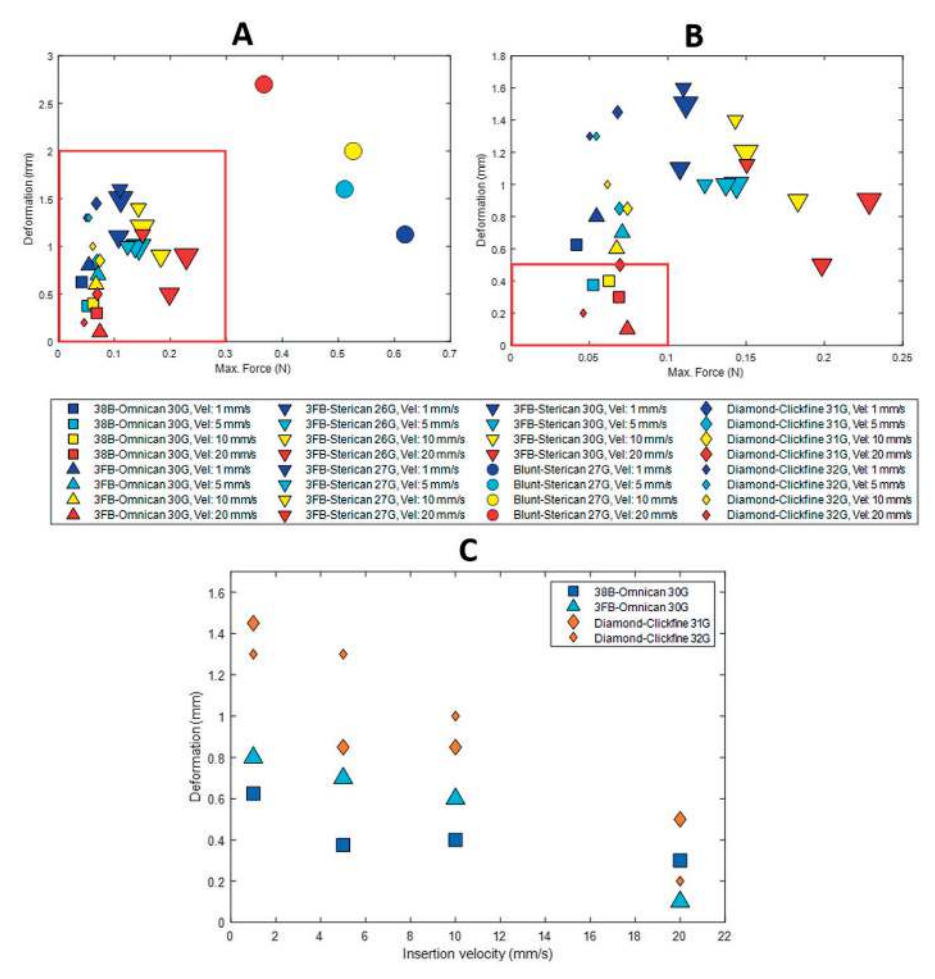


Figure 5.6. The size of the symbols is correlated with the diameter of the needles. A. Deformation versus maximum insertion force for all insertion velocities and needles. B. Showing all needles in the red rectangle of A, excluding the needle with the blunt tip geometry. C. Deformation as a function of insertion velocity for the needles that showed the lowest deformation and lowest maximum insertion force in the red rectangle of B.

The performance of pre-selected needles (3FB-Omnican 30G, 38BOmnican 30G, Diamond-Clickfine 31G, and Diamond-Clickfine 32G) was further evaluated in an endurance test. It consisted of up to 100 consecutive insertions of a needle in tongue tissue while recording the insertion force. The maximum force was determined for each in-

sertion and plotted as a function of the insertion number. The results are shown in **Figure 5.7.** The endurance test was performed at two insertion velocities: 10 mm/s (blue) and 20 mm/s (red). For each of the four needle types, the maximum insertion force remains constant during the endurance tests.

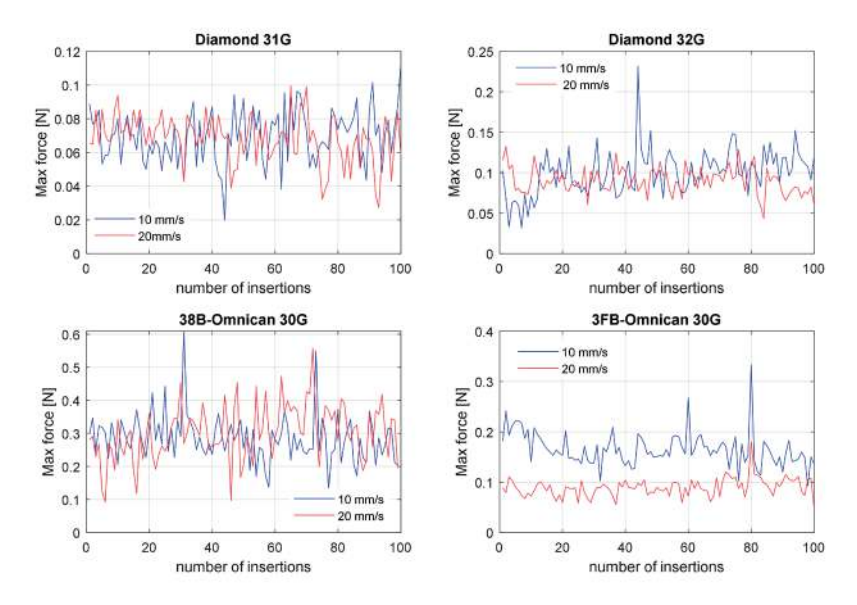


Figure 5.7. Maximum insertion force as a function of the number of consecutive needle insertions in tongue tissue for the four needle types and two insertion velocities (10 mm/s (blue) and 20 mm/s (red)).

DISCUSSION

Our study aimed to gain insights into tissue deformation during the insertion of a needle into tongue tissue and the effect of multiple insertions. This study showed that the tissue deformation and the maximum insertion force strongly depend on the tip geometry and the insertion velocity. Moreover, the endurance experiments showed no notable difference in the maximum insertion force during 100 insertions.

For the intended application, tissue deformation should be limited to ≤ 0.5 mm. In our experiments, four needles (3FB-Omnican 30G, 38BOmnican 30G, Diamond-Clickfine 31G, and Diamond-Clickfine 32G) met this requirement at high velocities (10 mm/s and 20 mm/s). However, in the system under development, the maximum insertion velocity should be limited to about 5 mm/s to allow longer Raman signal collection

time and further improve Raman signal quality. Only one needle (38B-Omnican 30G) met our requirement of ≤ 0.5 mm deformation at a velocity of 5 mm/s.

Throughout the experiments, multiple puncturing events were recognized, as shown in **Figure 5.5**. This is a well-described effect in the literature for biological tissue^{21,22}. The multiple puncturing events are most likely due to the different orientations of the muscle fibers of the calf tongue. In most cases, the maximum insertion force does not correspond to the tissue surface puncture force, but to a puncture event that occurs inside the tissue. Before the puncture event, the tissue is pushed away by the needle tip, resulting in tissue deformation and an increase in force. For our intended application of fiber-optic needles, it is important to minimize tissue deformation both at the tissue surface and inside the tissue.

In the system under development, a single needle will be used for the assessment of tumor resection margins at many locations of the resected tissue. This means that the needle must endure multiple insertions in soft tissue. All of the selected commercial needles are intended for single use only. Reports have shown that a needle tip can deteriorate after multiple insertions, which might lead to an increase in the maximum insertion force^{23,24}. We tested this but did not observe an increase of insertion force during 100 insertions in tongue tissue. This might be due to the tissue characteristics of calf tongue and the design of the tested needles (3FB-Omnican 30G, 38B-Omnican 30G, Diamond-Clickfine 31G, and Diamond-Clickfine 32G). Moreover, in the endurance experiments, 3 of the 4 needles show essentially no difference in the insertion force between 10 and 20 mm/s. The exception is the 3FB-Omnican 30G needle which shows a markedly, not yet understood, higher insertion force for the 10 mm/s.

The literature shows that the tip geometry is an important determining factor for the insertion force 18,25-27. Hirsch et al. showed that by adding 2 cutting edges (5 facet bevel instead of 3 facet bevel), the puncture force could be reduced by 23%28. This was also observed in this work, the needles with a blunt tip performed the worst followed by the 3FB-Sterican needles. Even for needles with a similar tip shape such as the 3FB-Omnican and 3FB-Sterican we observed a difference in the insertion force, which is possibly due to the angles of the tip. A smaller maximum force and a smaller deformation were observed for the 3FB-Omnican 30G in comparison to the 3FB-Sterican 30G. The diamond tip needles that were included in this study, are 6 facet beveled needles. However, the 3 facet beveled and the 38° beveled needles performed equally well or better than the diamond tip needles.

To visualize and measure the tissue deformation, the needles were inserted 3 mm from the wall of the measuring cubes. This could possibly affect the boundary conditions compared to real ex-vivo experiments and thereby change tissue deformation and insertion force. However, we do not expect that this will affect our conclusions with respect to the most suitable needle and insertion velocity given the very small deformation that was observed.

According to the literature, the force needed to create a puncture event increases with the needle's outer diameter¹⁶. In the current study, we examined a set of needles with small diameters (26G - 32G) compared to the ones studied in the literature (7G to 30G)¹⁶. However, for the thinnest needles (30G - 32G), no correlation between insertion force and needle diameters was found.

The insertion velocity had a great impact on tissue surface deformation, which supports the literature²⁹. **Figure 5.6C** shows that the deformation decreases with the increase of the insertion velocity, which was the case for nearly all needles. However, only four different insertion velocities (1 mm/s, 5 mm/s, 10 mm/s, and 20 mm/s) were tested and more insertion velocities should be investigated in the future. Moreover, to optimize needles for any intended application and any biological tissue, future research should focus on selecting comparable biological tissue and selecting needles with different tip geometries.

CONCLUSIONS

This study showed that the tissue deformation and the maximum insertion force strongly depend on the tip geometry and the insertion velocity for needles with a small outer diameter (30G - 32G). An increase in the insertion velocity decreases tissue deformation. Moreover, the needle tip geometry is an important factor to consider when optimizing the needle for any intended application. Of all the tested needles in this study, the 3FB-Omnican 30G and 38B-Omnican 30G needles performed the best in tongue tissue in regards to the maximum insertion force and tissue deformation. The needles selected for the endurance test showed no notable difference in the maximum insertion force during 100 insertions. Based on these outcomes the 38B-Omnican 30G needle was selected for the device under development **Figure 5.7**.

REFERENCES

- Ferlay J, Soerjomataram I, Dikshit R, et al. Cancer incidence and mortality worldwide: sources, methods and major patterns in GLOBOCAN 2012. *Int J Cancer*. 2015;136:E359-86. doi:10.1002/ijc.29210
- Vigneswaran N, Williams MD. Epidemiologic trends in head and neck cancer and aids in diagnosis. Oral Maxillofac Surg Clin North Am. 2014;26:123-41. doi:10.1016/j. coms.2014.01.001
- 3. Helliwell TR, Woolgar JA. Standards and datasets for reporting cancers. Dataset for histopathology reporting of mucosal malignancies of the head and neck. London: Royal College of Pathologists; 2013.
- 4. Dillon JK, Brown CB, McDonald TM, et al. How does the close surgical margin impact recurrence and survival when treating oral squamous cell carcinoma? *J Oral Maxillofac Surg.* 2015;73:1182-8. doi:10.1016/j.joms.2014.12.014
- 5. Slootweg PJ, Hordijk GJ, Schade Y, van Es RJJ, Koole R. Treatment failure and margin status in head and neck cancer: a critical view on the potential value of molecular pathology. *Oral Oncol*. 2002;38:500-3. doi:10.1016/s1368-8375(01)00092-6
- Al-Rajhi N, Khafaga Y, El-Husseiny J, et al. Early stage carcinoma of oral tongue: prognostic factors for local control and survival. *Oral Oncol*. 2000;36:508-14. doi:10.1016/ S1368-8375(00)00042-7
- 7. Binahmed A, Nason RW, Abdoh AA. The clinical significance of the positive surgical margin in oral cancer. *Oral Oncol*. 2007;43:780-4. doi:10.1016/j.oraloncology.2006.10.001
- 8. Loree TR, Strong EW. Significance of positive margins in oral cavity squamous carcinoma. Am J Surg. 1990;160:410-4. doi:10.1016/s0002-9610(05)80555-0
- 9. Smits RWH, van Lanschot CGF, Aaboubout Y, et al. Intraoperative assessment of the resection specimen facilitates achievement of adequate margins in oral carcinoma. *Front Oncol*. 2020;10:614593. doi:10.3389/fonc.2020.614593
- Varvares MA, Poti S, Kenyon B, Christopher K, Walker RJ. Surgical margins and primary site resection in achieving local control in oral cancer resections. *Laryngoscope*. 2015;125:2298-307. doi:10.1002/lary.25397
- 11. Smits RWH, Koljenović S, Hardillo JA, et al. Resection margins in oral cancer surgery: room for improvement. *Head Neck*. 2016;38:E2197-203. doi:10.1002/hed.24075
- 12. Dik EA, Willems SM, Ipenburg NA, et al. Resection of early oral squamous cell carcinoma with positive or close margins: relevance of adjuvant treatment in relation to local recurrence. *Oral Oncol.* 2014;50:611-5. doi:10.1016/j.oraloncology.2014.02.014
- 13. Aaboubout Y, Ten Hove I, Smits RWH, et al. Specimen-driven intraoperative assessment of resection margins should be standard of care for oral cancer patients. *Oral Dis.* 2021;27:111-6. doi:10.1111/odi.13619
- Santos IP, Barroso EM, Schut TCB, et al. Raman spectroscopy for cancer detection and cancer surgery guidance: translation to the clinics. *Analyst*. 2017;142:3025-47. doi:10.1039/C7AN00957G

- 15. Barroso EM, Smits RWH, Bakker Schut TC, et al. Discrimination between oral cancer and healthy tissue based on water content determined by Raman spectroscopy. *Anal Chem*. 2015;87:2419-26. doi:10.1021/ac504362y
- 16. Jiang S, Li P, Yu Y, et al. Experimental study of needle-tissue interaction forces: effect of needle geometries, insertion methods and tissue characteristics. *J Biomech*. 2014;47:3344-53. doi:10.1016/j.jbiomech.2014.08.007
- Bao X, Li W, Lu M, Zhou ZR. Experiment study on puncture force between MIS suture needle and soft tissue. Biosurf Biotribol. 2016;2:49-58. doi:10.1016/j.bsbt.2016.05.001
- van Gerwen DJ, Dankelman J, van den Dobbelsteen JJ. Needle-tissue interaction forces: a survey of experimental data. *Med Eng Phys.* 2012;34:665-80. doi:10.1016/j.medeng-phy.2012.04.007
- Naemura K, Uchino Y, Saito H. Effect of the needle tip height on the puncture force in a simplified epidural anesthesia simulator. In: 2007 29th Annual International Conference of the IEEE Engineering in Medicine and Biology Society. 2007. p. 3504-7. doi:10.1109/ IEMBS.2007.4353086
- 20. Mahvash M, Dupont PE. Mechanics of dynamic needle insertion into a biological material. *IEEE Trans Biomed Eng.* 2010;57:934-43. doi:10.1109/TBME.2009.2036856
- Mahvash M, Dupont PE. Fast needle insertion to minimize tissue deformation and damage.
 In: Proceedings of the 2009 IEEE International Conference on Robotics and Automation (ICRA). 2009. p. 3097-102. doi:10.1109/ROBOT.2009.5152617
- 22. Westbrook JL, Uncles DR, Sitzman BT, Carrie LE. Comparison of the force required for dural puncture with different spinal needles and subsequent leakage of cerebrospinal fluid. *Anesth Analg.* 1994;79:769-72. doi:10.1213/00000539-199410000-00026
- 23. van Lanschot C, Klazen YP, de Ridder M, et al. Depth of invasion in early stage oral cavity squamous cell carcinoma: the optimal cut-off value for elective neck dissection. *Oral Oncol*. 2020;111:104940. doi:10.1016/j.oraloncology.2020.104940
- 24. Aaboubout Y, van der Toom QM, de Ridder MAJ, et al. Is the depth of invasion a marker for elective neck dissection in early oral squamous cell carcinoma? *Front Oncol*. 2021;11:628320. doi:10.3389/fonc.2021.628320
- 25. Qi Y, Jin J, Chen T, Cong Q. Modeling of geometry and insertion force of a new lancet medical needle. *Sci Prog.* 2020;103:36850419891074. doi:10.1177/0036850419891074
- 26. Jushiddi MG, Cahalane RM, Byrne M, et al. Bevel angle study of flexible hollow needle insertion into biological mimetic soft-gel: simulation and experimental validation. *J Mech Behav Biomed Mater*. 2020;111:103896. doi:10.1016/j.jmbbm.2020.103896
- 27. Abolhassani N, Patel R, Moallem M. Needle insertion into soft tissue: a survey. *Med Eng Phys*. 2007;29:413-31. doi:10.1016/j.medengphy.2006.07.003
- 28. Hirsch L, Gibney M, Berube J, Manocchio J. Impact of a modified needle tip geometry on penetration force as well as acceptability, preference, and perceived pain in subjects with diabetes. *J Diabetes Sci Technol*. 2012;6:328-35. doi:10.1177/193229681200600216
- 29. Pereira IB, Oliveira MMM, Ferreira PBP, et al. Ultra-structural evaluation of needles and their role for comfort during subcutaneous drug administration. *Rev Esc Enferm USP*. 2018;52:e03307. doi:10.1590/s1980-220x2017024003307



IS THE DEPTH OF INVASION A MARKER FOR ELECTIVE NECK DISSECTION IN EARLY ORAL SQUAMOUS CELL CARCINOMA?

Yassine Aaboubout, Quincy M van der Toom, Maria A J de Ridder, Maria J De Herdt, Berdine van der Steen, Cornelia G F van Lanschot, Elisa M Barroso, Maria R Nunes Soares, Ivo Ten Hove, Hetty Mast, Roeland W H Smits, Aniel Sewnaik, Dominiek A Monserez, Stijn Keereweer, Peter J Caspers, Robert J Baatenburg de Jong, Tom C Bakker Schut, Gerwin J Puppels, José A Hardillo, Senada Koljenović

Front Oncol. 2021 Mar 12;11:628320.



ABSTRACT

Objective

The depth of invasion (DOI) is considered an independent risk factor for occult lymph node metastasis in oral cavity squamous cell carcinoma (OCSCC). It is used to decide whether an elective neck dissection (END) is indicated in the case of a clinically negative neck for early stage carcinoma (pT1/pT2). However, there is no consensus on the cut-off value of the DOI for performing an END. The aim of this study was to determine a cut-off value for clinical decision making on END, by assessing the association of the DOI and the risk of occult lymph node metastasis in early OCSCC.

Methods

A retrospective cohort study was conducted at the Erasmus MC, University Medical Centre Rotterdam, The Netherlands. Patients surgically treated for pT1/pT2 OCSCC between 2006 and 2012 were included. For all cases, the DOI was measured according to the 8th edition of the American Joint Committee on Cancer guideline. Patient characteristics, tumor characteristics (pTN, differentiation grade, perineural invasion, and lymphovascular invasion), treatment modality (END or watchful waiting), and 5-year follow-up (local recurrence, regional recurrence, and distant metastasis) were obtained from patient files.

Results

A total of 222 patients were included, 117 pT1 and 105 pT2. Occult lymph node metastasis was found in 39 of the 166 patients who received END. Univariate logistic regression analysis showed DOI to be a significant predictor for occult lymph node metastasis (odds ratio (OR) = 1.3 per mm DOI; 95% CI: 1.1-1.5, p = 0.001). At a DOI of 4.3 mm the risk of occult lymph node metastasis was >20% (all subsites combined).

Conclusion

The DOI is a significant predictor for occult lymph node metastasis in early stage oral carcinoma. A NPV of 81% was found at a DOI cut-off value of 4 mm. Therefore, an END should be performed if the DOI is >4 mm.

INTRODUCTION

Oral cavity cancer has a worldwide incidence of 350,000, with a male:female ratio of 2.1:1¹. The 5-year survival rate is approximately 50% in Europe². Histologically, more than 90% of all oral cavity cancers are squamous cell carcinoma (OCSCC)³. The most common risk factors for developing OCSCC are tobacco and alcohol consumption⁴. In Southern Asia (India, Sri Lanka, China, and Thailand), the incidence of OCSCC is even higher due to the chewing of tobacco with or without betel quid². The estimated annual mortality in patients with OCSCC is 145,000 worldwide⁵.

Factors that are known to contribute to a patients prognosis are tumor size, regional lymph node involvement and distance metastasis (TNM classification), tumor differentiation grade, perineural invasion (PNI), and lymphovascular invasion (LVI)⁶. The treatment of choice is surgery with tumor resection and neck dissection in case of clinical lymph node involvement. An elective neck dissection in OCSCC patients is recommended if the risk of occult lymph node metastasis is >20%⁷.

An END increases the disease-specific survival (DSS) and overall survival (OS) compared to watchful waiting (WW), supported by a therapeutic lymph node dissection when needed^{8, 9}. A neck dissection can be associated with several adverse effects such as edema, pain, and disability of the shoulder. The severity of these effects is often related to the extent of dissection; neck and shoulder discomfort is still reported even if the vital structures are well preserved^{10, 11}. Therefore, the current international consensus is that an END should only be performed if the risk of occult lymph node metastasis is >20%.

The DOI and sentinel lymph node biopsy are currently the best predictors for occult lymph node metastasis¹². Sentinel node biopsy has high accuracy for identifying occult lymph node metastasis¹³⁻¹⁵. However, this accuracy is very dependent on experience and technical expertise, which makes the sentinel node biopsy procedure difficult for wide implementation¹².

The DOI is used as a marker for elective neck dissection (END) in a number of centers, including ours. However, there is no unanimous cut-off value, varying from 2 mm - 10 mm between the centers^{16, 17}. The lack of common definition and guidelines on how to measure DOI has led to this large variation. This shortcoming has been recently addressed by the 8th edition of the cancer staging manual from the American Joint Committee on Cancer (AJCC)¹⁸.

The aim of this study was to estimate a cut-off value of DOI for clinical decision making on END, by assessing the association of DOI and the risk of occult lymph node metastasis in early OCSCC.

METHODS

Study Design and Patients

A single-center retrospective cohort study was conducted at the Erasmus University Medical Center (Erasmus MC), Rotterdam, the Netherlands after Institutional Review Board approval (MEC-2016-751). Surgically treated patients with primary OCSCC (pT1 or pT2, based on the 8th edition of the AJCC) and clinically negative lymph nodes (cN0) were identified from January 2006 until December 2012¹⁸. Clinical lymph node status was determined by palpation of the neck, and/or by imaging (ultrasound with fine-needle aspiration biopsy, CT, and/or MRI).

Exclusion criteria were a history of head and neck cancer, presence of synchronous oral cavity tumor, unreliable assessment of the DOI, and loss to follow-up.

All patient and tumor characteristics, except the DOI, were recorded from the patient files, including age, gender, tumor localization, cTNM, pTN, differentiation grade, perineural invasion (PNI), and lymphovascular invasion (LVI). Lymphovascular invasion was regarded as positive when appreciated in the tumor and/or in the cases of a positive lymph node (pN+).

Neck lymph node treatment (i.e., END or WW), follow-up (e.g., local recurrence, regional recurrence, and cause of death) were also recorded. Patients were divided into two groups based on the neck treatment: the END group and the WW group. All patients were followed for at least 5 years. Patients from the END group received clinical examination and ultrasonography when indicated. Patients in the WW group always underwent ultrasonography in the first 2 years of follow-up in addition to clinical examination. The frequency of the follow-up in the first 2 years was every 2-3 months, in the 3rd year 4-6 months, and in the 4th and 5th years 6-12 months. If regional recurrence occurred, the side (ipsilateral or contralateral) was recorded.

Measurement of the Depth of Invasion

The DOI was measured for all surgical specimens based on the hematoxylin and eosin slide. The DOI was defined and measured as a plumb-line from the basal membrane of

the closest normal adjacent mucosa to the deepest point of invasion, in line with the recommendation from the 8th edition of the AJCC¹⁸.

All hematoxylin and eosin slides were collected from the Department of Pathology of the Erasmus University Medical Center and scanned by the NanoZoomer 2.0-HT slide scanner (Hamamatsu Photonics, Hamamatsu, Japan). Slides were reviewed by a head and neck pathologist (SK) using the NanoZoomer digital pathology (NDP) viewer 2.5.19 (Hamamatsu Photonics, Hamamatsu, Japan).

The patients were divided based on DOI into a group with DOI \leq 4 mm and a group with DOI >4 mm, based on the DOI cut-off value >4 mm used at our institute.

Statistical Analysis

Statistical analysis was performed using the IBM SPSS Statistics version 25 software. Patients' characteristics between the two groups (DOI ≤ 4 mm DOI > 4 mm) were compared using student T-test for continuous variables and Chi-square test for categorical variables. Univariate logistic regression was performed to assess the correlation between predictor variables and occult lymph node status. A Receiver Operator Curve (ROC) was utilized to determine the optimal cut-off value for predicting occult lymph node metastasis using DOI, for all sub-sites combined. Follow-up was calculated from the date of surgery. Regional recurrence-free survival (i.e., time until an isolated regional recurrence occurs; RRFS) and disease-specific survival (i.e., time until death due to disease; DSS) were assessed by Kaplan-Meier analysis and log-rank test for the DOI ≤4 mm and >4 mm and for the WW and END in the DOI group ≤4 mm. The overall survival (i.e., time until the death of patients; OS) was assessed by Kaplan-Meier analysis and log-rank test for the DOI ≤4 mm and >4 mm. Two-tailed statistical tests were performed. A p-value of less than 0.05 was considered statistically significant.

RESULTS

Study Population

A total of 318 patients were seen in our hospital with pT1/pT2 OCSCC during the study period. Patients were excluded due to the following reasons: a history of head and neck tumor (n = 91), unreliable assessment of the depth of invasion (n = 3), loss to follow-up (n = 2). After exclusion, 222 patients were included for the final analysis, **Table 6.1**. Of the 222 patients included, the cN0 status was determined by both, clinical examination and imaging in 124 patients (55.9%), by clinical examination only in 51 patients (23%), and by imaging only in 42 patients (18.9%). For the remaining five patients (2.2%) no data was available.

Table 6.1. Patient and tumor characteristics.

Table 6.1. Patient and tumor characteristic		
	Number (n = 222)	%
Gender		
Male	138	62.2
Female	84	37.8
Age (years)		
Median (range)	64.5 (16.1 - 93.1)	
pT status (8 th edition)		
1	117	52.7
2	105	47.3
Tumor diameter (cm)		
Median (range)	1.5 (0.2 - 4)	
Depth of invasion (mm)		
Median (range)	4.48 (0.05 - 9.97)	
Subsite		
Tongue	128	57.6
Floor of mouth	65	29.3
Buccal mucosa	12	5.4
Retromolar trigone	7	3.2
Gingiva mandible*	7	3.2
Gingiva maxilla*	2	0.9
Lip	1	0.4
Hard palate	0	0.0
Differentiation grade		
Well	59	26.6
Moderate	149	67.1
Poor	14	6.3
Perineural invasion		
Yes	36	19.7
No	147	80.3
Unknown	39	
Lymphovascular invasion		
Yes	56	31.1
No	124	68.9
Unknown	42	
Neck treatment		
Ipsilateral END	146	65.8
Bilateral END	20	9.0
ww	56	25.2

^{*}In this small group all patients had SCC arising from the gingiva. However, in five cases the tumor was extending to the adjacent floor of mouth, reaching the maximum DOI at that location.

Depth of Invasion

Median DOI for all cases was 4.48 mm; mean was 4.8 mm with a standard deviation of 2.5 mm. In 97 cases the DOI was ≤ 4 mm and in 125 cases the DOI was > 4 mm. Of all adverse histopathologic characteristics, only PNI was associated with DOI > 4 mm (p = 0.001). The other adverse tumor characteristics such as differentiation grade and LVI were similar in both groups, **Table 6.2**.

Table 6.2. Comparison of patient and tumor characteristics for the two depth of invasion groups.

	DOI ≤ 4 mm	%	DOI > 4 mm	%	p-value*
pT status (8 th edition)					< 0.001
1	89	91.8	28	22.4	
2	8	8.2	97	77.6	
Tumor diameter **	1.23 ± 0.69		1.94 ± 0.83		< 0.001
DOI **	2.47 ± 0.95		6.62 ± 1.75		< 0.001
Subsite					0.670
Tongue	59	60.8	69	55.2	
Floor of mouth	28	28.9	37	29.6	
Buccal mucosa	3	3.1	9	7.2	
Retromolar trigone	3	3.1	4	3.2	
Gingiva mandible	3	3.1	4	3.2	
Gingiva maxilla	0	0.0	2	1.6	
Lip	1	1.0	0	0.0	
Hard palate	0	0.0	0	0.0	
Differentiation grade					0.259
Well	31	32.0	28	22.4	
Moderate	61	62.8	88	70.4	
Poor	5	5.2	9	7.2	
Perineural invasion					0.001
Yes	6	8.2	30	27.3	
No	67	91.8	80	72.7	
Unknown	24		15		
Lymphovascular invasion					0.10
Yes	7	10.4	16	15.1	
No	60	89.6	90	84.9	
Unknown	30		19		

^{*}Chi-square test for categorical data, unpaired T-test for numeric data.

Elective Neck Dissection Versus Watchful Waiting

Thirty-nine patients of the 166 patients treated with an END had occult lymph node metastasis. The DOI of all patients was categorized into whole mm (0 mm < DOI \leq 1

^{**}Expressed as mean ± SD.

mm, 1 mm < DOI \leq 2 mm, etc), **Table 6.3**. A separate analysis was performed for 128 patients with SCC of the tongue, **Table 6.4**.

Table 6.3. Association between depth of invasion and occult lymph node metastasis.

DOI (mm)	Total patients (n)	pN0 (n)	pN+** n (%)	Cut-off value (mm)	Sens* (%)	Spec* (%)	PPV* (%)	NPV* (%)
1 (0 < DOI ≤ 1)	2	2	0 (0)	>1	100	2	24	100
2 (1 < DOI ≤ 2)	6	6	0 (0)	>2	100	6	25	100
3 (2 < DOI ≤ 3)	24	20	4 (17)	>3	90	22	26	88
4 (3 < DOI ≤ 4)	21	15	6 (29)	>4	74	34	26	81
5 (4 < DOI ≤ 5)	26	20	6 (23)	>5	59	50	26	80
6 (5 < DOI ≤ 6)	16	14	2 (12)	>6	54	61	30	81
7 (6 < DOI ≤ 7)	24	21	3 (12)	>7	46	77	38	82
$8 (7 < DOI \le 8)$	16	9	7 (44)	>8	28	84	35	79
9 (8 < DOI ≤ 9)	15	9	6 (40)	>9	13	91	31	77
10 (9 < DOI ≤ 10)	16	11	5 (31)	>10	0	100	#N/B	77

^{*}Sensitivity, specificity, PPV, and NPV were calculated using the upper limit of the category as a cut-off.

Table 6.4. Association between depth of invasion and occult lymph node metastasis in tongue.

Total patients (n)	pN0 (n)	pN+** n (%)	Cut-off value (mm)	Sens* (%)	Spec* (%)	PPV* (%)	NPV* (%)
4	4	0 (0)	>1	100	4	31	100
12	10	2 (17)	>2	95	16	33	88
23	16	7 (30)	>3	77	34	34	77
20	12	8 (40)	>4	56	47	32	71
19	14	5 (26)	>5	44	63	34	72
8	7	1 (12)	>6	41	71	38	73
15	12	3 (20)	>7	33	84	48	74
7	4	3 (43)	>8	26	89	50	73
9	4	5 (56)	>9	13	93	45	71
11	6	5 (45)	>10	0	100	#N/A	70
	patients (n) 4 12 23 20 19 8 15 7 9	patients (n) 4	patients (n) (%) 4	patients (n) (%) value (mm) 4	patients (n) (%) value (mm) (%) 4	patients (n) (%) value (mm) (%) (%) (%) 4	patients (n) (%) value (mm) (%) (%) (%) (%) 4

^{*}Sensitivity, specificity, PPV, and NPV were calculated using the upper limit of the category as a cut-off.

Figure 6.1 shows predictions from a logistic regression analysis. This leads to a cut-off value of 4.3 mm, considering the 20% risk (NPV = 80%)⁷. In the logistic regression analysis for the tongue population, the risk of 20% (NPV = 80%) is reached between 3 mm and 4 mm.

^{**}Percentage is based on the pN+ per categorized DOI (mm).

^{**}Percentage is based on the pN+ per categorized DOI (mm).

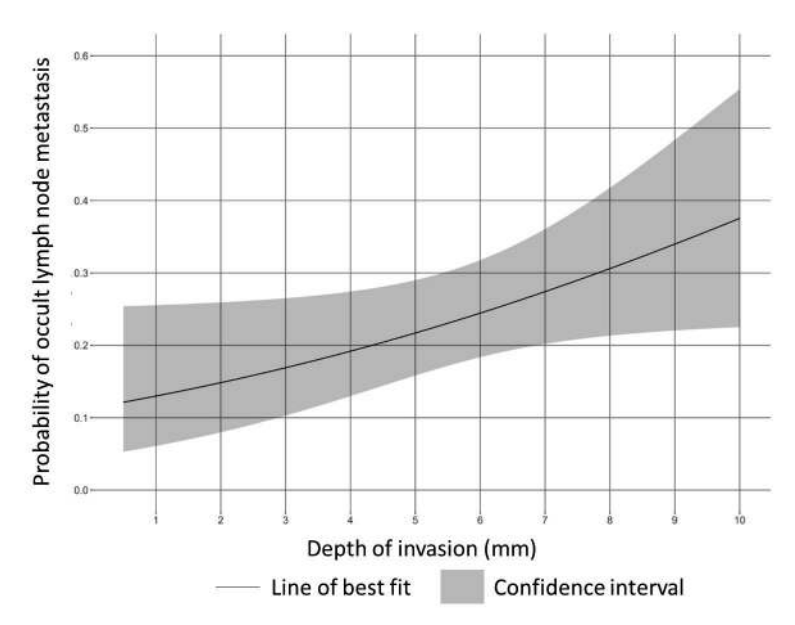


Figure 6.1. Association between depth of invasion and occult lymph node metastasis.

Predictors for Occult Lymph Node Metastasis

Univariate logistic regression analysis showed depth of invasion (OR = 1.3 per mm DOI; 95% CI: 1.1-1.5, p = 0.001) and tumor diameter (OR = 2.0; 95% CI: 1.3-3.1, p = 0.002) as predictors for occult lymph node metastasis. Perineural invasion (p = 0.204) and differentiation grade (p = 0.194) were non-predictors for occult lymph node metastasis.

Follow-Up

The mean follow-up was 67 ± 34 months, ranging from 0.2 to 156 months. No difference was found in the duration of follow-up between the DOI ≤ 4 mm and >4 mm, p = 0.969 (66.7 \pm 33.5 months; 66.5 \pm 34.9 months, respectively).

No difference was found between the groups DOI \leq 4 mm and > 4 mm in local recurrence, and distant metastasis. Local recurrence occurred in 19 patients, 8 patients (8.2%) in the group DOI \leq 4 mm and 11 patients (8.8%) in the group DOI > 4 mm, p = 1.0. Distant metastasis occurred in 12 patients, 6 patients (6.2%) in the group DOI \leq 4 mm and 6 patients (4.8%) in the group DOI > 4 mm, p = 0.878.

Regional recurrence was also analyzed per DOI group (≤4 mm versus >4 mm) and per type of treatment (WW versus END), **Table 6.5**. Regional recurrence occurred in 15

patients (15.5%) in the group DOI \leq 4 mm and in 12 patients (9.6%) in the group DOI >4 mm, p = 0.263.

Table 6.5.	Regional	recurrence	for the	two dep	th of	invasion	groups.

	DOI ≤	4 mm			DOI > 4 mm				
	Number of	Region	nal Recur	rence (n)	Number of	Regio	onal Recu	rrence (n)	
	patients (n=97)	2 yr	5 yr	Total	patients (n=125)	2 yr	5 yr	Total	
WW	44 (45.4%)	8	3	11 (25%)	12 (9.6%)	1	1	2 (16.7%)	
END	53 (54.6%)				113 (90.4%)				
pN0	43 (81.1%)	2	1	4 (7.7%)	84 (74.3%)	3	3	10 (8.8%)	
pN+	10 (18.9%)	0	1	. (/ / / /	29 (25.7%)	3	1	10 (010/0)	

In the WW group, regional recurrence was seen in 13 patients (23.2%) (11 in the group DOI \leq 4 mm and two in the group DOI \geq 4 mm) and 14 patients (8.4%) in the END group (four in the group DOI \leq 4 mm and 10 in the group DOI \geq 4 mm), p = 0.007.

In this END group, in nine of 14 cases regional recurrence was contralateral (tumor subsite: tongue six, floor of mouth two, and retromolar trigone one). In the remaining five cases the regional recurrence was ipsilateral, four in a level which was not included in the END, one in the level that was included.

Regional recurrence-free survival was similar for a DOI ≤ 4 mm and a DOI > 4 mm (5-year RRFS 86.0 vs 90.1%, logrank test p = 0.317).

Disease specific survival was similar for a DOI \leq 4 mm and a DOI >4 mm (both 5-year DSS 89.1 vs 91.3%, log-rank test p = 0.605).

Overall survival was similar for a DOI ≤ 4 mm and a DOI > 4 mm (5-year OS 73.6 vs 70.1%, log-rank test p = 0.527).

The differences in RRFS and DSS were calculated between WW and END only for the group DOI \leq 4 mm, because in the group DOI >4 mm the number of patients with WW was not sufficient for statistical analysis.

For the group DOI \leq 4 mm, the RRFS for patients with an END compared to those with WW was not different (5-year RRFS 92.2 vs 78.4%, log-rank test p = 0.055), **Figure 6.2**.

For the DOI \leq 4 mm, the DSS was similar for the END and WW (5-year DSS 94.3 vs 82.6%, log-rank test p = 0.097).

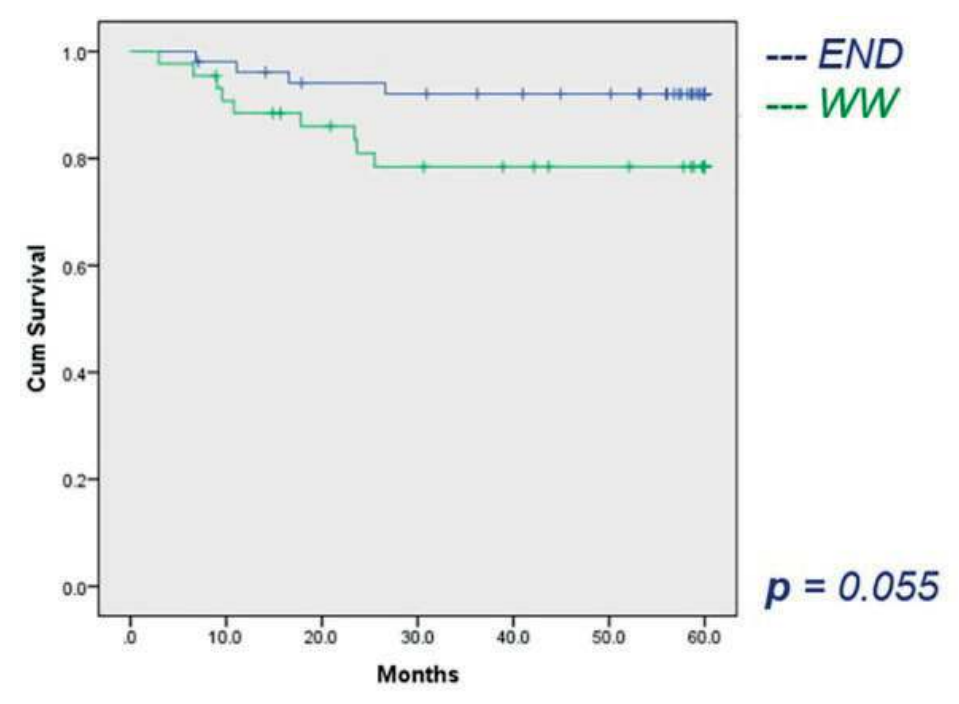


Figure 6.2. The 5-year regional recurrence-free survival.

DISCUSSION

Several studies report the DOI as a predictor of occult lymph node metastasis, and it is used as a criterion to decide on END in early OCSCC¹⁹⁻²⁶.

However, large differences exist between studies in regard to the definition and reliable measurement of the DOI and in the number of cases included from different subsites. This makes comparison of the results between studies unreliable.

The lack of consensus on the DOI cut-off value for the clinical decision on END is caused by the fact that it is used interchangeably with tumor thickness (TT) in different studies^{16, 17, 19, 20, 27, 28}. The DOI is considered a better prognostic factor than TT because it compensates for exophytic or ulcerative tumors²⁸. The 8th edition of the AJCC guideline, published in January 2017, provides a clear definition of the DOI (i.e., the distance between the basal membrane of normal adjacent mucosa and the deepest point of tumor invasion)¹⁸. Therefore, many studies are outdated^{9, 19, 28-30}.

Moreover, the studies published after the release of the 8th edition of the AJCC show large variances. A number of studies do not confirm the DOI cut-off value of 4 mm. For instance, Faisal et al. showed 10 mm DOI cut-off value for decision making on END, Tam et al. showed 7.25 mm, and Kozak et al. did not specify another DOI cut-off value^{23, 24, 31}. On the other hand, van Lanschot et al. confirmed the DOI cut-off value of 4 mm, and Brockhoff et al. calculated DOI cut-off values for most subsites (i.e., tongue = 2 mm, floor of mouth = 3 mm, and Proc alv/hard palate = 4 mm)^{20, 22}.

The strength of the current study is that the DOI was measured for all cases, according to the current AJCC guideline, on digital H&E slides with high precision. In order to have comparable data, it would be desirable that in future studies the DOI is used and that the conclusions of already published studies based on TT are reassessed based on the DOI.

It is known that the frequency of occult lymph node metastasis differs per OCSCC subsite. It has been reported that occult lymph node metastasis is present in 20-30% of the cases for tongue cancer, 41.7% for the floor of mouth, and 15.4% for the buccal mucosa^{20, 32}. Therefore, the DOI cut-off value should be determined per subsite. The limited number of cases per subsite included in this study did not allow this analysis.

Aside from the DOI, other tumor characteristics like diameter, differentiation grade, worst pattern of invasion, perineural invasion, and tumor budding can also be associated with occult lymph node metastasis³³⁻³⁶. In this study, it was not possible to confirm the other tumor characteristics because the multivariate analysis was not performed due to the incomplete pathology reporting between 2006 and 2012. Data on LVI, PNI, and tumor diameter were sometimes missing. Besides, margin status was often not annotated exactly. Instead of numerical values, there was only a description of margins (e.g., radical, free of tumor). The previously published study on this subject by our group involved a relatively recent cohort (2013-2018), in which our protocol for END was based on the DOI (>4 mm = END). On contrary, in the current study an older cohort was involved for which the guideline for END was based on either DOI >5 mm or tumor diameter >1.0 cm. Moreover, for the old cohort the reliable data for LVI, PNI, tumor diameter and margin status were missing and therefore not further analyzed and compared with the newer cohort. Finally, the patient outcome (locoregional recurrence and survival) in the previously published study may be influenced by the fact that our institute started with intra-operative assessment of resection margins in 2013^{22, 37, 38}.

However, it was shown that a predictive model for occult lymph node metastasis including all the tumor characteristics is the best approach³⁹. Objective methods for predicting occult lymph node metastasis are being investigated, like gene-expression profiling or molecular markers⁴⁰⁻⁴³.

In this study, we showed that the DOI is a significant predictor for occult lymph node metastasis (p = 0.001) in OCSCC. Therefore, the DOI can be regarded as a parameter for decision making on END. At our institute, the DOI cut-off value >4 mm is used, based on the National Comprehensive Cancer Network (NCCN) guideline¹². Here we confirm with a NPV of 81% the DOI cut-off value >4 mm for decision making on END.

We showed that performing an END in patients with an DOI ≤ 4 mm had no significant effect on the 5-year DSS compared to WW (94.3 vs 82.6%, log-rank test p = 0.097). The strength of this study is that this analysis was possible because of the large number of patients treated with an END in the group with a DOI ≤ 4 mm. In this group, the RRFS reached near significance (p = 0.055) for END, when compared to WW. For the group DOI ≥ 4 mm, the difference in DSS and RRFS could not be calculated because the number of patients was not sufficient for statistical analysis.

Despite the fact that END was performed, regional recurrence occurred in 8.4% of patients (14 of 166). The recurrences were either ipsilateral and mostly at a neck level that was not included in the END(5), or contralateral(9) to END side. The effectiveness of END is shown by the fact that only one patient had a regional recurrence at a level that was included in the END.

Most authors base their decision on END according to 20% (NPV 80%) risk of occult lymph node metastasis^{19, 20, 22-26}. The origin of this risk cut-off value is the publication of Weiss et al. in 1994⁷. In this study, the decision for intervention was determined by the side effects of surgery (END) and radiotherapy at that time. It may be assumed that nowadays, 25 years later, the treatment modalities have substantially improved. Therefore, we suggest that a risk lower than 20% should be taken into consideration when deciding on END. This of course, should only be done in agreement with patients, based on the clear information on both, side effects of the END and the risk of occult lymph node metastasis.

REFERENCES

- Bray F, Ferlay J, Soerjomataram I, Siegel RL, Torre LA, Jemal A. Global cancer statistics 2018: GLOBOCAN estimates of incidence and mortality worldwide for 36 cancers in 185 countries. CA Cancer J Clin. 2018;68(6):394-424. doi:10.3322/caac.21492
- 2. Shield KD, Ferlay J, Jemal A, Sankaranarayanan R, Chaturvedi AK, Bray F, et al. The global incidence of lip, oral cavity, and pharyngeal cancers by subsite in 2012. CA Cancer J Clin. 2017;67(1):51-64. doi:10.3322/caac.21384
- Vigneswaran N, Williams MD. Epidemiologic trends in head and neck cancer and aids in diagnosis. Oral Maxillofac Surg Clin North Am. 2014;26(2):123-41. doi:10.1016/j. coms.2014.01.001
- 4. Hashibe M, Brennan P, Chuang SC, Boccia S, Castellsague X, Chen C, et al. Interaction between tobacco and alcohol use and the risk of head and neck cancer: pooled analysis in the International Head and Neck Cancer Epidemiology Consortium. Cancer Epidemiol Biomarkers Prev. 2009;18(2):541-50. doi:10.1158/1055-9965.EPI-08-0347
- Ferlay J, Soerjomataram I, Dikshit R, Eser S, Mathers C, Rebelo M, et al. Cancer incidence and mortality worldwide: sources, methods and major patterns in GLOBOCAN 2012. Int J Cancer. 2015;136(5):E359-86. doi:10.1002/ijc.29210
- 6. Liu SA, Wang CC, Jiang RS, Lee FY, Lin WJ, Lin JC. Pathological features and their prognostic impacts on oral cavity cancer patients among different subsites a single institute's experience in Taiwan. Sci Rep. 2017;7(1):7451. doi:10.1038/s41598-017-08022-w
- 7. Weiss MH, Harrison LB, Isaacs RS. Use of decision analysis in planning a management strategy for the stage N0 neck. Arch Otolaryngol Head Neck Surg. 1994;120(7):699-702. doi:10.1001/archotol.1994.01880310005001
- Xie Y, Shen G. Association of neck dissection with survival for early stage N0 tongue cancer: a SEER population-based study. Medicine (Baltimore). 2018;97(51):e13633. doi:10.1097/MD.0000000000013633
- 9. D'Cruz AK, Vaish R, Kapre N, Dandekar M, Gupta S, Hawaldar R, et al. Elective versus therapeutic neck dissection in node-negative oral cancer. N Engl J Med. 2015;373(6):521-9. doi:10.1056/NEJMoa1506007
- Gane EM, Michaleff ZA, Cottrell MA, McPhail SM, Hatton AL, Panizza BJ, et al. Prevalence, incidence, and risk factors for shoulder and neck dysfunction after neck dissection: a systematic review. Eur J Surg Oncol. 2017;43(7):1199-218. doi:10.1016/j.ejso.2016.10.026
- 11. Bradley PJ, Ferlito A, Silver CE, Takes RP, Woolgar JA, Strojan P, et al. Neck treatment and shoulder morbidity: still a challenge. Head Neck. 2011;33:1060-7. doi:10.1002/hed.21495
- 12. National Comprehensive Cancer Network. NCCN Clinical Practice Guidelines in Oncology (NCCN Guidelines®) Head and Neck. Version 1. 2016.
- Civantos FJ, Zitsch RP, Schuller DE, Agrawal A, Smith RB, Nason R, et al. Sentinel lymph node biopsy accurately stages the regional lymph nodes for T1-T2 oral squamous cell carcinomas: results of a prospective multi-institutional trial. J Clin Oncol. 2010;28(8):1395-400. doi:10.1200/JCO.2008.20.8777

- 14. Alkureishi LWT, Ross GL, Shoaib T, Soutar DS, Robertson AG, Thompson R, et al. Sentinel node biopsy in head and neck squamous cell cancer: 5-year follow-up of a European multicenter trial. Ann Surg Oncol. 2010;17(9):2459-64. doi:10.1245/s10434-010-1111-3
- Govers TM, Hannink G, Merkx MAW, Takes RP, Rovers MM. Sentinel node biopsy for squamous cell carcinoma of the oral cavity and oropharynx: a diagnostic meta-analysis. Oral Oncol. 2013;49(8):726-32. doi:10.1016/j.oraloncology.2013.04.006
- 16. Kuan EC, Clair JM-S, Badran KW, St. John MA. How does depth of invasion influence the decision to do a neck dissection in clinically NO oral cavity cancer? Laryngoscope. 2016;126(3):547-8.
- 17. Shinn JR, Wood CB, Colazo JM, Harrell FE, Rohde SL, Mannion K. Cumulative incidence of neck recurrence with increasing depth of invasion. Oral Oncol. 2018;87:36-42.
- 18. Lydiatt WM, Patel SG, O'Sullivan B, Brandwein MS, Ridge JA, Migliacci JC, et al. Head and neck cancers—major changes in the American Joint Committee on Cancer eighth edition cancer staging manual. CA Cancer J Clin. 2018;68(1):55-63.
- 19. Melchers LJ, Schuuring E, van Dijk BAC, de Bock GH, Witjes MJH, van der Laan BFAM, et al. Tumour infiltration depth ≥4 mm is an indication for an elective neck dissection in pT1cN0 oral squamous cell carcinoma. Oral Oncol. 2012;48(4):337-42.
- 20. Brockhoff HC, Kim RY, Braun TM, Skouteris C, Helman JI, Ward BB. Correlating the depth of invasion at specific anatomic locations with the risk for regional metastatic disease to lymph nodes in the neck for oral squamous cell carcinoma. Head Neck. 2017;39(5):974-9.
- 21. Pentenero M, Gandolfo S, Carrozzo M. Importance of tumor thickness and depth of invasion in nodal involvement and prognosis of oral squamous cell carcinoma: a review of the literature. Head Neck. 2005;27(12):1080-91.
- 22. van Lanschot CGF, Klazen YP, de Ridder MAJ, Mast H, ten Hove I, Hardillo JA, et al. Depth of invasion in early stage oral cavity squamous cell carcinoma: the optimal cut-off value for elective neck dissection. Oral Oncol. 2020;111:104940.
- 23. Faisal M, Abu Bakar M, Sarwar A, Adeel M, Batool F, Malik KI, et al. Depth of invasion (DOI) as a predictor of cervical nodal metastasis and local recurrence in early stage squamous cell carcinoma of oral tongue (ESSCOT). PLoS One. 2018;13(8):e0202632.
- 24. Tam S, Amit M, Zafereo M, Bell D, Weber RS. Depth of invasion as a predictor of nodal disease and survival in patients with oral tongue squamous cell carcinoma. Head Neck. 2018;7:hed.25506.
- 25. Liao CT, Wang HM, Ng SH, Yen TC, Lee LY, Hsueh C, et al. Good tumor control and survivals of squamous cell carcinoma of buccal mucosa treated with radical surgery with or without neck dissection in Taiwan. Oral Oncol. 2006;42(8):800-9.
- 26. Massey C, Dharmarajan A, Bannuru RR, Rebeiz E. Management of NO neck in early oral squamous cell carcinoma: A systematic review and meta-analysis. Laryngoscope. 2019;129(8):E284-E298.
- 27. Fukano H, Matsuura H, Hasegawa Y, Nakamura S. Depth of invasion as a predictive factor for cervical lymph node metastasis in tongue carcinoma. Head Neck. 1997;19(3):205-10.
- 28. Kane SV, Gupta M, Kakade AC, D'Cruz A. Depth of invasion is the most significant histological predictor of subclinical cervical lymph node metastasis in early squamous carcinomas of the oral cavity. Eur J Surg Oncol. 2006;32(7):795-803.

- 29. Almagush A, Bello IO, Coletta RD, Makitie AA, Makinen LK, Kauppila JH, et al. For early-stage oral tongue cancer, depth of invasion and worst pattern of invasion are the strongest pathological predictors for locoregional recurrence and mortality. Virchows Arch. 2015;467(1):39-46.
- 30. Chen YW, Yu EH, Wu TH, Lo WL, Li WY, Kao SY. Histopathological factors affecting nodal metastasis in tongue cancer: analysis of 94 patients in Taiwan. Int J Oral Maxillofac Surg. 2008;37(10):912-6.
- 31. Kozak MM, Shah J, Chen M, Schaberg K, von Eyben R, Chen JJ, et al. Depth of invasion alone as a prognostic factor in low-risk early-stage oral cavity carcinoma. Laryngoscope. 2019;129(9):2082-6.
- 32. Hanai N, Asakage T, Kiyota N, Homma A, Hayashi R. Controversies in relation to neck management in N0 early oral tongue cancer. Jpn J Clin Oncol. 2019;49(4):297-305.
- 33. An S, Jung E-J, Lee M, Kwon T-K, Sung M-W, Jeon YK, et al. Factors Related to Regional Recurrence in Early Stage Squamous Cell Carcinoma of the Oral Tongue. Clin Exp Otorhinolaryngol. 2008;1(3):166.
- 34. Lanzer M, Gander T, Kruse A, Luebbers H-T, Reinisch S. Influence of histopathologic factors on pattern of metastasis in squamous cell carcinoma of the head and neck. Laryngoscope. 2014;124(5):E160-6.
- 35. Kademani D, Bell RB, Bagheri S, Holmgren E, Dierks E, Potter B, et al. Prognostic Factors in Intraoral Squamous Cell Carcinoma: The Influence of Histologic Grade. J Oral Maxillofac Surg. 2005;63(11):1599-605.
- 36. Chatterjee D, Bansal V, Malik V, Bhagat R, Punia RS, Handa U, et al. Tumor Budding and Worse Pattern of Invasion Can Predict Nodal Metastasis in Oral Cancers and Associated With Poor Survival in Early-Stage Tumors. Ear Nose Throat J. 2019;98(7):E112-9.
- 37. Smits RWH, van Lanschot CGF, Aaboubout Y, de Ridder M, Hegt VN, Barroso EM, et al. Intraoperative Assessment of the Resection Specimen Facilitates Achievement of Adequate Margins in Oral Carcinoma. Front Oncol. 2020;10:1-9.
- 38. Aaboubout Y, ten Hove I, Smits RWH, Hardillo JA, Puppels GJ, Koljenovic S. Specimendriven intraoperative assessment of resection margins should be standard of care for oral cancer patients. Oral Dis. 2021;27(1):111-6.
- 39. Wermker K, Belok F, Schipmann S, Klein M, Schulze H-J, Hallermann C. Prediction model for lymph node metastasis and recommendations for elective neck dissection in lip cancer. J Craniomaxillofac Surg. 2015;43(4):545-52.
- 40. Roepman P, Wessels LFA, Kettelarij N, Kemmeren P, Miles AJ, Lijnzaad P, et al. An expression profile for diagnosis of lymph node metastases from primary head and neck squamous cell carcinomas. Nat Genet. 2005;37(2):182-6.
- 41. van Hooff SR, Leusink FKJ, Roepman P, Baatenburg de Jong RJ, Speel E-JM, van den Brekel MWM, et al. Validation of a Gene Expression Signature for Assessment of Lymph Node Metastasis in Oral Squamous Cell Carcinoma. J Clin Oncol. 2012;30(33):4104-10.
- 42. Melchers L, Clausen M, Mastik M, Slagter-Menkema L, van der Wal J, Wisman G, et al. Identification of methylation markers for the prediction of nodal metastasis in oral and oropharyngeal squamous cell carcinoma. Epigenetics. 2015;10(9):850-60.

43. Takes RP, Baatenburg de Jong RJ, Alles MJRC, Meeuwis CA, Marres HAM, Knegt PPM, et al. Markers for Nodal Metastasis in Head and Neck Squamous Cancer. Arch Otolaryngol Neck Surg. 2002;128(5):512.



7

SPECIMEN-DRIVEN INTRAOPERATIVE ASSESSMENT OF RESECTION MARGINS SHOULD BE STANDARD OF CARE FOR ORAL CANCER PATIENTS

Yassine Aaboubout, Ivo Ten Hove, Roeland W H Smits, Jose A Hardillo, Gerwin J Puppels, Senada Koljenovic

Oral Dis. 2021 Jan;27(1):111-116



ABSTRACT

With an incidence of 350.000 new cases per year, cancer of the oral cavity ranks among the 10 most common solid organ cancers. Most of these cancers are squamous cell carcinomas. Five-year survival is about 50%. It has been shown that clear resection margins (>5 mm healthy tissue surrounding the resected tumor) have a significant positive effect on locoregional control and survival. It is not uncommon that the resection margins of oral tumors are inadequate. However, when providing the surgeon with intraoperative feedback on the resection margin status, it is expected that obtaining adequate resection margins is improved. In this respect, it has been shown that specimen-driven intraoperative assessment of resection margins is superior to defect-driven intraoperative assessment of resection margins. In this concise report, it is described how a specimen-driven approach can increase the rate of adequate resections of oral cavity squamous cell carcinoma as well as that it is discussed how intraoperative assessment can be further improved with regard to the surgical treatment of oral cavity squamous cell carcinoma.

INTRODUCTION

Each year about 350.000 patients are diagnosed with cancer in the oral cavity worldwide, the vast majority of which are squamous cell carcinoma (90% of the cases)¹. Oral cavity squamous cell carcinoma (OCSCC) ranks among the ten most common solid organ cancers. The 5-year survival of OCSCC patients is about 50%, with little improvement over the last decades².

Surgery is the mainstay of treatment for OCSCC and aims for complete resection of the tumor with adequate margins, while sparing healthy tissue as much as possible³.

The most widely accepted definition of margins in oral cancer surgery is that of The Royal College of Pathologists⁴. A clear (or adequate) margin means a distance of more than 5 mm from resection surface to the tumor border, a distance of 1-5 mm is called a close margin. A distance of <1 mm is called a positive margin⁵.

Of all oncological prognostic factors (i.e., patient and tumor characteristics), the surgeon and pathologist can only influence the resection margins. Adequate resection margins in OCSCC lead to higher survival and a marked reduction in local recurrence^{6,7}. Inadequate resection margins result in the need for adjuvant therapy in the form of postoperative (chemo-) radiotherapy. Adjuvant therapy brings an additional burden for the patient, which in the vast majority of cases results in increased morbidity and reduced quality of life⁸.

There is a debate in the literature about the margin definition. Although there is evidence that margins of >5 mm improve patient outcome (e.g., local control, disease-free survival, overall survival) and that there should be agreement on 5 mm margin as a clear margin^{4,6,7}, several studies found that margins of <5 mm are sufficient, especially for early-stage OCSCC. Nason et al. unequivocally stated that survival improves with each additional millimeter of clear surgical margin and proposes a minimum margin of 3 mm to be considered an adequate resection⁹. Zanoni et al. showed that for tongue cancer, resection margins between 2.2 and 5 mm show no greater risk of local recurrence, than margins >5 mm¹⁰. Jang et al. reported little or no effect of resection margin status on local recurrence, but only for small (<3 mm diameter) T1 tumors¹¹, as did Barry et al. for T1/T2 tumors¹². Dik et al. concluded that a margin of 3 mm with ≤2 other adverse histological features is as safe as a margin of 5 mm in relation to local recurrence¹³. Another recent study showed that only a margin of <1 mm was associated with an increased risk of local recurrence¹⁴. However, the evidence put forward to decide what is an adequate margin is still very fragmented.

Until sufficient evidence is accumulated in a meta-analysis on the basis of which a new consensus can be reached, a margin >5 mm should be pursued.

A separate discussion concerns the recommended adjuvant therapy in connection with margin status. Many centers regard a positive margin to be an absolute indication for adjuvant treatment. There is no consensus on when to indicate adjuvant therapy in case of a close margin. However, many authors do not regard close margin (<5 mm) as adequate, but do not recommend postoperative radiotherapy for OCSCC patients if a close margin is the only adverse tumor feature (i.e., without perineural invasion and infiltrative growth pattern)¹⁵. Dik et al. showed that there was no evidence of benefit for any local adjuvant therapy in case of a margin of 3 mm with only one or two more adverse histological features¹³. They compared the impact of re-resection, postoperative radiotherapy, and watchful waiting.

Working in the complex oral anatomy and having to rely solely on visual inspection, palpation, and preoperative imaging, the surgeon is caught between the goals of achieving an adequate tumor resection and safeguarding satisfactory remaining function and acceptable physical appearance.

Recent studies have shown that an adequate tumor resection is often only achieved in a minority (15%-26%) of cases^{6,7,13}.

However, there is a wide range of adequate resection margins reported in the literature, varying from 35% to 70%. Surprisingly, clinical outcomes in terms of overall survival and recurrence seemed comparable among the centers, irrespective of the reported rate of adequate resections. This variation in results is caused by a lack of unanimous agreement on resection margins and differences in surgicopathological approaches. This prevents a genuine comparison of the results between the centers.

Clearly, the hands and eyes of the surgeon cannot warrant an adequate resection. Moreover, the definitive margin status, as determined during the final pathology, follows only several days after the operation. If at that point an inadequate margin is encountered, a second operation is not an option, nor effective, because an accurate relocation of the site of an inadequate margin is impossible in most cases. Therefore, there is a need for the introduction of techniques to improve getting adequate surgical margins.

HOW TO ACHIEVE "FIRST TIME RIGHT" SURGERY?

It is evident that for optimal control of resection margin, the surgeon needs additional information. Intraoperative assessment of resection margins (IOARM) can provide such valuable information, enabling additional tissue resection when needed to turn an otherwise inadequate tumor resection into an adequate operation. Two methods of IOARM can be distinguished: the traditional defect-driven IOARM based on frozen sections and the recently recommended specimen-driven assessment.

Defect-Driven IOARM

For defect-driven intraoperative assessment, the surgeon takes tissue samples from the wound bed for frozen section histopathologic analysis. Of all surgical disciplines, intraoperative assessment of the resection margins based on the frozen section procedure is most often performed for head and neck cancers¹⁶.

Although the frozen section analysis is a well-known procedure available in many centers, studies have reported that it has no impact on regional control or an improvement in survival in OCSCC patients^{7,14, 17-20}.

Frozen section analysis during defect-driven IOARM has a high accuracy in classification of the tissue samples, but is poorly predictive of the final margin status. The obvious reason is that the method is time-consuming and laborious, so that relatively few tissue samples can be analyzed intraoperatively. Hence, the method is fraught with sampling error. Recent large cohort studies showed no benefit with respect to local recurrence or survival, when a re-resection was performed because of a positive frozen section margin based on defect-driven intraoperative assessment^{14,18}. This is caused by the well-known difficulty of relocation of the exact location of the frozen section tissue sample in the wound bed. Relocation is particularly difficult in the head and neck region, and therefore, an optimal additional resection is not always achieved²¹⁻²⁵.

Thus, the defect-driven frozen section procedure is presumed to be insufficient for decision making regarding the need for additional resection to achieve "first time right" surgery.

Specimen-driven IOARM

A 2005 survey reported that over 90% of surgeons performed a defect-driven frozen section analysis and only 14%-24% performed a specimen-driven margin assessment during OCSCC surgery⁴.

Since that time, there is growing evidence that specimen-driven IOARM is superior to defect-driven assessment^{7,24,26-28}. A recent study showed that specimen-driven IOARM by macroscopic examination and measurement of margins is as accurate as specimen-driven IOARM accompanied by sampling of tissue for microscopic evaluation of frozen sections¹⁹

In 2017, the American Joint Committee on Cancer (AJCC) has recommended specimen-driven intraoperative assessment as a standard of care²⁹. At our institute, we have implemented a comprehensive specimen-driven IOARM since 2013. The method has become our standard of care in 2015 (**Figure 7.1**). A pathologist and the surgeon inspect the resection specimen macroscopically (by visual inspection, palpation, and by making incisions in the specimen perpendicular to the resection plane) and when necessary microscopically (by sampling tissue for frozen section analysis, from the suspicious areas if the location of the tumor border is not clear by macroscopic inspection).

The specimen-driven IOARM procedure is accompanied by a simple method for the relocation of inadequate margins in the wound bed, that have been identified on the resection specimen, to enable confident additional resection. The relocation method is described in detail by van Lanschot et al.³⁰.

Preferably, the entire IOARM process, including the conclusion and the recommendation for additional resection, is recorded (including photographs) and stored in the patient file. This information can then be used during the final pathologic assessment and multi-disciplinary consultations.

Although specimen-driven IOARM has led to a significant improvement in obtaining adequate OCSCC surgical margins, which underlines the necessity of intraoperative feedback to the surgeon, the level of its wide implementation still leaves a lot to wish for.

The main concerns to perform specimen-driven IOARM include the fact that grossing fresh tissue is counter-intuitive to pathologists as wells as that grossing fresh tissue might deteriorate the anatomical orientation and the shape or size of the specimen.

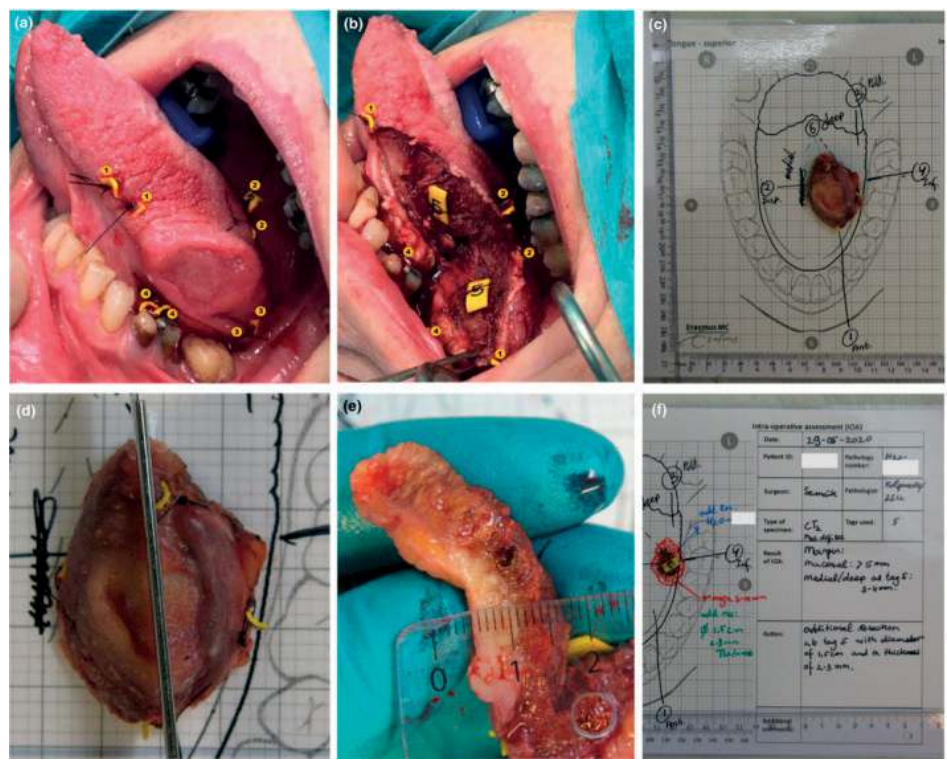


Figure 7.1. Illustration of the IOARM procedure including the relocation method by parallel tagging. (a) The surgeon attaches numbered tags in a pair-wise manner on both sides of the resection line, superficial and deep during the resection. (b) After the tumor resection has been completed, one numbered tag of each pair is attached to the specimen and the other tag remains in the wound bed. (c) Anatomical template of the tongue with the specimen, patient information, and the annotated tags. These templates have been designed to facilitate the preservation of anatomical orientation of the specimen during the IOARM. (d) The pathologist and surgeon inspect and palpate the specimen for suspicious areas (i.e., areas where margin might be less than ≤ 5 mm). If a suspicious area is found, the pathologist makes one or more parallel incisions perpendicular to the resection surface (with a mutual distance of 5-6 mm). This enables the visualization and measurement of the margin. (e) Measuring the margin with a ruler. If an inadequate margin is detected, its location is indicated based on the numbered tags. Advice is given for an additional resection in the indicated area, including the thickness. (f) Result of IOARM (e.g., at the location of tag nr. 5, the margin is 3-4 mm) is recorded at the template, together with the recommendation for additional resection (e.g., area of tissue enclosing tag 5, with a diameter of 1.5 cm and the thickness 3-4 mm).

These obstacles potentially can affect the final, postoperative pathologic assessment^{31,32}. Another concern is the assumption that a specimen-driven IOARM might be more time-consuming than defect-driven IOARM, because of the distance between the operating room and department of pathology. Finally, it is not realistic to expect that this approach can be commonly adopted because a dedicated team of head and neck surgeons and pathologists is not available in every center.

FUTURE

Specimen-driven IOARM works, but it is important to be open for innovative modalities with the goals to further improve its accuracy and to enable more widespread implementation. For example, technology is needed that will enable objective inspection of the entire resection surface. Raman spectroscopy is among the most promising optical techniques to fill this gap. Raman spectroscopy is an optical technique that does not require sample preparation. This technique provides real-time information about the molecular composition of the tissue. Earlier studies have shown that Raman spectroscopy discriminates between OCSCC and healthy tissue, with a sensitivity of 99% and a specificity of 92%^{33,34}.

Currently, Raman spectroscopy is implemented in a prototype instrument employing a fiber-optic needle probe (**Figure 7.2**). This fiber-optic needle is driven into the specimen, from the resection surface toward the tumor. Based on the Raman spectra collected along the insertion path, it is determined whether the needle tip is in healthy or tumor tissue. This principle is used to measure the resection margin (i.e., distance between the resection surface and the tumor border, given in millimeters). This takes a few seconds per measurement and enables objective measurement of resection margins without the need for grossing of the specimen.

In addition, to be used for soft tissue intraoperative assessment, Raman spectroscopy can also be used to assess osseous resection margins in the OCSCC patients treated with bone resection³⁵. When shown to be feasible and reliable, this Raman spectroscopic approach could solve the persisting problem of the lack of IOARM for bone resection margins (for both segmental and marginal bone resections)^{36,37}.

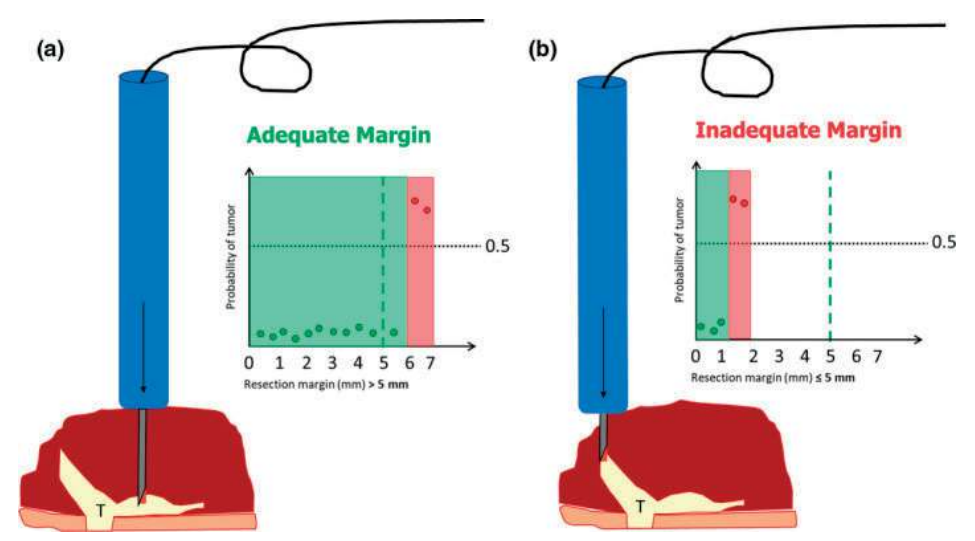


Figure 7.2. Illustration of specimen-driven IOARM based on Raman spectroscopy. The fiber-optic needle determines the resection margin as a distance between the resection surface and tumor border, given in millimeters. The fiber-optic needle is driven into the specimen, from the resection surface toward the tumor border. Raman spectra are collected along the insertion path at each 0.5 mm of depth. In the graphs, each measurement is presented as a dot; the x-axis shows the measured resection margin in millimeters, and the y-axis shows the probability of individual measurements to be classified as tumor or not. (a) Example of adequate margin (6 mm) between tags 1 and 2, no additional resection is needed. (b) Example of inadequate margin (1.5 mm) between tags 0 and 1, an additional resection is needed.

CONCLUSION

Radical tumor resection is the goal of surgery since ancient times, when Galen recommended that the whole tumor with its all "roots" should be removed³⁸. Unfortunately, after almost two millennia this goal is still not achieved for many patients. The importance of adequate tumor resection cannot be overemphasized, and specimen-driven intraoperative assessment of resection margins is crucial to this. In addition to the upcoming specimen-driven IOARM approach, new technology is needed to further improve its accuracy and to enable its widespread implementation.

The literature on IOARM is clear in its verdict that a specimen-driven approach is superior to defect-driven IOARM in guiding surgeon and pathologist toward adequate resection.

REFERENCES

- Bray F, Ferlay J, Soerjomataram I, Siegel RL, Torre LA, Jemal A. Global cancer statistics 2018: GLOBOCAN estimates of incidence and mortality worldwide for 36 cancers in 185 countries. CA Cancer J Clin. 2018;68(6):394-424. doi:10.3322/caac.21492
- van der Ploeg T, Datema F, Baatenburg de Jong RJ, Steyerberg EW. Prediction of survival with alternative modeling techniques using pseudo values. *PLoS One*. 2014;9(6):e100234. doi:10.1371/journal.pone.0100234
- 3. Shah JP, Gil Z. Current concepts in management of oral cancer Surgery. *Oral Oncol*. 2009;45(4-5):394-401. doi:10.1016/j.oraloncology.2008.05.017
- 4. Meier JD, Oliver DA, Varvares MA. Surgical margin determination in head and neck oncology: Current clinical practice. *Head Neck*. 2005;27(11):952-8. doi:10.1002/hed.20269
- 5. Helliwell T, Woolgar J. Dataset for histopathology reporting of mucosal malignancies of the oral cavity. *Royal College of Pathologists*; 2013.
- 6. Smits RWH, Koljenović S, Hardillo JA, ten Hove I, Meeuwis CA, Sewnaik A, et al. Resection margins in oral cancer surgery: Room for improvement. *Head Neck*. 2016;38(S1):E2197-203. doi:10.1002/hed.24075
- 7. Varvares MA, Poti S, Kenyon B, Christopher K, Walker RJ. Surgical margins and primary site resection in achieving local control in oral cancer resections. *Laryngoscope*. 2015;125(10):2298-307. doi:10.1002/lary.25397
- 8. Lin A. Radiation therapy for oral cavity and oropharyngeal cancers. *Dent Clin North Am*. 2018;62(1):99-109. doi:10.1016/j.cden.2017.08.007
- 9. Nason RW, Binahmed A, Pathak KA, Abdoh AA, Sándor GK. What is the adequate margin of surgical resection in oral cancer? *Oral Surg Oral Med Oral Pathol Oral Radiol Endod*. 2009;107(5):625-9. doi:10.1016/j.tripleo.2008.11.013
- 10. Zanoni DK, Migliacci JC, Xu B, Katabi N, Montero PH, Ganly I, et al. A proposal to redefine close surgical margins in squamous cell carcinoma of the oral tongue. *JAMA Otolaryngol Head Neck Surg.* 2017;143(6):555-60. doi:10.1001/jamaoto.2016.4238
- 11. Jang JY, Choi N, Ko YH, Chung MK, Son YI, Baek CH, et al. Differential impact of close surgical margin on local recurrence according to primary tumor size in oral squamous cell carcinoma. *Ann Surg Oncol*. 2017;24(6):1698-706. doi:10.1245/s10434-016-5497-4
- 12. Barry CP, Ahmed F, Rogers SN, Lowe CD, Bekiroglu F, Brown JS, et al. Influence of surgical margins on local recurrence in T1/T2 oral squamous cell carcinoma. *Head Neck*. 2014;36(10):1391. doi:10.1002/HED
- Dik EA, Willems SM, Ipenburg NA, Adriaansens SO, Rosenberg AJWP, Van Es RJJ. Resection of early oral squamous cell carcinoma with positive or close margins: Relevance of adjuvant treatment in relation to local recurrence. *Oral Oncol*. 2014;50(6):611-5. doi:10.1016/j.oraloncology.2014.02.014
- 14. Buchakjian MR, Tasche KK, Robinson RA, Pagedar NA, Sperry SM. Association of main specimen and tumor bed margin status with local recurrence and survival in oral cancer surgery. *JAMA Otolaryngol Head Neck Surg*. 2016;142(12):1191-8. doi:10.1001/jamaoto.2016.2329

- 15. Ch'ng S, Corbett-Burns S, Stanton N, Gao K, Shannon K, Clifford A, et al. Close margin alone does not warrant postoperative adjuvant radiotherapy in oral squamous cell carcinoma. *Cancer*. 2013;119(13):2427-37. doi:10.1002/cncr.28081
- McIntosh ER, Harada S, Drwiega J, Brandwein-Gensler MS, Gordetsky J. Frozen section: Guiding the hands of surgeons? *Ann Diagn Pathol*. 2015;19(5):326-9. doi:10.1016/j.anndiagpath.2015.07.004
- 17. Abbas SA, Ikram M, Tariq MU, Raheem A, Saeed J. Accuracy of frozen sections in oral cancer resections, an experience of a tertiary care hospital. *J Pak Med Assoc.* 2017;67(5):806-9.
- 18. Buchakjian MR, Ginader T, Tasche KK, Pagedar NA, Smith BJ, Sperry SM. Independent predictors of prognosis based on oral cavity squamous cell carcinoma surgical margins. *Otolaryngol Head Neck Surg.* 2018;159(4):675-82. doi:10.1177/0194599818773070
- 19. Mair M, Nair D, Nair S, Dutta S, Garg A, Malik A, et al. Intraoperative gross examination vs frozen section for achievement of adequate margin in oral cancer surgery. *Oral Surg Oral Med Oral Pathol Oral Radiol*. 2017;123(5):544-9. doi:10.1016/j.oooo.2016.11.018
- Pathak KA, Nason RW, Penner C, Viallet NR, Sutherland D, Kerr PD. Impact of use of frozen section assessment of operative margins on survival in oral cancer. *Oral Surg Oral Med Oral Pathol Oral Radiol Endod*. 2009;107(2):235-9. doi:10.1016/j.tripleo.2008.09.028
- 21. Gokavarapu S, Rao LMC, Mahajan M, Parvataneni N, Raju KVVN, Chander R. Revision of margins under frozen section in oral cancer: A retrospective study. *Br J Oral Maxillofac Surg.* 2015;53(9):875-9. doi:10.1016/j.bjoms.2015.08.257
- 22. Kerawala CJ, Ong TK. Relocating the site of frozen sections? Is there room for improvement? Head Neck. 2001;23(3):230-2. doi:10.1002/1097-0347(200103)23:3<230::AID-HED1023>3.0.CO;2-V
- 23. Magliocca KR. Surgical margins: The perspective of pathology. *Oral Maxillofac Surg Clin North Am.* 2017;29(3):367-75. doi:10.1016/j.coms.2017.05.002
- 24. Maxwell JH, Thompson LDR, Brandwein-Gensler MS, Weiss BG, Canis M, Purgina B, et al. Early oral tongue squamous cell carcinoma sampling of margins. *JAMA Otolaryngol Head Neck Surg.* 2015;141(12):1104-10. doi:10.1001/jamaoto.2015.1351
- 25. Williams MD. Determining adequate margins in head and neck cancers: Practice and continued challenges. *Curr Oncol Rep.* 2016;18(9):54. doi:10.1007/s11912-016-0540-y
- Amit M, Na'ara S, Leider-Trejo L, Akrish S, Cohen JT, Billan S, et al. Improving the rate of negative margins after surgery. Head Neck. 2016;38(S1):E1803-9. doi:10.1002/hed.24320
- 27. Hinni ML, Zarka MA, Hoxworth JM. Margin mapping in transoral surgery for head and neck cancer. *Laryngoscope*. 2013;123(5):1190-8. doi:10.1002/lary.23900
- 28. Kain JJ, Birkeland AC, Udayakumar N, Morlandt AB, Stevens TM, Carroll WR, et al. Surgical margins in oral cavity squamous cell carcinoma: Current practices and future directions. *Laryngoscope*. 2020;130(1):128-38. doi:10.1002/lary.27943
- 29. Amin MB, Greene FL, Edge SB, Compton CC, Gershenwald JE, Brookland RK, et al. The Eighth Edition AJCC Cancer Staging Manual. *CA Cancer J Clin*. 2017;67(2):93-9. doi:10.3322/caac.21388
- van Lanschot CGF, Mast H, Hardillo JA, Monserez D, ten Hove I, Barroso EM, et al. Relocation of inadequate resection margins. Head Neck. 2019;41(7):2159-66. doi:10.1002/hed.25690

- 31. Pangare TB, Waknis PP, Bawane SS, Patil MN, Wadhera S, Patowary PB. Effect of formalin fixation on surgical margins. *J Oral Maxillofac Surg*. 2017;75(6):1293-8. doi:10.1016/j.joms.2016.11.024
- 32. Umstattd LA, Mills JC, Critchlow WA, Renner GJ, Zitsch RP. Shrinkage in oral squamous cell carcinoma. *Am J Otolaryngol*. 2017;38(6):660-2. doi:10.1016/j.amjoto.2017.08.011
- 33. Barroso EM, Smits RWH, Schut TCB, Ten Hove I, Hardillo JA, Wolvius EB, et al. Discrimination between oral cancer and healthy tissue. *Anal Chem.* 2015;87(4):2419-26. doi:10.1021/ac504362y
- Barroso EM, Smits RWH, Van Lanschot CGF, Caspers PJ, Ten Hove I, Mast H, et al. Water concentration analysis by Raman spectroscopy. *Cancer Res.* 2016;76(20):5945-53. doi:10.1158/0008-5472.CAN-16-1227
- 35. Barroso EM, ten Hove I, Bakker Schut TC, Mast H, van Lanschot CGF, Smits RWH, et al. Raman spectroscopy for assessment of bone resection margins. *Eur J Cancer*. 2018;92:77-87. doi:10.1016/j.ejca.2018.01.068
- 36. Nieberler M, Häusler P, Drecoll E, Stoeckelhuber M, Deppe H, Hölzle F, et al. Evaluation of intraoperative cytological assessment. *Cancer Cytopathol*. 2014;122(9):646-56. doi:10.1002/cncy.21428
- 37. Smits RWH, ten Hove I, Dronkers EAC, Bakker Schut TC, Mast H, Baatenburg de Jong RJ, et al. Evaluation of bone resection margins. *Int J Oral Maxillofac Surg.* 2018;47(8):959-64. doi:10.1016/j.ijom.2018.03.006
- Papavramidou N, Papavramidis T, Demetriou T. Ancient Greek and Greco-Roman methods in modern surgical treatment. Ann Surg Oncol. 2010;17(3):665-7. doi:10.1245/s10434-009-0886-6



8 GENERAL DISCUSSION AND OUTLOOK



THE FINE LINE

Surgery is the mainstay treatment for OCSCC¹. In the perfect world, the surgeon would excise the tumor with the utmost finesse, meaning the excision of the tumor with a margin of more than 5 millimeters, as recommended by the AJCC, but never exceeding this boundary². This would result in an adequate resection margin while preserving as much healthy tissue as possible.

Currently, in some parts of the world, the surgeon may have a more aggressive approach (reminiscent of the well-known Dr. William Halsted) due to the lack of postoperative radiotherapy. In these cases, the surgery might result in more adequate resections. However, at the same time, it is a very mutilating procedure that also affects functionality (e.g., mastication, swallowing, and speech). Conversely, the surgeon may adopt a more conservative approach to preserve as much of the aesthetics and functionality. In these cases, the surgery is more likely to result in an inadequate resection of the tumor (Chapter 2), which usually necessitates postoperative radiotherapy.

THE RELEVANCE OF RESECTION MARGINS IN OCSCC

Currently, the AJCC guidelines differentiate margins as clear, close, or positive². Clear margins are defined as adequate whereas close and positive margins are defined as inadequate. The literature shows that an adequate resection improves patient outcomes (e.g., lower local recurrence and longer disease-free survival)³⁻⁷.

However, in the last few years, there has been a growing debate in the literature about the definition of margins. More and more studies are being performed to show whether or not a surgical margin of 4 mm or 3 mm would suffice as an adequate resection. Lin et al. recently showed, in a Taiwanese national database analysis with roughly 15.000 patients, that the group of patients with a resection margin of 4.0-4.9 mm had similar disease-specific survival as the group of patients with a resection margin of ≥ 5 mm. They finally recommend that a resection margin of > 4.0 mm should be defined as adequate⁸. Sadly, they did not perform an analysis of local recurrence.

Another study even recommended a margin of ≥ 3 mm based on the 5-year survival and local recurrence rate. This study showed a 5-year recurrence-free survival of 69.5% in the 3 to 4.9 mm group in comparison to the 70.5% in the ≥ 5 mm group. The

recurrence rate was 24.4% in the 3 to 4.9 mm in comparison to 25.3% in the \geq 5 mm group. However, their analysis also shows that for each millimeter of progression towards the 5 millimeter boundary, the risk of death at 5 years decreases by 8%. These results should carefully be interpreted as only 277 patients were included and divided into 4 groups. Moreover, the patients with an inadequate margin were treated with adjunctive radiotherapy, which could have a disruptive effect on the recurrence rates and survival.

Some studies state that the definition of an adequate margin differs per anatomical location. For example, in tongue resections, Zanoni et al. showed that the 2-year local recurrence-free survival between the 2.3 - 5.0 mm group and the > 5 mm group, were 93.5% and 91.8%, respectively. Based on these results, they proposed new definitions for margins in squamous cell carcinoma of the tongue: 0.1 - 2.2 mm as a close margin and ≥ 2.3 mm as a clear margin¹⁰.

To genuinely compare the results of these previously mentioned and future studies, the implementation of a worldwide pathology protocol is much needed. Currently, different national protocols are used^{11,12}.

This worldwide pathology protocol should address the following:

- 1. Systematic grossing of the specimen.
- 2. Standard/synoptic reporting.
- 3. Standard meetings of pathologists and surgeons to evaluate the number of adequate resections.

Grossing - Depending on the institute either the pathologist, pathology resident or a specialized pathology assistant does the grossing. The main objective is the appropriate sampling of the resection specimen to generate a complete pathology report. Therefore, this process is of the utmost importance, mistakes or incomplete sampling can lead to a faulty pathology report which can affect further treatment decisions. Therefore, multiple sections of the tumor should be sampled including the deepest invasion, to determine the differentiation grade, tumor size, invasion depth, lymphovascular invasion, and perineural invasion. Furthermore, the resection margins (mucosal and deep) should be sampled in all directions.

Pathology report - The quality of the pathology report depends heavily on the experience and skills of the pathologist. Therefore, a dedicated head and neck pathologist should preferably take care of the pathology report. A systematic approach in which all information (i.e., differentiation grade, tumor size, invasion depth, lymphovascu-

lar invasion, perineural invasion, resection margins, and pTNM) is reported, not only for further treatment but also for future studies.

Meetings - Measurement brings knowledge, to evaluate the performance of the institute, regular meetings with the pathologist and surgeons are necessary. This will allow for close monitoring of the number of adequate resections and also allows for timely adjustments if needed. One must remember that the best performance can only be achieved by a dedicated team of surgeons and pathologists.

IOARM IS A MUST

As described at the beginning of this discussion, we are far from the ideal surgical procedure. Currently, during the resection of a tumor, the surgeon relies on preoperative imaging, visual inspection, and palpation. The preoperative imaging might be weeks old at the time of surgery. The tumor may have grown in this period and therefore the tumor border may be changed. As it is, the surgeon intraoperatively relies mostly on visual and palpatory information. Therefore, intraoperative assessment of the resection margins is very necessary and we would state that it should be mandatory.

The evidence of the effect of IOARM in the literature is unmistakable and growing, much so that even the AJCC strongly recommends its implementation for standard care². This thesis adds evidence to the literature that IOARM is essential for patient care.

This thesis is a petition for the wide adoption of specimen-driven IOARM, as described in **Chapter 3**. This method can easily be implemented and the materials used for this method are cheap and available worldwide. However, it does require a dedicated team of healthcare providers (e.g., surgeons, pathologists, assistants, trainees, and researchers) to make and keep it as a standard of care.

In this method, the margins are assessed together by the surgeon and pathologist through visual inspection, palpation, and perpendicular incisions of the suspicious areas. This approach provides an estimation of margins in millimeters and allows for an additional resection if needed. However, Kubik et al reported several causes (e.g., the incorrect orientation of the additional resection, incorrect dimensions of the additional resection, and additional resection at an incorrect location) for additional resections to fail during the intraoperative assessment¹³. To circumvent these causes, any IOARM method needs to be accompanied by a relocation method. Our institute

developed a paired tagging system that allows us to accurately relocate inadequate margins from the resection specimen back into the patient¹⁴.

The IOARM method (**Chapter 3**) is occasionally supported by the frozen section procedure if the tumor border is macroscopically hard to distinguish (e.g., fibrosis of tissue after radiotherapy or scar formation after previous surgery, or salivary gland tissue). However, the implementation of the IOARM drastically decreases the number of frozen sections needed, which are known to be costly, time-consuming, and not accessible for all institutes. This protocol is following previous reports, that standard frozen section analysis is not cost-effective and, in most cases, does not improve the accuracy of specimen-driven IOARM¹⁵⁻¹⁷. Physicians have shown that they cannot reliably detect inadequate resection margins. For example, sampling error by the use of frozen sections or sampling error with the IOARM method as described in **Chapter 3** (even though this method did significantly increase performance).

Despite the evident improvement in the number of adequate resections as a result of the implementation of the specimen-driven IOARM, its wide adoption is lacking because pathologists find the grossing of fresh tissue counterintuitive. They are fearful that the grossing of the freshly resected tissue will lead to the deterioration of the shape, size, and anatomical orientation of the specimen, which therefore will affect the final histopathologic assessment ^{18,19}. The measures prescribed in **Chapter 3**, prevent these possible negative effects. Since the implementation of this protocol in our hospital, the final pathologic assessment has never become compromised.

According to a recent survey, intraoperative assessment is practiced by 96,8% of head and neck surgeons by performing frozen sections. Unfortunately, this survey also shows that only 55% of surgeons use a specimen-driven approach²⁰. Even so, this is a significant increase compared to the 2005 survey, in which only 16% of the surgeons used a specimen-driven approach³.

However, the evidence of the superiority of the specimen-driven approach is overwhelming^{6,13,21-25}. **Chapter 2**, a literature review of the performance of both the defect-driven and specimen-driven approach, confirms this. It shows that the performance (i.e., accuracy, sensitivity, specificity, PPV, and NPV) is better for the specimen-driven approach. In the conventional defect-driven approach, the surgeon extracts one or more suspicious fragments of tissue from the surgical wound bed for analysis by frozen section (i.e., a tissue sample that has been quick-frozen, cut by a microtome, and stained immediately for rapid microscopic diagnosis). However, the significant handicap of this approach lies in its limited ability to solely indicate the

presence of a tumor-positive margin. The defect-driven approach cannot provide the exact margin value in millimeters, which the specimen-driven method can. One could state that the defect-driven intraoperative assessment is like navigating through a dense dark forest armed with a dim candle and a narrow scope.

This shows that new methods (the specimen-driven approach) in medicine can take a long time to be adopted worldwide and that an old method like frozen section sampling from the wound bed can be practiced long overdue. For example, the radical mastectomy was introduced in 1891 by Halsted. Only in 1981, nearly 100 years later, the horrifying and disfiguring surgical procedure was abandoned for a less invasive procedure. It took this long, even though the evidence was readily available in 1924. The most likely cause of this delay is the internal culture and the rituals of practice in the world of medicine²⁶.

Even though IOARM could be easily implemented with a willing team and has a great impact on patient care, there is still much to be improved. As previously described the number of adequate resections varies a lot, due to the subjective nature of the procedure. The performance of the IOARM is based on the experience of the pathologist and the number of possible incisions on the fresh tissue. The grossing of fresh tissue is performed based on the palpation of the resection specimen and small parts of the tumor cannot be detected by palpation, which results in missed close margins. Moreover, fresh tissue can only be grossed in tissue sections of at least 5 mm, compared to the 2 to 3 mm after fixation, which can also result in missed close margins. The conclusion is that the sampling error needs to be improved to create the best IOARM procedure. The procedure as described in **Chapter 3** has reached its potential, so a new method must be developed. Therefore, objective methods are needed in which an entire resection surface can be scanned.

RAMAN SPECTROSCOPY-BASED IOARM

In **Chapter 4**, we report on the development and validation of a Raman spectroscopy-based device to objectively measure the distance from the resection surface to the tumor border by a thin fiber-optic needle probe that is inserted into the resection specimen.

To realize this procedure, first, the needle and an insertion strategy had to be developed. **Chapter 5** shows that the thickness of the needle and the velocity of the insertion matter greatly on the tissue deformation during the insertion in tongue

tissue. We selected a velocity based on these results and further optimized the fiber-optic needle to suit our needs (such as deformation, contamination, and leaving no marks behind in the tissue during measurements). This resulted in a disposable thin fiber-optic needle probe, which left no visible marks in the resection tissue. The design of the needle prevents needle tip contamination and allows for fast consecutive measurements. However, the deformation could not be completely solved by optimizing the thickness of the needle, tip geometry, or insertion velocity. Therefore, we developed a vacuum chamber around the fiber-optic needle probe, that keeps the tissue in place during insertion.

Raman spectroscopy has been a focus for many oncological applications, such as the detection of pre-malignant lesions, detection of cancer, reduction of unnecessary biopsies, and guidance towards complete tumor removal²⁷⁻³².

Our institute has a long-standing Raman research line in oral cancer, that has progressed for many years. Cals et al showed that Raman spectroscopy could distinguish tumor tissue from adipose tissue, nerves, muscle tissue, salivary gland tissue, connective tissue, and squamous epithelium in 100%, 100%, 97%, 94%, 93%, and 75% of the cases, respectively^{33,34}. In 2016 Barroso et al showed that oral cavity squamous cell carcinoma could be distinguished from healthy surrounding tissue based on the water concentration³⁵. Oral cavity squamous cell carcinoma has higher water content compared to the surrounding healthy tissue. This information could be used to distinguish tumor from healthy tissue and, therefore, to detect the tumor border.

Due to these previous efforts, we were able to implement all this knowledge into the newly designed Raman fiber-optic needle probe, as described in **Chapter 4**. The previous measurements were performed with a confocal microscope, whereas now we used a needle that concomitantly collected data as it was inserted into a freshly resected specimen. Early on, we noticed that water concentration alone was insufficient to differentiate between tumor and healthy tissue, particularly at the tumor border. However, we did notice that the Raman signal intensity ratio of the CH-stretching region (indicative of the lipid-to-protein ratio) and the Raman signal-to-autofluorescence ratio could contribute to distinguishing tumor tissue from healthy tissue. In this way, a tissue classification model was developed and tested, which allowed for the margin length prediction model to be developed and also tested, as shown in **Chapter 4**.

This resulted in an easy-to-use device that allows its user to objectively assess the resection margin at a chosen location within 5 seconds. Moreover, the speedy measurement also allows its user to perform measurements at many locations. Lastly, the

measurements could be carried out by anyone with little training, so that the device could be in, or nearby the operating room.

OUTLOOK

In this thesis, we have demonstrated an easy-to-use and accessible method for IO-ARM, which had a great impact on improving the percentage of adequate resections. Finally, we have also established a way to objectively measure the resection margin on freshly resected tissue employing Raman spectroscopy.

However, to truly create an objective method, we must develop a systematic process to measure the entire resection surface, a so-called measurement strategy. The goal of the development of a measurement strategy is to guarantee that the entire resection surface is assessed within a limited time frame.

After the measurement strategy has been devised and has been tested, the last remaining step is a multi-center study to compare the performance of the device with the standard of care of the selected institutes. In most cases, this means the Raman device will be compared with the defect-driven intraoperative assessment (many institutes still use this inferior and outdated method). The following situations will be compared: 1) Raman device versus the retrospective numbers (surgeon), 2) Raman device versus the IOARM method from **Chapter 3** (pathologist and surgeon).

Finally, we want to investigate if the device with the measurement strategy can perform better or equally well as the pathologist. Even if it is equally good, the device is easier to implement, in or nearby the operation room, does not require a pathologist, leaves the specimen intact, and lastly does not need a dedicated team of physicians.

Another application of the device would be the measurement of the depth of invasion. Conceptually, at least two measurements are needed: one from the closest normal adjacent mucosa and another from the tumor to the deepest point of invasion. This aligns with the recommendations from the 8th edition of the AJCC³⁶. If feasible, this measurement could be performed during outpatient clinics, allowing for an instant decision on whether to perform an elective neck dissection. Currently, this decision is made roughly two weeks after the initial surgery, necessitating a secondary operation in some cases. This application could potentially reduce the number of second operations needed and brings us a step closer to "first-time-right" surgery. As Pedro Domingos, a specialist in artificial intelligence has said, "It is not man versus

machine; it is man with machine versus man without"³⁷. This is the way to ensure that all patients around the world could receive what they are entitled to, namely, intraoperative assessment of resection margins.

REFERENCES

- Shah JP, Gil Z. Current concepts in management of oral cancer Surgery. Oral Oncol. 2009;45(4-5):394-401. doi:10.1016/j.oraloncology.2008.05.017
- 2. Amin MB, Greene FL, Edge SB, et al. The Eighth Edition AJCC Cancer Staging Manual: Continuing to build a bridge from a population-based to a more "personalized" approach to cancer staging. CA Cancer J Clin. 2017;67(2):93-99. doi:10.3322/caac.21388
- Meier JD, Oliver DA, Varvares MA. Surgical margin determination in head and neck oncology: Current clinical practice. Head Neck. 2005;27(11):952-958. doi:10.1002/hed.20269
- 4. Varvares MA, Poti S, Kenyon B, Christopher K, Walker RJ. Surgical margins and primary site resection in achieving local control in oral cancer resections. Laryngoscope. 2015;125(10):2298-2307. doi:10.1002/lary.25397
- Smits RWH, Koljenović S, Hardillo JA, et al. Resection margins in oral cancer surgery: Room for improvement. Head Neck. 2016;38(Suppl 1):E2197-E2203. doi:10.1002/hed.24075
- 6. Smits RWH, van Lanschot CGF, Aaboubout Y, et al. Intraoperative assessment of the resection specimen facilitates achievement of adequate margins in oral carcinoma. Front Oncol. 2020;10:614593. doi:10.3389/fonc.2020.614593
- 7. Kang CJ, Wen YW, Lee SR, et al. Surgical margins status and prognosis after resection of oral cavity squamous cell carcinoma: Results from a Taiwanese nationwide registry-based study. Cancers (Basel). 2021;14(1):15. doi:10.3390/cancers14010015
- 8. Lin MC, Leu YS, Chiang CJ, et al. Adequate surgical margins for oral cancer: A Taiwan cancer registry national database analysis. Oral Oncol. 2021;115:105358. doi:10.1016/j. oraloncology.2021.105358
- 9. Nason RW, Binahmed A, Pathak KA, Abdoh AA, Sándor GKB. What is the adequate margin of surgical resection in oral cancer? Oral Surg Oral Med Oral Pathol Oral Radiol Endod. 2009;107(5):625-629. doi:10.1016/j.tripleo.2008.11.013
- 10. Zanoni DK, Migliacci JC, Xu B, et al. A proposal to redefine close surgical margins in squamous cell carcinoma of the oral tongue. JAMA Otolaryngol Head Neck Surg. 2017;143(6):555-560. doi:10.1001/jamaoto.2016.4238
- 11. Casparie M, Tiebosch ATMG, Burger G, et al. Pathology databanking and biobanking in The Netherlands, a central role for PALGA. Cell Oncol. 2007;29(1):19-24. doi:10.1155/2007/971816
- 12. Woolgar JA, Triantafyllou A. A histopathological appraisal of surgical margins in oral and oropharyngeal cancer resection specimens. Oral Oncol. 2005;41(10):1034-1043. doi:10.1016/j.oraloncology.2005.06.008
- 13. Kubik MW, Sridharan S, Varvares MA, et al. Intraoperative margin assessment in head and neck cancer: A case of misuse and abuse? Head Neck Pathol. 2020;14(1):124-132. doi:10.1007/s12105-019-01121-2
- 14. Lanschot CGF, Mast H, Hardillo JA, et al. Relocation of inadequate resection margins in the wound bed during oral cavity oncological surgery: A feasibility study. Head Neck. 2019;41(7):2159-2166. doi:10.1002/hed.25690

- 15. Chaturvedi P, Datta S, Nair S, et al. Gross examination by the surgeon as an alternative to frozen section. Head Neck. 2014;36(7):957-961. doi:10.1002/hed.23313
- Mair M, Nair D, Nair S, et al. Intraoperative gross examination vs frozen section for achievement of adequate margin in oral cancer surgery. Oral Surg Oral Med Oral Pathol Oral Radiol. 2017;123(4):453-459. doi:10.1016/j.oooo.2016.11.018
- 17. Datta S, Mishra A, Chaturvedi P, et al. Frozen section is not cost beneficial for the assessment of margins in oral cancer. Indian J Cancer. 2019;56(1):44-47. doi:10.4103/ijc. IJC_41_18
- 18. Umstattd LA, Mills JC, Critchlow WA, Renner GJ, Zitsch RP. Shrinkage in oral squamous cell carcinoma: Tumor and margin measurements. Am J Otolaryngol. 2017;38(6):673-679. doi:10.1016/j.amjoto.2017.08.011
- 19. Pangare TB, Waknis PP, Bawane SS, et al. Effect of formalin fixation on surgical margins in oral squamous cell carcinoma. J Oral Maxillofac Surg. 2017;75(6):1293-1298. doi:10.1016/j.joms.2016.11.024
- 20. Bulbul MG, Zenga J, Tarabichi O, et al. Margin practices in oral cavity cancer resections: Survey of American Head and Neck Society members. Laryngoscope. 2021;131(7):E2193-E2199. doi:10.1002/lary.28976
- 21. Barroso EM, Aaboubout Y, van der Sar LC, et al. Performance of intraoperative assessment of resection margins in oral cancer surgery: A review of literature. Front Oncol. 2021;11:628297. doi:10.3389/fonc.2021.628297
- 22. Namin AW, Bruggers SD, Panuganti BA, et al. Efficacy of bone marrow cytologic evaluations in detecting occult cancellous invasion. Laryngoscope. 2015;125(12):2717-2721. doi:10.1002/lary.25063
- 23. Maxwell JH, Thompson LDR, Brandwein-Gensler MS, et al. Early oral tongue squamous cell carcinoma: Sampling of margins from tumor bed and worse local control. JAMA Otolaryngol Head Neck Surg. 2015;141(12):1104-1110. doi:10.1001/jamaoto.2015.1351
- 24. Kain JJ, Birkeland AC, Udayakumar N, et al. Surgical margins in oral cavity squamous cell carcinoma: Current practices and future directions. Laryngoscope. 2020;130(1):128-138. doi:10.1002/lary.27943
- Hinni ML, Zarka MA, Hoxworth JM. Margin mapping in transoral surgery for head and neck cancer. Laryngoscope. 2013;123(5):1190-1198. doi:10.1002/lary.23900
- Mukherjee S. The Emperor of All Maladies: A Biography of Cancer. 1st ed. New York: Scribner; 2010.
- Santos IP, Barroso EM, Bakker Schut TC, et al. Raman spectroscopy for cancer detection and cancer surgery guidance: Translation to the clinics. Analyst. 2017;142(17):3025-3047. doi:10.1039/C7AN00957G
- 28. Jermyn M, Mok K, Mercier J, et al. Intraoperative brain cancer detection with Raman spectroscopy in humans. Sci Transl Med. 2015;7(274):274ra19. doi:10.1126/scitranslmed. aaa2384
- Haka AS, Volynskaya Z, Gardecki JA, et al. Diagnosing breast cancer using Raman spectroscopy: Prospective analysis. J Biomed Opt. 2009;14(5):054023. doi:10.1117/1.3247154

- 30. Kallaway C, Almond LM, Barr H, et al. Advances in the clinical application of Raman spectroscopy for cancer diagnostics. Photodiagnosis Photodyn Ther. 2013;10(3):207-219. doi:10.1016/j.pdpdt.2013.01.008
- 31. Krafft C, Schie IW, Meyer T, Schmitt M, Popp J. Developments in spontaneous and coherent Raman scattering microscopic imaging for biomedical applications. Chem Soc Rev. 2016;45(7):1819-1849. doi:10.1039/C5CS00564G
- 32. Wang W, McGregor H, Short M, Zeng H. Clinical utility of Raman spectroscopy: Current applications and ongoing developments. Adv Healthc Technol. 2016;2:13-25. doi:10.2147/AHCT.S96486
- 33. Cals FLJ, Bakker Schut TC, Hardillo JA, et al. Investigation of the potential of Raman spectroscopy for oral cancer detection in surgical margins. Lab Invest. 2015;95(10):1186-1196. doi:10.1038/labinvest.2015.85
- 34. Cals FLJ, Koljenović S, Hardillo JA, et al. Development and validation of Raman spectroscopic classification models to discriminate tongue squamous cell carcinoma from non-tumorous tissue. Oral Oncol. 2016;62:28-35. doi:10.1016/j.oraloncology.2016.06.012
- 35. Barroso EM, Smits RWH, van Lanschot CGF, et al. Water concentration analysis by Raman spectroscopy to determine the location of the tumor border in oral cancer surgery. Cancer Res. 2016;76(20):5945-5953. doi:10.1158/0008-5472.CAN-16-1227
- 36. Lydiatt WM, Patel SG, O'Sullivan B, et al. Head and neck cancers—Major changes in the American Joint Committee on Cancer eighth edition cancer staging manual. CA Cancer J Clin. 2018;68(1):55-63. doi:10.3322/caac.21389
- 37. Domingos P. The master algorithm: How the quest for the ultimate learning machine will remake our world. Choice Rev Online. 2016;53(7):53-3100. doi:10.5860/CHOICE.194685



9 Summary



Per year, 350,000 patients are diagnosed with oral cavity cancer worldwide. This is primarily squamous cell carcinoma (OCSCC). Surgery is the main treatment, aiming for complete tumor resection with a margin of more than 5 mm of healthy tissue (adequate resection margin). Sadly, adequate tumor resections are only achieved in 15%-26% of the cases. Most surgeons currently rely on preoperative imaging and intraoperative visual inspection and palpation to achieve an adequate resection. The intraoperative assessment of resection margins (IOARM) is needed to improve the number of adequate resections.

In this thesis, we investigated the potential of different forms of intraoperative assessment of the resection margins. This thesis shows that there are limited studies that have investigated intraoperative assessment in oral cancer surgery. However, the studies that were found show that the specimen-driven IOARM approach has higher performance for both soft tissue and bone. Furthermore, our institute's specimen-driven IOARM approach - which is based on visual inspection, palpation, and grossing of the fresh tissue - is described in detail with a protocol and a short video. This method is easy to adopt by any pathologist and/or surgeon worldwide, as no expensive materials are needed. The performance of our specimen-driven IOARM shows an improvement from 15% to 58% adequate resections. The implementation of our method shows drastic improvements, nonetheless, it remains a subjective and labor-intensive method that requires the availability of a highly dedicated and specialized team of surgeons and pathologists. This hinders the widespread adoption of our method and therefore an easy-to-use technology is necessary.

Such a technology is Raman spectroscopy, which is a non-destructive optical technique, that provides information about the overall molecular composition of tissues, without the need for labels. We developed a Raman spectroscopy-based IOARM-device (RIOARM-device). It employs a thin fiber-optic needle probe that is inserted into the specimen to rapidly (5 seconds) determine the distance between the resection surface and the tumor border. To discriminate OCSCC from healthy oral tissue, a tissue classification model was developed, with a sensitivity of 0.87 and a specificity of 0.91. An independent validation of this model showed a sensitivity of 0.85 and a specificity of 0.92. Then, the tissue classification model was used to develop a margin length prediction model, which showed after an independent validation, a mean difference of -0.17 mm between the margin length predicted by Raman spectroscopy and histopathology.

Additionally, for the development of the fiber-optic needle probe, we investigated which needle characteristics were optimal for insertion into oral tissue. Tissue defor-

mation due to the insertion of a needle is strongly influenced by the tip geometry and insertion velocity. Moreover, an endurance test was performed with 100 insertions per needle, which showed no notable difference.

Lastly, the depth of invasion (DOI) is a significant predictor for occult lymph nodes and is used to decide whether an elective neck dissection is indicated. Sadly, the DOI can only be measured after a resection is performed and a second operation is needed. However, with the RIOARM-device, the DOI could be measured preoperatively.

In conclusion, the RIOARM-device enables widespread adoption of IOARM in oral cancer surgery, could be used to measure the DOI, and should not be limited to oral cancer surgery only.



10 Samenvatting



Per jaar worden wereldwijd 350.000 patiënten gediagnosticeerd met mondholtekanker. Dit is voornamelijk plaveiselcelcarcinoom. Chirurgie is de belangrijkste behandeling, gericht op volledige tumorresectie met een marge van meer dan 5 mm gezond weefsel (adequate resectiemarge). Helaas worden adequate tumorresecties slechts behaald bij 15%-26% van de gevallen. De meeste chirurgen vertrouwen momenteel op preoperatieve beeldvorming en intra-operatieve visuele inspectie en palpatie om een adequate resectie te bereiken. De intra-operatieve beoordeling van resectiemarges is nodig om het aantal adequate resecties te verbeteren.

In dit manuscript hebben we het potentieel van verschillende vormen van intraoperatieve beoordeling van resectiemarges onderzocht. Dit manuscript toont aan dat er een beperkte aantal studies zijn die intra-operatieve beoordeling bij mondholtekankerchirurgie hebben onderzocht. De gevonden studies tonen echter aan dat het preparaat-gedreven intra-operatieve beoordeling een betere prestatie heeft voor zowel wekedelen als voor bot. Bovendien wordt het preparaat-gedreven intra-operatieve beoordeling van ons instituut - die is gebaseerd op visuele inspectie, palpatie en bewerking van vers weefsel - gedetailleerd beschreven met een protocol en een korte video. Deze methode is eenvoudig over te nemen door elke patholoog en/of chirurg wereldwijd, omdat er geen dure materialen nodig zijn. De prestaties van onze specimen-gedreven intra-operatieve beoordeling tonen een verbetering van 15% naar 58% adequate resecties. Hoewel de implementatie van onze methode drastische verbeteringen laat zien, blijft het een subjectieve en arbeidsintensieve methode die de beschikbaarheid van een zeer toegewijd team van chirurgen en pathologen vereist. Dit belemmert de brede implementatie van onze methode, daarom is een gebruiksvriendelijke technologie noodzakelijk.

Een dergelijke technologie is Raman-spectroscopie, een niet-destructieve optische techniek die informatie geeft over de algehele moleculaire samenstelling van weefsels, zonder de noodzaak van labels. We hebben een Raman-spectroscopie-gebaseerd IOARM-apparaat (RIOARM-apparaat) ontwikkeld. Het maakt gebruik van een dunne fiber-optische naald die in het preparaat wordt ingebracht om snel (5 seconden) de afstand tussen het resectieoppervlak en de tumorrand te bepalen. Om plaveiselcelcarcinoom te onderscheiden van gezond mondslijmvlies, werd een weefselclassificatiemodel ontwikkeld met een sensitiviteit van 0,87 en een specificiteit van 0,91. Een onafhankelijke validatie van dit model toonde een sensitiviteit van 0,85 en een specificiteit van 0,92. Vervolgens werd het weefselclassificatiemodel gebruikt om een model voor de voorspelling van de marge-lengte te ontwikkelen, dat na een onafhankelijke validatie een gemiddeld verschil van -0,17 mm liet zien tussen de marge-lengte voorspeld door Raman-spectroscopie en de histopathologie.

Daarnaast hebben we voor de ontwikkeling van de fiber-optische naald onderzocht welke eigenschappen van de naald optimaal waren voor inbrengen in mondweefsel. Weefseldeformatie als gevolg van de inbreng van een naald wordt sterk beïnvloed door de geometrie van de punt en insertie snelheid. Bovendien werd een uithoudingstest uitgevoerd waarbij er 100 keer een insertie met één naald werd uitgevoerd, waarbij geen opmerkelijk verschil werd waargenomen.

Ten slotte is de invasiediepte een belangrijke voorspeller voor occulte lymfeklieren en wordt gebruikt om te beslissen of een electieve halsklierdissectie is geïndiceerd. Helaas kan de invasiediepte pas worden gemeten nadat een resectie is uitgevoerd en is een tweede operatie daardoor soms nodig. Met het RIOARM-apparaat kan de invasiediepte echter voorafgaand aan de operatie worden gemeten.

Samengevat maakt het RIOARM-apparaat een brede acceptatie van intra-operatieve beoordeling van resectiemarges bij mondholtekankerchirurgie mogelijk, kan het worden gebruikt om de invasiediepte te meten en hoeft het gebruik niet beperkt te blijven tot alleen mondholtekankerchirurgie.



11 Appendix



LIST OF ABBREVIATIONS

AJCC American joint committee on cancer

AF autofluorescence
AUC area under the curve
BCE before (the) common era
CCD charge coupled device

CE common era
CIS carcinoma insitu
DM distant metastasis
DOI depth of invasion

DSS disease specific survival

EGFR epidermal growth factor receptor

END elective neck dissection EPF electronic patient file

ESI extra supplementary information

FWHM full width at half maximum

FS frozen section GR grossing room

H&E hematoxylin and eosin
HWVN high wavenumber
IE interpretation error

IOARM intraoperative assessment of resection margins

IR inadequate resections

LR local recurrence

LVI lymphovascular invasion NBI narrowband imaging

NDP Nanozoomer digital pathology NPV negative predictive value

OCSCC oral cavity squamous cell carcinoma

OR operation room or odds ratio

OS overall survival

PALGA pathologisch-anatomisch landelijk geautomatiseerd archief

PIM potentially inadequate margin

PMMA polymethylmetacrylate PNI perineural invasion

PORT post-operative radiotherapy
PPB positive predictive value
RCP royal college of pathologist

RIOARM Raman spectroscopy-based objective intraoperative assessment of

resection margins

ROC receiver operating characteristic

RR regional recurrence

RRFS regional recurrence-free survival RSNR Raman signal-to-noise ratio

RT radiotherapy

SCC squamous cell carcinoma

SD standard deviation
SE sampling error
TT tumor thickness

UICC union for international cancer control

US ultrasound

WHO world health organisation
WPOI worst pattern of invasion

WW watchful waiting

AFFILIATIONS OF CONTRIBUTING AUTHORS

Department of Pathology, Erasmus MC, University Medical Center Rotterdam, Rotterdam, The Netherlands.

Yassine Aaboubout, Elisa M Barroso, Mahesh Algoe, Patricia C Ewing-Graham, Maria R Nunes Soares, Lisette C van der Sar Lars Ottevanger, Sanne E Matlung, Vera van Dis, Robert M Verdijk, Senada Koljenović

Department of Otorhinolaryngology and Head and Neck Surgery, Erasmus MC, University Medical Center Rotterdam. Rotterdam. The Netherlands.

Yassine Aaboubout, Quincy M van der Toom, Cornelia G F van Lanschot, Roeland W H Smits, Maria J De Herdt, Berdine van der Steen, Stijn Keereweer, Aniel Sewnaik, Dominiek A Monserez, José A Hardillo, Robert J Baatenburg de Jong

Department of Oral and Maxillofacial Surgery, Erasmus MC, University Medical Center Rotterdam, Rotterdam, The Netherlands.

Elisa M Barroso, Hetty Mast, Brend P Jonker, Eppo B Wolvius

Department of Oral and Maxillofacial Surgery, LUMC, Leiden University Medical Center, Leiden, The Netherlands.

Ivo Ten Hove

Department of Medical informatics, Erasmus MC, University Medical Center Rotterdam, Rotterdam, Netherlands.

Maria A J de Ridder

Department of Dermatology, Erasmus MC, University Medical Center Rotterdam, Rotterdam, The Netherlands.

Maria R Nunes Soares, Lars Ottevanger, Peter J Caspers, Tom C Bakker Schut, Gerwin J Puppels

Department of Biomechanical Engineering, Delft University of Technology, Delft, the Netherlands.

John J van den Dobbelsteen

Art Photonics GmbH, Berlin, Germany.

Alexex Bocharnikov, Iskander Usenov, Viacheslav Artyushenko

PALGA foundation, The nationwide network and registry of histo- and cytopathology.

Paul A Seegers

RiverD International B. V., Rotterdam Science Tower, Marconistraat 16, 3029 AK Rotterdam, The

Martin van der Wolf, Elena Sokolova, Maria R Nunes Soares, Peter J Caspers, Tom C Bakker Schut, Gerwin J Puppels

Chapter 11

192

Department of Pathology, Antwerp University Hospital, 2650 Antwerpen, Belgium. Senada Koljenović

University of Antwerp, Faculty of Medicine, 2610 Antwerpen, Belgium.

Senada Koljenović

LIST OF PUBLICATIONS

Aaboubout, Y., Ten Hove, I., Smits, R. W. H., Hardillo, J. A., Puppels, G. J., & Koljenovic, S. (2021). Specimen-driven intraoperative assessment of resection margins should be standard of care for oral cancer patients. Oral diseases, 27(1), 111-116. https://doi.org/10.1111/odi.13619

Barroso, E. M., Aaboubout, Y., van der Sar, L. C., Mast, H., Sewnaik, A., Hardillo, J. A., Ten Hove, I., Nunes Soares, M. R., Ottevanger, L., Bakker Schut, T. C., Puppels, G. J., & Koljenović, S. (2021). Performance of Intraoperative Assessment of Resection Margins in Oral Cancer Surgery: A Review of Literature. Frontiers in oncology, 11, 628297. https://doi.org/10.3389/fonc.2021.628297

Aaboubout, Y., Nunes Soares, M. R., Barroso, E. M., van der Sar, L. C., Bocharnikov, A., Usenov, I., Artyushenko, V., Caspers, P. J., Koljenović, S., Bakker Schut, T. C., van den Dobbelsteen, J. J., & Puppels, G. J. (2021). Experimental study on needle insertion force to minimize tissue deformation in tongue tissue. Medical engineering & physics, 97, 40-46. https://doi.org/10.1016/j.medengphy.2021.10.003

Aaboubout, Y., Barroso, E. M., Algoe, M., Ewing-Graham, P. C., Ten Hove, I., Mast, H., Hardillo, J. A., Sewnaik, A., Monserez, D. A., Keereweer, S., Jonker, B. P., van Lanschot, C. G. F., Smits, R. W. H., Nunes Soares, M. R., Ottevanger, L., Matlung, S. E., Seegers, P. A., van Dis, V., Verdijk, R. M., Wolvius, E. B., ... Koljenović, S. (2021). Intraoperative Assessment of Resection Margins in Oral Cavity Cancer: This is the Way. Journal of visualized experiments: JoVE, (171), 10.3791/62446. https://doi.org/10.3791/62446

Aaboubout, Y., Nunes Soares, M. R., Bakker Schut, T. C., Barroso, E. M., van der Wolf, M., Sokolova, E., Artyushenko, V., Bocharnikov, A., Usenov, I., van Lanschot, C. G. F., Ottevanger, L., Mast, H., Ten Hove, I., Jonker, B. P., Keereweer, S., Monserez, D. A., Sewnaik, A., Hardillo, J. A., Baatenburg de Jong, R. J., Koljenović, S., ... Puppels, G. J. (2023). Intraoperative assessment of resection margins by Raman spectroscopy to guide oral cancer surgery. The Analyst, 148(17), 4116-4126. https://doi.org/10.1039/d3an00650f

Bugter, O., Aaboubout, Y., Algoe, M., de Bruijn, H. S., Keereweer, S., Sewnaik, A., Monserez, D. A., Koljenović, S., Hardillo, J. A. U., Robinson, D. J., & Baatenburg de Jong, R. J. (2021). Detecting head and neck lymph node metastases with white

light reflectance spectroscopy; a pilot study. Oral oncology, 123, 105627. https://doi.org/10.1016/j.oraloncology.2021.105627

Aaboubout, Y., van der Toom, Q. M., de Ridder, M. A. J., De Herdt, M. J., van der Steen, B., van Lanschot, C. G. F., Barroso, E. M., Nunes Soares, M. R., Ten Hove, I., Mast, H., Smits, R. W. H., Sewnaik, A., Monserez, D. A., Keereweer, S., Caspers, P. J., Baatenburg de Jong, R. J., Bakker Schut, T. C., Puppels, G. J., Hardillo, J. A., & Koljenović, S. (2021). Is the Depth of Invasion a Marker for Elective Neck Dissection in Early Oral Squamous Cell Carcinoma?. Frontiers in oncology, 11, 628320. https://doi.org/10.3389/fonc.2021.628320

Smits, R. W. H., van Lanschot, C. G. F., **Aaboubout, Y.**, de Ridder, M., Hegt, V. N., Barroso, E. M., Meeuwis, C. A., Sewnaik, A., Hardillo, J. A., Monserez, D., Keereweer, S., Mast, H., Hove, I. T., Bakker Schut, T. C., Baatenburg de Jong, R. J., Puppels, G. J., & Koljenović, S. (2020). Intraoperative Assessment of the Resection Specimen Facilitates Achievement of Adequate Margins in Oral Carcinoma. Frontiers in oncology, 10, 614593. https://doi.org/10.3389/fonc.2020.614593

De Herdt, M. J., van der Steen, B., van der Toom, Q. M., Aaboubout, Y., Willems, S. M., Wieringa, M. H., Baatenburg de Jong, R. J., Looijenga, L. H. J., Koljenović, S., & Hardillo, J. A. (2021). The Potential of MET Immunoreactivity for Prediction of Lymph Node Metastasis in Early Oral Tongue Squamous Cell Carcinoma. Frontiers in oncology, 11, 638048. https://doi.org/10.3389/fonc.2021.638048

van Lanschot, C. G. F., Klazen, Y. P., de Ridder, M. A. J., Mast, H., Ten Hove, I., Hardillo, J. A., Monserez, D. A., Sewnaik, A., Meeuwis, C. A., Keereweer, S., **Aaboubout, Y.**, Barroso, E. M., van der Toom, Q. M., Bakker Schut, T. C., Wolvius, E. B., Baatenburg de Jong, R. J., Puppels, G. J., & Koljenović, S. (2020). Depth of invasion in early stage oral cavity squamous cell carcinoma: The optimal cut-off value for elective neck dissection. Oral oncology, 111, 104940. https://doi.org/10.1016/j.oraloncology,2020.104940

Nicholson, O. A., Van Lanschot, C. G. F., van den Besselaar, B. N., **Aaboubout**, Y., Iseli, T., Hardillo, J. A. U., Mast, H., McDowell, L., Koljenović, S., Kranz, S., Baatenburg de Jong, R. J., Keereweer, S., & Wiesenfeld, D. (2024). Management of the neck in T1 and T2 buccal squamous cell carcinoma. International journal of oral and maxillofacial surgery, 53(4), 259-267. https://doi.org/10.1016/j.ijom.2023.07.004

PHD PORTOFOLIO

Name PhD student: Yassine Aaboubout

Erasmus MC department: Pathology and Otorhinolaryngology and Head and Neck

Surgery

PhD period: 2018 -2024

Promotor: Prof. dr. S. Koljenović and Prof. dr. R.J. Baatenburg de Jong

PhD training	Year	Workload
Courses		
Raman Summerschool	2018	3.0
Research integrity	2021	0.3
Presentations/Conferences		
Rotterdamse Werkgroep Hoofd Hals Tumoren	2018	0.2
Symposium Experimenteel Onderzoek Heelkundig Specialismen	2018	0.5
7th World Congress of the International Academy of Oral Oncology	2019	2.0
237e jaarcongres van de Nederlandse KNO Vereniging	2019	2.0
Quartly Progress meeting - Raman Group Oak Institute	2021	1.0
European Congress on Head and Neck Oncology	2023	2.0
8e Landelijke Enter Dag	2023	0.3
2-Daags Symposium	2023	2.0
241e jaarcongres van de Nederlandse KNO Vereniging	2023	0.3
Refereeravonden KNO	2018-2024	2.0
Teaching/Supervision		
Technical Medicine Bachelor Student	2019	1.0
Medicine master student	2019	1.0
Applied physics student	2019	1.0
Applied physics student	2019	1.0
Technical Medicine Bachelor Students	2019	1.0
Applied physics studen	2019	1.0
Technical Medicine Bachelor Students	2019	1.0
Histopathology (VO digimic) - airway	2020	1.0
Histopathology (VO digimic) - male reproductive system	2020	1.0
Technical Medicine Bachelor Student	2020	2.0
Technical Medicine Bachelor Student	2020	1.0
Histopathology (VO digimic) - oral cavity	2018-2021	3.0
PKV education otorhinolaryngology medical students	2019-2023	0.2
		30.80

DANKWOORD

Allereerst wil ik alle **patiënten en hun familieleden** bedanken voor hun inzet en welwillendheid om deel te nemen aan het onderzoek. Zonder hen was dit onderzoek nooit tot stand gekomen.

Mijn ouders (Marzouk Aaboubout en Nadia Erahoutan), jullie vormen de basis van wie ik ben, als mens en als arts. Zonder jullie enorme inspanningen en voortdurende motivatie was ik nooit naar het vwo gegaan en had ik nooit geneeskunde gestudeerd. Waar docenten van de basisschool weinig vertrouwen hadden in mijn kunnen en mij een laag schooladvies gaven, bleven jullie altijd optimistisch. Jullie namen mij mee op sleeptouw en investeerden ontzettend veel tijd en energie. Dankzij jullie onvoorwaardelijke steun en toewijding ben ik nu arts, en is dit proefschrift tot stand gekomen. Jullie hebben mij geleerd dat doorzettingsvermogen en hard werken een vereiste zijn.

Mijn dankbaarheid is te groot om in woorden uit te drukken, maar ik hoop dat jullie weten dat ik jullie elke dag dankbaar ben.

Geachte **Prof. dr. Koljenović**, beste Senada, jij bent de drijvende kracht achter dit onderzoek. Met jouw onvermoeibare inzet, genadeloos en onuitputtelijk, heb je dit project voortgestuwd. Dagen, avonden, nachten en weekenden: altijd was je beschikbaar, altijd stond je klaar voor de volgende horde. Op de afdeling Pathologie kon ik op elk moment binnenlopen, en je maakte áltijd tijd vrij, zelfs als dat eigenlijk niet goed uitkwam.

Jij bent het bindmiddel van de Raman-groep. Dat bleek niet alleen uit je overweldigende toewijding, maar ook uit de vele gezellige etentjes en borrels. Je directheid siert je en maakt de samenwerking soms intens (lees: vaak), maar zoals het gezegde luidt: ijzer smeden doe je als het heet is.

Moju zahvalnost je nemoguće izraziti riječima.

Geachte **Prof. dr. Baatenburg de Jong**, beste Rob, de eerste keer dat ik je sprak, was tijdens mijn sollicitatie voor een PhD-traject met mogelijk een opleidingsplek bij de KNO nadien. Dat gesprek kan ik mij nog goed herinneren: daar zat je dan, formeel, maar toch ook informeel, en met veel bravoure stelde je de ene na de andere vraag.

Altijd nieuwsgierig en altijd op zoek naar meer antwoorden. Die nieuwsgierigheid uitte zich tijdens het onderzoek regelmatig in een WhatsApp-bericht, dat soms overdag, soms 's avonds en soms in het weekend verscheen, vaak met nieuwe ideeën.

Prof, dank voor je enthousiasme en je vertrouwen in mij.

Geachte **dr. ir. Puppels**, beste Gerwin, voor mij ben jij "the Raman Godfather". Tijdens elke meeting zit je daar aandachtig te luisteren naar ieders input, om vervolgens, met slechts een paar rake opmerkingen of een creatieve, out-of-the-box gedachtegang, de hele groep (en vooral mij) weer in beweging te brengen.

Je weet precies wanneer je moet ingrijpen en hoe je richting geeft zonder te sturen.

Ondanks je drukke agenda was ook jij bereid om aan te schuiven bij onze overleggen, of dat nu in de avonden, nachten of weekenden was. Jouw betrokkenheid is voor mij altijd van grote waarde geweest. Ik ben je dan ook zeer dankbaar voor al je hulp en inzet.

Geachte prof. dr. B. Kremer, prof. dr. I.W. Schie en prof. dr. B. Weynand, hartelijk dank voor het plaatsnemen in mijn leescommissie. Geachte prof. dr. W. Huvenne, dr. J.A. Hardillo en prof. dr. K. Zwaenepoel, dank voor het opponeren tijdens mijn promotie.

Geachte **dr. Barroso**, beste Elisa, Je bent een geweldig en warm mens, altijd op zoek naar kennis, altijd nieuwsgierig en enorm gedreven. Je bent bescheiden en timide, maar je rol binnen mijn PhD-traject was van groot belang.

De uitwisseling van gedachten tussen ons, jouw technische achtergrond en mijn medische achtergrond, heeft ons beiden verrijkt en versterkt. In de loop der jaren ben ik een beetje een engineer geworden en jij een beetje een medicus.

Onze samenwerking verliep altijd op een zeer prettige manier. Waar je ook werkt, je bent zonder twijfel een grote meerwaarde voor elk team.

Geachte **dr. Nunes Soares**, beste Rosa, toen Elisa vertrok voor een nieuwe uitdaging buiten het ziekenhuis, was jij daar opeens. Bijna een kloon van Elisa: wederom een kleine Portugese, ook erg bescheiden en timide. Jij nam moeiteloos over waar zij was gebleven.

De snelheid waarmee je alles onder de knie kreeg en je uitzonderlijke werkethos waren indrukwekkend, alsof je dit al jaren deed. Het was altijd prettig en gezellig samenwerken.

Als jij iets toezegt, weet je zeker dat het met grote zorg en precisie wordt uitgevoerd.

Cara **Elisa** e **Rosa**, obrigada de coração pelo vosso apoio e pela parceria tão boa, caralho.

Geachte **dr. ir. Bakker Schut**, beste Tom, op de 16e verdieping, tijdens borrels of etentjes, hoor je vaak jouw kenmerkende bulderende lach. Jouw humor, gecombineerd met een scherpe visie op het leven, heeft altijd voor een geweldige sfeer gezorgd.

Daarnaast heb je ook een serieuze kant: je weet complexe technische vraagstukken op een heldere en begrijpelijke manier uit te leggen. Dankzij jouw vermogen om met eenvoudige woorden de essentie over te brengen, werd het voor mij snel duidelijk wat er technisch mogelijk was, en minstens zo belangrijk: wat de beperkingen waren.

Tom, zonder jou was dit alles niet mogelijk geweest. Ik wil je dan ook enorm bedanken voor je onvermoeibare inzet, je betrokkenheid en je onmisbare rol.

Geachte dr. Meeuwis, dr. Hardillo, dr. Sewnaik, drs. Monserez, dr. Keereweer, drs. ten Hove, drs. Mast en dr. Jonker. Beste allen, hartelijk dank voor jullie inzet en waardevolle hulp tijdens dit onderzoek.

Geachte heer Algoe, beste Mahesh, vanaf dag één was het een enorm plezier om met jou samen te werken. Niet alleen beschikte je over brede kennis en ervaring, maar je manier van samenwerken was ook altijd bijzonder prettig. Je was voortdurend op zoek naar oplossingen, wat het proces op de uitsnijkamer en alles daaromheen altijd soepel liet verlopen. Dank je wel, Mahesh, voor je welwillendheid om altijd mee te denken en voor je waardevolle bijdrage.

Geachte heer Ottenvanger, beste Lars, in de eerste fase van mijn onderzoek zag ik je af en toe en leek je vooral veel achter de schermen te werken. Vanuit mijn perspectief had je toen al veel invloed, maar later werd je veel meer betrokken en stond je echt naast mij in de loopgraven. Je frisse blik, perspectief en honger naar kennis en oplossingen maakten je tot een topcollega.

Geachte **ir. de Wolf**, beste Martin, ik was altijd blij je te zien. Om de zoveel tijd stond je ineens weer in ons lab, nog in je motorkleding, bezig met het aanpassen van de apparatuur. Steeds weer was er een nieuw onderdeel, iets dat werd omgewisseld, of een slimme ontwikkeling van jou om het design te verbeteren. Dank je wel voor al je hulp, je eindeloze aanpassingen en jouw betrokkenheid.

Geachte **dr. ir. Caspers**, beste Peter, jou wil ik speciaal bedanken voor je kritische blik. Geen enkel artikel ontsnapte eraan; steevast kreeg ik minstens twintig opmerkingen terug. Dankzij jouw scherpe en grondige feedback zijn al onze publicaties merkbaar beter geworden.

Geachte **dr. de Ridder,** beste Maria, dank voor je zorgvuldige analyse, je heldere uitleg en je scherpe inzichten. Je was altijd bereidheid om te ondersteunen waar nodig, wat voor mij van onschatbare waarde is geweest.

Beste Ian, Remko, Silvy, Mandy, Jennifer, Sabine, Ilya, Elly, Remco en alle anderen van de pathologie afdeling, dank allen voor de gezellige en fijne samenwerking.

Beste collega arts-onderzoekers, (oud-) arts-assistenten en stafleden van de KNO-afdeling, dank voor jullie ondersteuning, het delen van kennis en voor de gezelligheid.

Geachte **dr. van Lanschot**, beste Florence, je was altijd een fijne collega, zowel tijdens de fulltime onderzoeksperiode als later tijdens onze gezamenlijke tijd als arts-assistenten. Jij had als voorganger alles uitstekend georganiseerd, waar ik enorm van heb kunnen profiteren. Veel dank voor alles.

Geachte **dr. Smits**, beste Roeland, ik leerde je kennen toen ik oudste coassistent was in het HagaZiekenhuis, en later werden wij collega's in het Erasmus MC. Door de jaren heen ben je uitgegroeid van een fijne collega tot een goede vriend. Dank je wel voor je vriendschap en voor het staan aan mijn zijde als paranimf.

Mijn zusje **Soumaya** en broertje **Farouk**, ik ben jullie veel dank verschuldigd. Jullie staan altijd voor mij klaar en weten dat ik er ook altijd voor jullie ben. We hebben het elkaar soms niet makkelijk gemaakt, maar ondanks alles is het altijd alleen maar liefde geweest. Ik houd van jullie.

Lieve **Naoual**, Ik houd enorm van je, en deze promotie is voor een groot deel aan jou te danken. Jij hebt zoveel opgeofferd, zodat ik mij steeds weer op mijn promotie kon focussen. Dank je wel voor je liefde, je onvoorwaardelijke steun en je eindeloze begrip. Jij, Amir, Nassim en onze nieuwe baby zijn mijn alles.

ABOUT THE AUTHOR

Yassine Aaboubout was born on the 29th of November 1988 in the Hague, the Netherlands. After completing his secondary education (Atheneum, Aloysius College, the Hague), he studied Medicine at the Erasmus University in Rotterdam and graduated in 2018. Early on in his study, he became interested in the otorhinolaryngology. A few months after graduating he started with a PhD-project on resection margins in oral cancer surgery within the Raman spectroscopy group at Erasmus Medical Center (promotor: Prof. dr. S. Koljenović and Prof.



dr. R.J. Baatenburg de Jong; co-promotor: dr. ir. G. J. Puppels).

From december 2021 he started his otorhinolaryngology residency under Prof. dr. R.J. Baatenburg de Jong, Prof. dr. B. Kremer, and dr. R.M. Metselaar at Erasmus Medical Center in Rotterdam, dr. P.G.J. ten Koppel at Maasstad Ziekenhuis in Rotterdam, and dr. G.K.A. van Wermeskerken at Amphia in Breda.

Yassine and his wife Naoual Tihouna, live in the Hague with their sons Amir, Nassim and a baby on the way.

Financial support for the printing of this thesis was kindly provided by:







Daleco Pharma b.v.





